LIGHT AND ELECTRON MICROSCOPIC STUDY OF THE TYROSINE HYDROXYLASE (TH) IMMUNOREACTIVE NEURONS WITHIN THE HYPOTHALAMIC ARCUATE NUCLEUS OF EARLY POSTNATAL, PREPUBERTAL AND ADULT RATS

by

Michèle Piotte

A thesis submitted to the Faculty of Graduate Studies and Research in partial fulfilment of the requirements for the degree of Doctor of Philosophy

Department of Anatomy
McGill University
Montreal, Quebec, Canada

May, 1986

ISBN 0-315-34456-3

IMMUNOCYTOCHEMICAL STUDY OF THE RAT DOPAMINERGIC ARCUATE NEURONS

by

Michèle Piotte

ABSTRACT

The hypothalamic arcuate nucleus contains a population of dopaminergic neurons that project to the median eminence, forming the tuberoinfundibular dopaminergic (TIDA) system. Although the topography of this system has been extensively studied, relatively little is known about its ultrastructure in general, and its patterns of connections in particular. In addition, although there is evidence for TIDA function very early in life, nothing is known about the fine structural differentiation and maturation of this system. Therefore, the organization of TIDA neurons and their connections was examined in neonatal, 15 day old, 30 day old, and adult female rats, and in adult male rats, by means of the peroxidase-anti-peroxidase (PAP) immunocytochemical method, using an antibody against tyrosine hydroxylase (TH).

In all animals examined, labeled dendrites were commonly observed in direct apposition to the following elements: labeled and unlabeled dendrites, labeled and unlabeled perikarya, and unlabeled tanycytic processes. These extensive contacts made by labeled dendrites suggested that TIDA cells may communicate with each other, influence other neuronal populations, and possibly play a role in the regulation of tanycytic function, by means of dendritic release of dopamine. The presence, in the neonate, of all types of connections (involving TH positive dendrites) seen in the adult indicated that the TIDA system is essentially differentiated and, therefore, potentially operative at birth. Maturational changes, however, involved quantitative alterations in the different types of dendritic connections. For example, the percentage of dendritic connections involving one labeled and one unlabeled element decreased with age.

No sexual dimorphism was apparent although staining intensity was greater in females than in males, possibly due to an estradiol enhancement and a testosterone suppression of TH expression. In fact, estradiol valerate-treated females exhibited the most intense immunoreactivity.

Name: Michèle Piotte

Thesis Title: Light and Electron Microscopic Study of the Tyrosine Hydroxylase -(TH) Immunoreactive Neurons within the Hypothalamic Arcuate Nucleus of Early Postnatal, Prepubertal and Adult Rats.

Department: Anatomy

Diploma: Doctor of Philosophy

RÉSUMÉ

Le noyau arqué de l'hypothalamus contient une population de neurones dopaminergiques dont les axones rejoignent l'éminence médiane, formant ainsi le système tuberoinfundibulaire dopaminergique (TIDA). Même si la topographie de ce système est déjà bien connue, il y a peu d'information sur son ultrastucture en général, et sur la disposition de ses connections intercellulaires en particulier. De plus, même s'il existe des preuves que le système TIDA entre en fonction très tôt au cours du développement, on ne sait rien sur sa différenciation et sa maturation au niveau ultrastructural. L'organisation des neurones TIDA et de leurs connections a donc été examinée chez des rates âgées de 2, 15 et 30 jours, ainsi que chez des rats et rates adultes. Les neurones dopaminergiques ont été visualisés par immunocytochimie, à l'aide d'un anticorps anti-tyrosine hydroxylase (TH) révélé par la méthode peroxidase-antiperoxidase (PAP).

Chez tous les animaux examinés, des dendrites immunomarquées ont communément été observées en apposition directe avec les éléments suivants: des dendrites marquées et non-marquées, des corps cellulaires marqués et non-marqués, et des processus tanycytaires non-marqués. L'étendue des contacts impliquant des dendrites marquées suggère que les cellules TIDA pourraient communiquer les unes avec les autres, influencer d'autres populations de neurones, et possiblement jouer un rôle dans la régulation des fonctions tanycytaires, au moyen de la libération dendritique de dopamine. La présence, chez le nouveau-né, de tous les types de connections (impliquant des dendrites marquées) observées chez l'adulte indique que le système TIDA est essentiellement différencié et, en conséquence, potentiellement fonctionel à la naissance. Au cours du développement on observe, cependant,

des modifications des différents types de connections dendritiques. Par exemple, le pourcentage des connections entre dendrites marquées et non-marquées diminue avec l'âge.

Il n'y a pas de dimorphisme sexuel apparent, quoique l'intensité du marquage est plus grande chez les femelles que chez les mâles, probablement à cause d'une stimulation par l'oestradiol et d'une suppression par la testosterone de l'expression de la TH. En fait, le système TIDA des femelles traitées a l'oestradiol montre l'immunoréactivité la plus intense.

Nom: Michèle Piotte

Titre de la Thèse: Étude en microscopie optique et électronique des neurones immunomarqués par la tyrosine hydroxylase (TH) dans le noyau arqué de l'hypothalamus du rat nouveau-né, prépubère et adulte.

Département: Anatomie

Diplôme: Docteur en Philosophie

To my parents,

my brother Pierre-Louis

and his wife Julia

ACKNOWLEDGEMENTS

I would first like to thank my supervisor, Dr. James R. Brawer, for his expert guidance throughout this project. His constructive criticisms were enlightning and deeply appreciated.

I am also grateful to Dr. Alain Beaudet for the use of his laboratory at the Montreal Neurological Institute, and for his many inspiring suggestions concerning the experimental approach.

I extend my appreciation to Miss Kathleen Leonard for instructing me on the use of the vibratome and immunostaining techniques. Furthermore, I am indebted to Mr. John Bertley for assisting me in perfusing the animals, collecting and immunostaining the material, and to Mrs. Jeannie Wong Mui for cutting and staining thin sections, and for the excellent work she has done in printing the electron micrographs included in this thesis.

I am also thankful to Mr. Anthony Graham for the photographic reproductions, Mrs. Margot Oeltzschner for tracing the neuronal maps, and Dr. Gerald McCarthy for reading the thesis.

Finally, I sincerely thank my parents for their constant encouragement.

This work was supported by a grant from the Medical Research Council of Canada to Dr. James R. Brawer.

TABLE OF CONTENTS

	Page no.
ABSTRACT	i
RÉSUMÉ	iii
ACKNOWLEDGEMENTS	v
TABLE OF CONTENTS	vi
LIST OF TABLES	ix
LIST OF PLATES AND FIGURES	x
LIST OF ABBREVIATIONS	xiii
INTRODUCTION	1
I- The Hypothalamic Arcuate Nucleus	1
II- Morphological Demonstration of a Dopaminergic System of Neurons within the Hypothalamic Arcuate Nucleus	2
III- The Role of the TIDA Neurons in Anterior Pituitary Function	7
IV- The Fine Structure of the TIDA System	10
A. Cytochemistry	11
B. Radioautography	12
C. Immunocytochemistry	14
V- Ontogeny of the TIDA System	18
SPECIFIC OBJECTIVES	20
MATERIALS AND METHODS	21
I- Animals	21
A) Housing	21
B) Adult Rats	21
1. Females	21
2. Males	22
C) Pubertal Animals	22
D) Prepubertal Animals and Neonates	22
II- Perfusion Procedures	22
A) Preparation of the Fixative	22
B) Perfusing Adult and Pubertal Animals	23
C) Prepubertal Animals	24
D) Neonates	24

III- Tissue Preparation..... 25
A) Adult and Pubertal Rats..... 25
B) Prepubertal Rats..... 25
C) Neonates..... 26

IV- Source of Antiserum..... 26

V- Immunocytochemical Staining..... 27
A) Specificity..... 27
B) Method Specificity..... 27
C) Specificity of the Antibody..... 28

VI- Immunocytochemical Procedures..... 28

VII- Tissue Processing for Light and Electron Microscopic Observations..... 30

VIII- Light and Electron Microscopy..... 31

RESULTS..... 34

I- The Adult TIDA System..... 34
A. Light Microscopic Observations..... 34
a) Normally Cycling Females..... 34
b) EV-treated Females..... 35
c) Intact Males..... 36

B. Electron Microscopic Observations..... 36
a) Normally Cycling Female Rats..... 36
1. Perikarya..... 36
2. Dendrites..... 37
3. Axon Terminals..... 41

b) EV-treated Females..... 43
1. Perikarya..... 43
2. Dendrites..... 43
3. Axon Terminals..... 46

c) Intact Males..... 47
1. Perikarya..... 47
2. Dendrites..... 47
3. Axon Terminals..... 49

II- Ontogeny of the TIDA System..... 49
A. Light Microscopic Observations..... 49
a) Neonatal Females..... 49
b) 15 Day Old Females..... 50
c) 30 Day Old Females..... 51

B. Electron Microscopic Observations..... 52
a) Neonatal Females..... 52
1. Perikarya..... 52
2. Dendrites..... 53
3. Axon Terminals..... 55

b) 15 Day Old Females..... 55
1. Perikarya..... 55
2. Dendrites..... 58
3. Axon Terminals..... 60

c) 30 Day Old Females..... 60
1. Perikarya..... 60
2. Dendrites..... 62
3. Axon Terminals..... 62

DISCUSSION..... 63

I- The Adult TIDA System..... 63
A. Topography..... 63
B. Ultrastructural Organization..... 64
C. Effects of Sex Steroids on Male and Female TIDA Neurons.. 74

II- Ontogeny of the TIDA System..... 76
A. Topography..... 76
B. Ultrastructural Organization..... 79

SUMMARY AND CONCLUSIONS..... 83

ORIGINAL CONTRIBUTIONS..... 85

BIBLIOGRAPHY..... 86

PLATES AND FIGURES..... 102

LIST OF TABLES

		Page no.
Table I	Number and Source of Sections Examined at the Ultrastructural Level.....	33
Table II	Types of Relationships Observed between TH Positive Dendrites and other Elements of the Arcuate Neuropil of Normally Cycling Females.....	39
Table III	Types of Relationships Seen between Labeled Axon Terminals and other Elements of the Arcuate Neuropil of Normally Cycling Females.....	42
Table IV	Number of Axo-Somatic Appositions and Synapses Involving Unlabeled Axon Terminals and both Labeled and Unlabeled Perikarya of Normally Cycling Females.....	44
Table V	Types of Relationships Observed between TH Positive Dendrites and other Elements of the Arcuate Neuropil in EV-treated Females.....	45
Table VI	Types of Relationships Observed between TH Positive Dendrites and other Elements of the Intact Male Arcuate Neuropil.....	48
Table VII	Types of Relationships Observed between TH Positive Dendrites and other Elements of the neonatal Arcuate Neuropil.....	54
Table VIII	Types of Relationships Observed between Labeled Axon Terminals and other Elements of the Neonatal Arcuate Neuropil.....	56
Table IX	Number of Axo-Somatic Appositions and Synapses involving Unlabeled Axon Terminals and both Labeled and Unlabeled Perikarya of Neonatal Females.....	57
Table X	Types of Relationships Observed between TH Positive Dendrites and other Elements of the Arcuate Neuropil of 15 Day Old Females.....	59
Table XI	Types of Relationships Observed between TH Positive Dendrites and other Elements of the Arcuate Neuropil of 30 Day Old Females.....	61

LIST OF PLATES AND FIGURES

		Page no.
Plate 1	TH positive nerve cell bodies from representative coronal sections taken from 4 different levels of the arcuate nucleus of a normally cycling female rat (CII).....	102
Plate 2	TH positive nerve cell bodies from representative coronal sections taken from 3 different levels of the arcuate nucleus of an EV-treated female rat (EVII).....	104
Plate 3	TH positive perikarya from representative coronal sections taken from 3 different levels of the male arcuate nucleus (animal C3).....	105
Plate 4	TH positive nerve cell bodies and processes from representative coronal sections taken from 4 different levels of a female neonatal (D1-3) arcuate nucleus	118
Plate 5	TH positive nerve cell bodies from representative coronal sections taken from 4 different levels of a 15 day old female (D15-2) arcuate nucleus.....	119
Figure 1	Transverse section of mid-arcuate nucleus, from which Plate 1d was obtained.....	103
Figure 2	TH immunoreactive perikaryon.....	106
Figure 3	Immunolabeled dendrite in longitudinal section.....	107
Figure 4	Immunolabeled dendrite in cross-section.....	107
Figure 5	Immunolabeled cross-sectioned dendritic profile in synaptic contact with an unlabeled terminal.....	107
Figure 6	Labeled dendrites in apposition to a tanycytic process.....	108
Figure 7	Labeled dendrite in apposition to unlabeled dendrite.....	109
Figure 8	Two labeled dendrites in apposition.....	109
Figure 9	Labeled dendro-somatic appositions.....	109
Figure 10	Labeled dendrite in apposition to unlabeled perikaryon.....	110

Figure 11	A glial sheath intercalated between a TH positive dendritic profile and an unlabeled nerve cell body.....	111
Figure 12	A labeled axon terminal.....	112
Figure 13a	Axo-dendritic synapse involving a labeled axon terminal and an unlabeled dendrite.....	113
Figure 13b	Apposition between a labeled and an unlabeled axon terminal.....	113
Figure 13c	Labeled axon terminal in direct apposition to a tanycytic process.....	114
Figure 13d	A labeled nerve terminal in direct apposition to a TH positive nerve cell body.....	114
Figure 13e	A labeled nerve terminal in direct apposition to an unlabeled nerve cell body.....	114
Figure 14	An unlabeled nerve cell body contacted by 4 unlabeled axon terminals.....	115
Figure 15	TH positive perikaryon from an intact male rat.....	116
Figure 16	Dendro-dendritic apposition involving 2 labeled dendrites.....	117
Figure 17	TH positive nerve cell body from a neonatal arcuate nucleus.....	120
Figure 18	TH positives nerve cell body from a neonatal arcuate nucleus.....	121
Figure 19	Dendro-somatic apposition between an unlabeled dendrite and a labeled perikaryon within the neonatal arcuate nucleus.....	122
Figure 20a	One TH positive dendrite in direct apposition to 2 unlabeled dendrites and an unlabeled axon terminal within the arcuate nucleus of a female neonate.....	123
Figure 20b	Dendro-dendritic apposition involving two labeled dendrites within the neonatal arcuate nucleus.....	123
Figure 20c	An unlabeled axon terminal synapses on a labeled dendrite.....	123
Figure 21	A neonatal dendritic profile in direct apposition to an extension of a tanycytic process.....	124

Figure 22 A labeled dendrite in direct apposition to an unlabeled perikaryon from a female neonatal arcuate nucleus..... 125

Figure 23 A labeled dendrite in direct apposition to a labeled and an unlabeled neonatal nerve cell body..... 126

Figure 24 Immunoreactive axon terminal within the neonatal arcuate nucleus..... 127

Figure 25 TH positive perikarya within the arcuate nucleus of a 15 day old female rat..... 128

LIST OF ABBREVIATIONS

ABC	Avidin-biotin-peroxidase complex
ACTH	Adrenocorticotropic hormone
CNS	Central nervous system
CO_2	Carbon dioxide
$CoCl_2$	Cobalt chloride
DA	Dopamine
DAB	Diaminobenzidine
DARP-32	Dopamine- and adenosine 3':5'-monophosphate-regulated phosphoprotein
DOPA	Dihydroxyphenylalanine
E_2	Estradiol
EB	Estradiol benzoate
EM	Electron microscopy
EV	Estradiol valerate
FITC	Fluoresceinisothiocyanate
FSH	Follicle stimulating hormone
GAD	Glutamic acid decarboxylase
GRF	Growth hormone releasing factor
H_2O_2	Hydrogen peroxide
HCl	Hydrochloric acid
5-HT	5-Hydroxytryptamine (serotonin)
LH	Luteinizing hormone
LM	Light microscopy
MAO	Monoamine oxidase

MBH	Medial basal hypothalamus
α-MT	α-methyl-p-tyrosine
NA	Noradrenaline
6-OH-DA	6-Hydroxydopamine
OsO_4	Osmium tetroxide
PAP	Peroxidase-antiperoxidase
PIF	Prolactin inhibiting factor
PRL	Prolactin
T	Testosterone
TH	Tyrosine hydroxylase
TIDA	Tuberoinfundibular dopaminergic

INTRODUCTION

I- THE HYPOTHALAMIC ARCUATE NUCLEUS

The hypothalamic arcuate nucleus consists of a dense collection of neurons located along the basal lateral wall of the third ventricle. This nucleus extends from the optic chiasm, anteriorly, to the end of the mamillary recess, posteriorly (Bleier et al., 1979). Arcuate neurons are, for the most part, small cells of about 10 µm in short diameter and 15 µm in long diameter (Bodoky and Réthelyi, 1977). They are positioned amongst non-neuronal elements such as macroglial cells, microglial cells, and long tanycytic processes extending from the ventricular wall (Brawer and van Houten, 1976). Golgi studies (Bodoky and Réthelyi, 1977; Millhouse, 1979; van den Pol and Cassidy, 1982) reveal that arcuate neurons are morphologically relatively homogeneous. Their small perikarya are generally fusiform or polygonal in shape, projecting two or three (occasionally one or four) dendritic processes. Despite this uniformity in shape, arcuate neurons comprise several distinct populations, containing different hypophysiotropic hormones and transmitters. Growth hormone releasing factor (GRF) (Merchenthaler et al., 1984), somatostatin (Dierickx and Vandesande, 1979; Johansson and Hökfelt, 1980), ACTH/ β-endorphin (Bloch et al, 1979; Sofroniew, 1979; Hisano et al., 1982), enkephalin (Johansson and Hökfelt, 1980), acetylcholine (Cuello and Sofroniew, 1984), GABA (Everitt et al., 1984), and dopamine (Björklund and Nobin, 1973; Hökfelt et al., 1976; Everitt et al., 1984) are amongst the numerous substances that have been detected within arcuate neurons.

Arcuate nerve cell bodies project to the primary capillary plexus of the hypothalamo-hypophyseal portal system (Szentágothai et al., 1972; Bodoky and Réthelyi, 1977), indicating their key role in the regulation of anterior pituitary function. This anatomical projection comprises part of the tuberoinfundibular tract, a highly heterogeneous anatomical pathway, which extends from diverse regions of medial hypothalamus and preoptic area to the median eminence. It is the final common neurosecretory pathway over which the brain influences hypophysiotropic function. One well delineated component of this system derives from dopaminergic cells within the arcuate nucleus. These cells project to the median eminence forming the tuberoinfundibular dopaminergic (TIDA) system. The TIDA system has been implicated in the regulation of prolactin and gonadotropin release from the anterior pituitary gland. It is this component of the neuronal circuitry regulating hypophyseal function that is the subject of this thesis.

II- MORPHOLOGICAL DEMONSTRATION OF A DOPAMINERGIC SYSTEM OF NEURONS WITHIN THE HYPOTHALAMIC ARCUATE NUCLEUS

The primary catecholamines, noradrenaline (NA) and dopamine (DA), were first detected within the mammalian hypothalamus (Vogt, 1954; Carlsson, 1959), using biological assays. Purified hypothalamic extracts were chromatographed on paper, eluted, and the amount of NA was assessed by observing the effect of the eluant on the blood pressure of the rat. (Crawford and Outschoorn, 1951). Cellular localization of these amines was not possible due to the lack of a specific histochemical technique. The first such

specific histochemical method was developed in the early 1960's (Falck, 1962; Falck et al., 1962). This so-called Falck-Hillarp formaldehyde fluorescence technique permitted the direct visualization of catecholaminergic neurons (Carlsson et al., 1962; Fuxe, 1964; Dahlström and Fuxe, 1964; Fuxe and Hökfelt, 1969). The method is based on the formaldehyde induced conversion of the primary catecholamines, DA and NA, and of the indolamine 5-hydroxytryptamine (serotonin:5-HT) to fluorescent isoquinolines and β-carbolines respectively. These reaction products fluoresce and can be visualized with a fluorescence microscope (Corrodi and Jonsson, 1967). Since the isoquinolines emit a green to yellow-green fluorescence while the β-carbolines give a yellow fluorescence (Falck, 1962), it was possible to differentiate the catecholamines from 5-HT. The green to yellow-green fluorescence of numerous nerve cell bodies, scattered throughout the hypothalamic arcuate nucleus, first indicated the presence and distribution of a sizeable population of catecholaminergic neurons in this nucleus (Carlsson et al., 1962; Fuxe, 1964; Dahlström and Fuxe, 1964; Fuxe and Hökfelt, 1969). Since both DA and NA have similar fluorescence characteristics (Falck, 1962), the exact nature of the transmitter found within the arcuate neurons remained uncertain. Indirect pharmacologic evidence, however, suggested that these fluorescent arcuate neurons were dopaminergic. The fluorescence of these cells was not, for example, affected by treatment with α-methyl-m-tyrosine, a false transmitter which causes a diminution of the brain NA levels, without appreciably affecting DA or 5-HT levels (Fuxe, 1964).

The Falck-Hillarp formaldehyde fluorescence method, used in conjunction with a variety of pharmacological and surgical manipulations, provided information, much of it indirect, on the size, distribution and axonal projections of the arcuate catecholaminergic system. Fuxe (1964),

for example, showed that reserpine, a drug that depletes monoamines, abolished the green fluorescence from the abundant fine varicose fibers in the external layer of the median eminence. The simultaneous decrease in the intensity of the green fluorescence observed within the small, round neurons of the arcuate nucleus, suggested that these neurons were, at least in part, the source of the fluorescent fibers in the external layer of the median eminence. Although visualizing catecholaminergic axons under normal conditions presented serious difficulties, due to their low amine content (Fuxe et al., 1969), Fuxe and Hökfelt (1966) were able to follow some axons emerging from arcuate perikarya by increasing amine content. They accomplished this by means of reserpine-nialamide-l-dopa treatment. Under such conditions, some fluorescent axons could be traced from neurons in the arcuate nucleus to the median eminence. This projection was also demonstrated by Lichtensteiger and Langemann (1966). After depleting the brain amine stores of mice with reserpine, and blocking monoamine oxidase inhibitor (MAO) with nialamide in order to eliminate catecholamine catabolism, these authors injected noradrenaline, dopamine, and dihydroxyphenylalanine (DOPA), intraperitoneally (i.p.), and observed, with the Falck-Hillarp method, an uptake of these exogenous catecholamines by arcuate neurons. Green fluorescent axons were observed projecting from green fluorescent arcuate nerve cell bodies to the external layer of the median eminence. Thus by 1966, the presence of a population of catecholaminergic cells scattered throughout the arcuate nucleus and projecting, at least in part, to the median eminence was fairly certain.

Confirmation of the existence of this tuberoinfundibular system of neurons was also obtained by means of lesion experiments. Following damage of the median eminence, an increase in both the number and fluorescence

intensity of catecholaminergic arcuate perikarya was observed (Fuxe and Hökfelt, 1966; Smith and Fink, 1972). This increase was reported to be directly proportional to the size of the lesion, that is, the larger the lesion, the greater the number of fluorescent cells and the more pronounced the fluorescence intensity of individual arcuate nerve cell bodies (Fuxe and Hökfelt, 1966). Conversely, lesions of the arcuate nucleus led to a diminution of the fluorescence intensity within the external layer of the median eminence (Smith and Fink, 1972; Björklund et al., 1973). More specifically, lesions of the most rostral arcuate region resulted in a diminution in catecholaminergic fibers throughout the external layer of the median eminence, whereas lesions of the middle or caudal arcuate regions caused a decreased fluorescence in the middle and caudal external median eminence respectively (Björklund et al., 1973). These results indicated that the catecholamine-containing neurons of the rostral arcuate nucleus project to all parts of the external median eminence, while those of the middle and caudal arcuate regions project to corresponding areas of the external median eminence.

In 1971, Weiner et al. provided additional indirect evidence for the dopaminergic nature of the arcuate infundibular catecholaminergic system. Following complete deafferentation of the medial basal hypothalamus (MBH), NA and DA levels were determined by the trihydroxyindole method. Each catecholamine was oxidized to its respective red indole derivative, and the concentration was then determined with a spectrofluorometer (Carlsson and Waldeck, 1958). A significant decrease in NA content of the MBH was observed while DA content remained unchanged, suggesting that DA but not NA originated in cells within the MBH. This finding was corroborated by the results of Jonsson et al. (1972) who showed a complete blockage of ^{3}H-NA formation

from ^{3}H-DA, in hypothalamic slices preincubated with 6-hydroxydopamine (6-OH-DA), a neurotoxin that causes selective degeneration of NA nerve terminals (Tranzer and Thoenen, 1968). A similar strategy was used to obtain evidence for the dopaminergic nature of the terminals in the median eminence originating from arcuate perikarya (Fuxe and Hökfelt, 1966). Jonsson et al. (1972) showed a marked resistance of these terminals to the depleting action of 6-OH-DA.

Finally, in 1972, Björklund et al., discovered that the fluorophores of DA and NA can be distinguished spectrally following their acidification. Subsequently, the dopaminergic nature of arcuate perikarya was directly demonstrated (Björklund and Nobin, 1973) when specific dopamine spectra were recorded from the arcuate nerve cell bodies of diencephalic sections that were previously exposed to formaldehyde and HCl vapours.

Combining the Falck-Hillarp fluorescence method with pharmacological and lesion experiments, researchers have shown that the arcuate nucleus contains dopaminergic nerve cell bodies, and that these cells provide extensive innervation to the external zone of the median eminence, forming the tuberoinfundibular dopaminergic (TIDA) system (Fuxe and Hökfelt, 1966). The close association of TIDA nerve terminals with the primary capillary plexus of the median eminence suggested that this system was involved in the regulation of hypophyseal hormonal release.

III-. THE ROLE OF THE TIDA NEURONS IN ANTERIOR PITUITARY FUNCTION

In 1954, about 10 years prior to the demonstration of the existence of the TIDA system, Everett showed that an interruption of the normal relationship between the pituitary gland and the hypothalamus resulted in an increase in prolactin (PRL) secretion. This suggested that the hypothalamus normally inhibits prolactin release. Kamberi et al. (1971) infused extracts of either cerebrocortical tissue (CE) or hypothalamus (HE) into the anterior pituitary of male rats, via a cannulated stalk portal vessel, and observed the resulting changes in arterial PRL plasma levels. CE extracts did not affect PRL levels, but HE extracts caused a marked diminution in the levels of this hormone. Moreover, lower doses of HE resulted in proportionally smaller decreases in prolactin.

Interestingly, indirect evidence already existed for a mononaminergic PRL inhibitory system located in the tuberal region of the hypothalamus (van Maanen and Smelik, 1968). Implantation of the monoamine-depleting drug reserpine into the medial basal hypothalamus, resulted in disappearance of the fluorescence normally observed in the TIDA neurons, as well as that associated with pseudopregnancy. It was assumed that, since the implant was very small, the depletion effect was restricted to its immediate surroundings. Furthermore, the implant did not provoke the effects usually observed after systemic injection (ACTH hypersecretion, piloerection, and sedation). Consequently, the induction of pseudopregnancy (a condition characterized by high PRL plasma levels) was attributed to the depletion of DA from the TIDA neurons, supporting the idea of an inhibitory action of these arcuate neurons upon PRL release.

Later work clearly demonstrated the inhibitory effect of dopamine on PRL secretion. Small amounts of DA have been shown to significantly inhibit PRL release from rat anterior pituitaries in vitro (Shaar and Clemens, 1974; MacLeod and Lehmeyer, 1974). Results from in vivo experiments similarly indicated that DA inhibits PRL release by acting directly at the anterior pituitary level. Takahara et al. (1974), for example, showed that an infusion of DA directly into a single portal vessel resulted in an inhibition of PRL secretion. However, it has also been proposed (McCann and Moss, 1975; Vijayan and McCann, 1978) that DA may stimulate the release of a prolactin-inhibiting factor (PIF), which would in turn inhibit hypophyseal PRL release. The presence of DA in portal blood (Ben-Jonathan et al., 1976; 1977; Plotsky et al., 1978) in amounts sufficient to inhibit PRL release (Gibbs and Neill, 1978), and the presence of DA receptors on pituitary lactotropes (Goldsmith et al., 1979; Ajika et al., 1982), indicate that at least part of the inhibitory action of DA upon PRL release occurs by a direct effect at the pituitary level.

Although the inhibitory role of DA upon PRL secretion has been well established (Leong et al., 1983), the function of this monoamine with respect to the regulation of gonadotropin release still remains equivocal. Kamberi et al. (1971) reported that a crude hypothalamic extract causes a simultaneous decrease in plasma PRL levels and an increase in the plasma gonadotropin levels, suggesting that the DA secreted by the TIDA cells may facilitate gonadotropin release. A number of investigators (Schneider and McCann, 1969; 1970; Kamberi et al., 1970 a,b,c; Kordon and Glowinski, 1972; Vijayan and McCann, 1978) have reinforced the concept of DA facilitation of gonadotropin secretion. Paradoxically, other laboratories have not only failed to observe DA stimulation of gonadotropin release, but have actually

reported DA to be inhibitory (Fuxe and Hökfelt, 1969; Miyachi et al., 1973; Fuxe et al., 1976 a,b; Löfström, 1977; Löfström et al., 1977; Fuxe et al., 1977). Yet others found no role at all for DA in the regulation of gonadotropin secretion (Rubinstein and Sawyer, 1970; Ojeda et al., 1974). Thus, evidence for a DA involvement in LH and FSH modulation is confusing and conflicting (Weiner and Ganong, 1978). Nevertheless, both the TIDA and the luteinizing hormone releasing hormone (LHRH) systems co-terminate in the perivascular region of the lateral external median eminence (Ajika and Hökfelt, 1973), clearly indicating a possible interaction by an axo-axonic mechanism (Schneider and McCann, 1969; Hökfelt and Fuxe, 1971; McCann et al., 1971; Fuxe et al., 1976 a; Barraclough, 1983).

Although little is known concerning the regulatory influences on the TIDA system, one direct input appears to be gonadal steroids. Indeed, estradiol (E_2) and androgen receptors have been demonstrated within TIDA neurons (Grant and Stumpf, 1973; 1981; Heritage et al., 1980; Sar, 1984). Furthermore, following the administration of estradiol benzoate (EB) to adult female rats, Tobias et al. (1981) observed a significant increase in tyrosine hydroxylase (TH) activity, accompanied by a decrease in plasma LH levels. EB has also been reported to simultaneously cause a decrease in LH plasma levels and an increase in LHRH content within, the MBH, both effects being partially reversible by the inhibition of DA synthesis with α-methyl-p-tyrosine (α-MT) (Tobias et al., 1983). Experimental evidence, therefore, suggests the possibility of an inhibitory feedback action of E_2 on LH release mediated by TIDA neurons (Löfström et al., 1977; Wiesel et al., 1978). The picture is far from clear, however, since E_2 treatment has also been reported to significantly reduce TH activity in the rat MBH (Luine et al., 1977).

There exist, therefore, histological, physiological and pharmacological evidence, which clearly demonstrate a population of dopaminergic neurons, within the hypothalamic arcuate nucleus, that project to the median eminence, and are directly involved in the regulation of prolactin and possibly gonadotropin secretion. To date, however, little is known about the fine structural organization of this system. This is due primarily to the technical difficulty of achieving simultaneous specific labeling for dopaminergic elements, while maintaining a high quality of fine structural preservation.

IV- THE FINE STRUCTURE OF THE TIDA SYSTEM

Until recently, the Falck-Hillarp formaldehyde fluorescence technique was the only selective staining method available for the study of specific central catecholaminergic systems of neurons. This method limited the observer to fluorescence light microscopy (Hökfelt et al., 1984a). In order to study the TIDA system at the fine structural level, an alternative method had to be found. Within the past decade, three such methods which could potentially be applied to the TIDA system have been developed or modified from preexisting procedures. These methods are: cytochemistry, radioautography and immunocytochemistry (Bosler and Calas, 1982; Descarries and Beaudet, 1983). Because of the inherent limitations of these techniques, however, only fragmentary information has thus far been obtained on the ultrastructural organization of the TIDA system.

A. Cytochemistry

The endogenous biogenic monoamines NA, DA and 5-HT, can be localized at the ultrastructural level by cytochemistry (Richards, 1983), using an improved chromaffin reaction (Tranzer and Richards, 1976). The chromaffin reaction is a dichromate or chromic acid method originally used to demonstrate the presence of catecholamines in the adrenal medulla (Wood and Barrnett, 1964). It has long been known that adrenomedullary cells turn brown when exposed to chromium salts (Tranzer and Richards, 1976). It has been shown, however, that this reaction does not differentiate between the various biogenic amines. Indeed, noradrenaline, dopamine and serotonin all give a precipitate when exposed to chromium salts in vitro (Wood, 1966). This lack of specificity theoretically should not preclude application to the ultrastructural study of the TIDA system since the hypothalamic arcuate nucleus is devoid of NA or 5-HT nerve cell bodies (Carlsson et al., 1962; Fuxe, 1964; Dahlström and Fuxe, 1964; Fuxe and Hökfelt, 1969; Björklund and Nobin, 1973; Swanson and Hartman, 1975). However, despite the efforts of Tranzer and Richards (1976) who modified this method, and successfully identified amine storage vesicles in some CNS regions (supra-ependymal nerve terminals throughout the ventricular system and palisade zone of the median eminence), results were still unsatisfactory in the caudate putamen, in the locus ceruleus and in the hypothalamic periventricular regions. The authors did not indicate why the method had failed in these specific CNS areas, and merely reported results as being inconsistent. In any case, since the TIDA system is located in a periventricular hypothalamic area, cytochemistry would not provide a reliable method for the ultrastructural study of this system. Consequently, there is, to our knowledge, no ultrastructural cytochemical data available concerning TIDA neurons.

B. Radioautography

Based on the ability of central dopaminergic neurons to accumulate their own transmitter by a high affinity uptake mechanism (Paton, 1980), radioautography may be applied to the study of the TIDA system, following the intraventricular injection of tritiated (^{3}H)-DA or its precursor L-DOPA. Bosler et al. (1982) demonstrated (at the LM level) that the TIDA neurons were radiolabeled following the intraventricular administration of ^{3}H-DA. Similarly, both ^{3}H-DA (Scott et al., 1976) and ^{3}H-L-DOPA (Scott et al., 1978 a,b) were shown to be taken up by a subpopulation of neurons located in the region of distribution of the TIDA cells as demonstrated by histofluorescence. At the EM level, the radiolabel was found mainly over the mitochondria and rough endoplasmic reticulum of the TIDA perikarya. Axon terminals were also labeled within the dorsal arcuate nucleus and in all zones of the median eminence. Dendrites, however, remained unlabeled, except may be proximal dendrites for very short distances (Scott et al., 1978b, Fig. 3A)]. Since a study of the ultrastructural organizational pattern of the TIDA system would require extensive labeling of its dendrites, radioautography is clearly not an ideal method. Furthermore, as will be discussed below, resolution and specificity of terminal labeling are two additional factors contraindicating the use of radioautography for the study of the patterns of connection of TIDA neurons.

Radioautography is the method of choice to label neurons in which the levels of transmitters, and/or their synthetic enzymes, are too low for histofluorescence or immunocytochemical detection, or when quantitation of the labeled material is required (Descarries and Beaudet, 1983). However, a major problem inherent in EM radioautography is resolution, that is, assigning a grain (label) to a specific underlying structure. On a radio-

autograph, the visualization of a grain over a particular organelle does not necessarily mean that this organelle is the source of the radioactivity producing the grain (Salpeter et al., 1978; Nadler, 1979). This is so for 2 reasons: firstly, radioautographic resolution (at best 50 nm) is not as good as the resolution achieved by the electron microscope (0.2-0.3 nm). Thus, for example, a grain located over a synaptic cleft [20-30 nm wide (Peters et al., 1976) and therefore beyond the radioautographic resolution], may have either the axon terminal or the dendrite as its radioactive source. Secondly, a β-particle emitted by a radioactive source travels in random direction for some distance, resulting in a grain (after development) which may not be directly adjacent to its radioactive site of origin. Consequently, complex statistics are required in order to assign grains to underlying structures, rendering radioautography somewhat imprecise and difficult to interpret when used to identify small elements such as dendritic or axonal profiles.

The specificity of uptake of the radiolabeled amines must also be considered when radioautography is used as a labeling tool for catecholamine-containing neurons. Indeed, both DA and NA can be taken up by either dopaminergic or noradrenergic neurons, and serotonergic neurons also have the ability to take up DA (Descarries and Beaudet, 1983; Berger and Glowinski, 1978). Consequently, determining the nature of radiolabeled terminals becomes a problem in regions of the CNS where DA-, NA-, and 5-HT-containing axons are present (Bosler and Calas, 1982). Although the hypothalamic arcuate nucleus contains exclusively dopaminergic cells (Björklund and Nobin, 1973; Swanson and Hartman, 1975; Ruggiero et al., 1985), DA, NA and 5-HT axon terminals are all present. Therefore, although radioautography provided some information about the distribution of DA and its precursor L-

DOPA within TIDA neurons (Scott et al., 1976; 1978 a, b), the limitations of this technique precluded the possibility of obtaining information about the ultrastructural connection patterns of these neurons. However, radioautography in conjunction with other labeling methods, such as immunocytochemistry, has been used to this end. For example, direct appositions between serotonergic axonal varicosities and dopaminergic dendrites were shown in studies of the arcuate nucleus (Bosler et al., 1984; Bosler and Beaudet, 1985). This approach, however, still did not provide information concerning the intrinsic connection patterns of the TIDA system.

C. Immunocytochemistry

Any substance capable of inducing the formation of specific antibodies, following its injection into a suitable host, can be localized by means of immunocytochemical techniques (Sternberger, 1974). The large proteins normally found in neural tissues, such as the neurotransmitter-synthesizing enzymes, can induce antibody formation (Pickel, 1981; 1982). Over the past several years, all of the enzymes of the catecholamine biosynthetic pathway (Pickel et al., 1976), including tyrosine hydroxylase (Joh et al., 1973; Joh and Ross, 1983), have been purified. Tyrosine hydroxylase (TH), the rate-limiting enzyme of the pathway (Levitt et al., 1965), is the first enzyme in the chain of reactions responsible for the synthesis of catecholamines (Nagatsu et al., 1964; Weiner, 1970; Hökfelt et al., 1973) and is thus found in dopaminergic, noradrenergic and adrenergic neurons (Fuxe et al., 1978; Hökfelt et al., 1984a). The immunocytochemical localization of rate-limiting enzymes in a biosynthetic pathway reflects the distribution of neurotransmitters (Sternberger, 1979a). Since the TH-containing perikarya and dendrites of the arcuate nucleus are exclusively

dopaminergic (Björklund and Nobin, 1973; Swanson and Hartman, 1975; Ruggiero et al., 1985), the organization of the dopamine-containing nerve cell bodies and processes within this nucleus can be studied through the immunocytochemical detection of TH. This concept is supported by direct experimental evidence. Hökfelt et al. (1976) showed that the distribution of the TH positive TIDA cells, marked using a fluoresceinisothiocyanate (FITC) conjugated immunoglobulin (which binds to the TH antibody), corresponded to that observed using the Falck-Hillarp technique (Carlsson et al. 1962; Fuxe, 1964; Dahlström and Fuxe, 1964; Fuxe and Hökfelt, 1969). Therefore, immunocytochemistry using an antibody against TH is a valid method for studying the TIDA system.

The peroxidase-antiperoxidase (PAP) method of Sternberger (1974; 1979b) permits the study of neuronal systems at both light and electron microscopic levels. Indeed, the brown reaction product, obtained when horseradish peroxidase is exposed to 3-3'-diaminobenzidine (DAB) and hydrogen peroxide (H_2O_2), is visible under the light microscope and, since it becomes electron dense when reacted with osmium tetroxide (OsO_4) (Graham and Karnovsky, 1966; Rees and Karnovsky, 1967; Sternberger, 1974), electron microscopic detection is also possible.

In the past decade, the topography of the TIDA system as demonstrated by fluorescence and immunofluorescence techniques (Carlsson et al., 1962; Fuxe, 1964; Dahlström and Fuxe, 1964; Fuxe and Hökfelt, 1969; Hökfelt et al., 1976; 1984a) has been confirmed by LM immunocytochemical studies using of the PAP method (Pickel et al., 1975; Bosler et al., 1984; Chan-Palay et al., 1984; van den Pol et al., 1984; Piotte et al., 1985). EM immunocytochemical studies, however, were not readily undertaken because of the difficulty in simultaneously obtaining satisfactory tissue morphology and

the good antibody diffusion required for proper immunostaining. A proper methodology for the study of the fine structural organization of the TIDA system was not available until a suitable perfusing medium (see Section II-A of Materials and Methods) was developed, and used in conjunction with a modified version of the unlabeled PAP method of Sternberger (1979b) (see below).

At present, one of the most extensively used methods for the ultrastructural localization of specific neuronal antigens, is the unlabeled PAP method of Sternberger (1979b) which has been modified for preembedding staining (Pickel et al., 1975; Pickel, 1981; 1982), following perfusion of the brain (for details see Materials and Methods). The preembedding methodology consists in exposing the tissue sections, which have been cut with a Vibratome, to the various steps of the immunocytochemical procedure prior to epon embedding. The advantages of this technique are: 1) a better membrane preservation resulting from exposure of the tissue to osmium tetroxide before embedding 2) better immunostaining since TH appears to be more reactive prior to plastic embedding and 3) the ability to select, prior to embedding, precise areas of the tissue, known to contain a high density of the immunolabeled elements (e.g. nerve cell bodies), for further examination at the EM level.

In a light and electron microscopic study of the hypothalamic TH immunoreactive neurons van den Pol et al. (1984), using the PAP preembedding methodology, described the ultrastructural morphology of the adult rat arcuate dopaminergic perikarya. They reported many synapses, mostly asymmetrical, involving unlabeled axon terminals and TH positive dendrites. The PAP preembedding method was also used in the combined radioautographic and immunocytochemical studies, and demonstrated the relationships between

TIDA cells and other identified neuronal elements, as described in the previous section (Bosler et al., 1984; Bosler and Beaudet, 1985).

Similarly, using the immunoperoxidase preembedding methodology but with a different marker, that is, the avidin-biotin-peroxidase complex (ABC) (Hsu et al., 1981), Léránth et al. (1985b) showed TH immunoreactive axons in synaptic connection with TH immunoreactive dendrites in the adult female arcuate nucleus. This was a most interesting observation in view of the evidence suggesting that the TIDA system is autoregulatory (Kizer et al., 1978). A preembedding double immunostaining procedure, permitting the simultaneous ultrastructural localization of two different antigens in the same tissue section, also made possible the demonstration of glutamic acid decarboxylase (GAD) immunoreactive nerve terminals (labeled with ferritin) in symmetrical synaptic contact with TH immunopositive dendrites and somata (labeled with both ferritin and peroxidase) (Léránth et al., 1985a).

In summary, previous EM studies combining radioautography and immunocytochemistry revealed that a relationship exists between the TIDA cells and both serotonergic and GABAergic nerve terminals (Bosler et al., 1984; Bosler and Beaudet, 1985; Léránth et al., 1985a). Furthermore, both labeled (TH positive) and unlabeled axon terminals were shown to synapse on TH positive dendrites (van den Pol et al., 1984; Léránth et al., 1985b). These results, however, especially concerning the intrinsic TIDA neuronal organizational pattern are, as of yet, incomplete and much remains to be determined regarding the types of connections established by TIDA elements.

V- ONTOGENY OF THE TIDA SYSTEM

Although some information (reviewed in the previous section) is presently available concerning the ultrastructure of the adult rat TIDA system, nothing is known about its early development at the fine structural level. In studies using the Falck-Hillarp formaldehyde fluorescence technique, DA nerve cell bodies were detected in the arcuate nucleus of the full term rat fetus (20-22 days of gestation) (Hyyppä, 1969; Seiger and Olson, 1973). Both the number and fluorescence intensity of these cells subsequently increased to reach a maximum within the first three postnatal weeks (Hyyppä, 1969; Loizou, 1971b; 1972), followed by a subsequent plateauing to the adult pattern by the 5th postnatal week (Loizou, 1971b; 1972). Application of the immunocytochemical technique, which is more sensitive than the histofluorescence method for the demonstration of cell bodies (Hökfelt et al., 1984a), enabled LM detection of the TIDA neuronal cell bodies as early as embryonic day 14.5, TH being first detectable at embryonic day 12.5 (Specht et al., 1981a). The topography of the TIDA cells closely resembled that of the adult by embryonic day 18 (Specht et al., 1981b).

These results show that the TIDA system is present in the newborn rat. In addition, pharmacological evidence indicates that neonatal DA arcuate neurons, like those of the adult, can be depleted of their neurotransmitter by reserpine and catecholamine synthesis inhibitors (Loizou, 1969; 1971b; 1972), and that they can also take up the amine precursor L-DOPA (Loizou, 1971b). Thus the TIDA system appears to be in place and capable of some function at birth. The question remains, however, as to the morphologic maturity of the TIDA system in the neonate. Despite some

expression of mature biochemical and physiological function, the TIDA neonatal neurons may exhibit neither adult patterns of connections nor mature perikaryal morphology. Indeed, in an EM study of the neonatal arcuate nucleus, Walsh and Brawer (1979) demonstrated a paucity of synapses, most of which were immature, an abundance of growth cones, and a predominance of undifferentiated immature-looking nerve cell bodies. Consequently, as was previously suggested by Loizou (1971a; 1972), the biochemical and functional differentiation of the catecholamine-containing neurons of the newborn probably precedes their morphological differentiation. Thus the neuronal circuitry regulating TIDA function is probably not present at birth, and must develop during the postnatal period. EM analysis of TIDA cell bodies, processes and patterns of connections is clearly needed to resolve this question.

SPECIFIC OBJECTIVES

Over the past several years, the evolution of techniques such as radioautography, fluorescence histochemistry and immunocytochemistry contributed to the acquisition of an extensive amount of information on the topography of the adult TIDA system. Such information about the immature TIDA system, however, is sparse. Furthermore, relatively little is known concerning the fine structural patterns of connections of the adult TIDA neurons, and data about the ultrastructure of the TIDA system of neonatal or prepubertal rats is non-existent. Consequently, the main objectives of the present study were to analyze the topography and fine structural organizational pattern of the adult female rat TIDA system by means of the preembedding PAP immunocytochemical method, and to compare the resulting data with that obtained in neonatal, 15 day old and 30 day old animals.

The questions of sex specificity and the effects of gonadal steroids were also addressed. The topography and fine structure of the male TIDA system was studied and compared to that of the female. Furthermore, since TIDA neurons contain estradiol receptors, and in view of the reported alterations in TH activity following estradiol treatment, the effects of chronic estrogenization on the fine structure of the TIDA system in the adult female was examined.

MATERIALS AND METHODS

I- Animals

A) Housing

All animals were obtained from Charles River Canada Inc. (St-Constant, Quebec). Upon arrival, they were housed in plastic cages containing heat-treated Hardwood Laboratory Bedding ("Beta Chips"). Food (Purina Rat Chow) and water were given ad libitum. The room temperature was kept at 23°C and the relative humidity varied between 50 and 55%. The animal quarters were illuminated from 06:00 to 20:00h.

B) Adult Rats

1. Females

Six five week old female rats (2 Sprague-Dawley and 4 Wistar) were used in this study. As soon as vaginal openings were visible, normal cyclicity was verified on a day to day basis by examining vaginal smears. After 2 weeks of normal cycles, three rats (1 Sprague-Dawley and 2 Wistar) received a single subcutaneous injection of 2 mg estradiol valerate (EV) in 0.2 ml vehicle (sesame oil). This treatment causes a permanent arrest of ovulatory cyclicity as was later indicated by persistent vaginal cornification. The remaining animals (1 Sprague-Dawley and 2 Wistar), which served as controls, were sesame oil injected and kept cycling normally up to the time of perfusion. All animals were killed by intra-aortic arch perfusion between 6 and 6 1/2 months of age.

2. Males

Three adult Wistar male rats, each weighing about 335 g, were killed by intra-aortic arch perfusion.

C) Pubertal Animals

Three female Wistar rats, received at 25 days of age, were perfused 5 days later, that is, at 30 days of age.

D) Prepubertal Animals and Neonates

Three pregnant Wistar female rats were housed in individual cages. The second day following parturition, 3 female pups were taken from 2 different litters and perfused. The neonatal females were distinguished on the basis of a shorter anogenital distance than that seen in male littermates. The pups that were not selected were left to age for 15 days, at which time 3 female pups, from 2 different litters, were taken for perfusion.

II- Perfusion Procedures

A) Preparation of the Fixative

Immunocytochemical studies require a compromise between good tissue preservation and retention of sufficient antigenicity to allow for the visualization of the antigenic sites since formaldehyde and/or glutaraldehyde, which are required for the preservation of cellular morphology (Ellar et al., 1971), impair tissue antigenicity. The extent of this impairment varies with the nature of the antigen (Pickel, 1982). In the case of tyrosine hydroxylase, a good balance between the preservation of tissue

morphology and immunoreactivity was obtained with a perfusing medium containing 4% paraformaldehyde and 0.2% glutaraldehyde in 0.1M phosphate buffer at pH 7.2 (Pickel, 1982). Furthermore, it has recently been suggested that the addition of picric acid in the aldehyde fixative improves immunostaining by preserving immunogenicity (Somogyi and Takagi, 1982). It has also been reported (van den Pol et al., 1984) that, in the case of tyrosine hydroxylase as the tissue antigen, immunostaining was still present with concentrations of glutaraldehyde up to 0.5%. Consequently, in order to maximize tissue preservation without sacrificing immunostaining, a solution containing a mixture of 4% paraformaldehyde, 0.5% glutaraldehyde and 0.1% picric acid in 0.1M Sorensen buffer, was used (modified from Pickel, 1982). The temperature of the fixative was always kept between 15 and 20°C.

B) Perfusing Adult and Pubertal Animals

Three brains from adult and three others from 30 day old rats were fixed by intra-aortic arch perfusion. Each animal was anesthetized by an intraperitoneal (i.p.) injection of sodium pentobarbital (0.12 cc/100 g body weight) in the left inferior abdominal quadrant. Once in deep anesthesia, CO_2 was given through a nose cone for a few seconds in order to produce vasodilation. The skin and muscle layers were then cut, the descending aorta clamped, and the thoracic cage opened and retracted with a hemostat. To avoid brain cell damage due to anoxia, the following steps had to be performed within 30 seconds of the thoracic cage opening: 1) free the heart from the pericardium 2) cut the apex of the heart 3) insert the cannula (connected to the rubber tubing leading to the pump delivering the fixative) into the left ventricle, and through the aortic valve into the origin of the aorta 4) clamp the aortic cannula in place 5) activate the pump. An

Advanced Varistaltic Pump (Fisher) was used. The pumping action consisted of a peristaltic effect produced by 2 rollers pressing a flexible tube against a horse-shoe shaped housing. The flow rate was set at 150 ml/min. for the first 2 minutes of the perfusion but was then decreased so that each animal received about 750 ml of fixative over a 10-minute interval.

C) Prepubertal Animals

The brains of three 15 day old rats were fixed by whole body gravity perfusion during which 100 ml of fixative was delivered (from a bottle hanging between 170 and 180 cm above the ground) over a 20 minute time interval. Animals were anesthetized by an i.p. injection of 0.05 to 0.08 ml of sodium pentobarbital in the left inferior abdominal quadrant. The rats were opened as described above but did not previously receive CO_2. Within 30 seconds of the rib cage opening, an 18 gage needle (with a dulled tip) was pushed through the left side of the heart into the left ventricle and the fixative flow was started.

D) Neonates

The perfusion procedure for three 2 day old rats was similar to that described for the 15 day old animals with the exception of the amount of fixative delivered per animal (50 ml during a 20 minute time interval), and the type of needle used (20 gage).

-III- Tissue Preparation

A) Adult and Pubertal Rats

Immediately after perfusion, brains were removed and the hypothalami were dissected out. Each block of hypothalamus was trimmed in the shape of a truncated pyramid by making four cuts : a rostral cut, just behind the optic chiasm; a caudal cut, just in front of the mamillary bodies; and two lateral cuts, each approximately 2.5 mm away from the third ventricle. The top of the pyramid contained part of the rostral hypothalamus while its base contained part of the caudal hypothalamus. The blocks were immersed in fresh fixative for not more than one hour at room temperature, after which time each block was glued on a glass stage secured to a Vibratome (Oxford), and immersed in cold ($4^{\circ}C$) phosphate buffer 0.1M. Coronal sections (about 30 µm thick) of the whole hypothalamic arcuate nucleus, from the optic chiasm/suprachiasmatic nucleus region to the mamillary bodies, were cut and placed in the wells of Porcelain Spot Test Plates (A.H. Thomas Co., Philadelphia, Pennsylvania) containing phosphate buffer 0.1M at room temperature. The sections were transferred to the wells individually with a small artist paint-brush. The immunocytochemical staining was done as soon as all the sections had been collected.

B) Prepubertal Rats

Following whole body perfusion, the brain of each 15 day old rat was taken out and put in fresh fixative at room temperature for 15 minutes. The hypothalamus was then dissected out (by the same method employed for adult and pubertal rats) and left in fixative for an additional 45 minutes. Before the hypothalamic blocks were prepared for Vibratome sectioning (see

previous section for description), they were put in cold (4°C) paraformaldehyde (4%) for a period of 2-4 hours. Coronal sections (about 30 µm thick) of the whole arcuate nucleus region were then cut and placed in phosphate buffer 0.1M at room temperature. The immunocytochemical staining was done as soon as all the sections had been collected.

C) Neonates

Tissue preparation for the neonates was similar to that described above for the 15 day old rats with 2 exceptions: 1) following whole body perfusion, the entire head of each neonate was put in fresh fixative for 15 minutes before the dissection of the hypothalamus 2) Vibratome sections were 50 µm in thickness instead of the usual 30 µm.

IV- Source of Antiserum

The antibody to tyrosine hydroxylase (TH) was obtained from Dr. Tong Hyub Joh (Laboratory of Neurobiology, Department of Neurology, Cornell University Medical College, New York, N.Y.). The TH antibody was produced in a rabbit using the enzyme from bovine adrenal medulla that was partially purified by ammonium sulfate precipitation and Sephadex G-200 column chromatography. For details on enzyme purification and antibody production, see Joh et al. (1973) and Joh and Ross (1983).

V- Immunocytochemical Staining

A) Specificity

Two requirements must be satisfied before any immunocytochemical staining is said to be specific: 1) method specificity and 2) antibody specificity (Petrusz et al., 1976). Method specificity requires that the staining be due exclusively to an interaction between the antibodies of the antiserum and the tissue antigen. Antibody specificity implies that there is no staining when the antibodies are blocked by the specific antigen prior to exposure to the tissue antigen.

B) Method Specificity

To determine method specificity, the specific antiserum is replaced by antibody-free serum in order to see if the specific labeling is removed (Sternberger, 1974; Petrusz et al., 1976; Pickel, 1981; Pickel, 1982). The "antibody-free" serum consists of the specific antiserum adsorbed by an excess of purified antigen or of serum taken from the host before immunization (Pickel, 1982). Within the rat hypothalamic arcuate nucleus, method specificity was tested by Pickel et al. (1975). These authors used two types of controls: in the first one, preimmune serum was substituted for immune serum. In the second control, the specific TH antibody was adsorbed with pure antigen, the antigen-antibody complex removed by centrifugation, and the antibody free supernatant was substituted for the specific antibody. There was no specific staining in any of the control sections.

C) Specificity of the Antibody

There are two ways of testing the antiserum specificity: 1) by performing immunoelectrophoresis or double immunodiffusion, which should result in a single precipitant arc between the purified antigen and the specific antiserum, or 2) by using the specific antiserum to inhibit the antigen activity (Joh et al. 1973; Pickel, 1981; 1982). Joh et al. (1973) found that the enzyme specificity of the TH antibody was high, since a single precipitin arc was seen when immunoelectrophoresis was performed on the antibody with either purified bovine-adrenal TH, or with a crude extract of the gland. Moreover, no precipitin arc formed when this same antibody was run against dopamine-β-hydroxylase, aromatic L-aminoacid decarboxylase, and phenylethanolamine-N-methyltransferase, the other enzymes of the catecholaminergic synthetic pathway. In addition, TH activity from both purified and crude bovine adrenal extract was inhibited almost 100% by the antibody, whereas this same antibody failed to inhibit the activities of the other enzymes of the catecholaminergic synthetic pathway. Joh et al. (1973) also reported that this TH antibody was highly cross-reactive with TH from rat adrenal gland, superior cervical ganglion and, most significantly for the present study, brain.

VI- Immunocytochemical Procedures

All sections were immunostained using the unlabeled antibody peroxidase-antiperoxidase (PAP) method of Sternberger (1979b). The protocol we used is a modification of that described by Pickel (1981): the Vibratome sections were first submitted to two 15 minute rinses with Tris-saline containing 0.1M lysine. Lysine, which was not included in the original

protocol, was used here since it may bind to the free aldehyde groups of the fixative (Oertel et al., 1982; Hodges et al., 1984) and thus contribute in reducing the background staining. Tris-saline was prepared by adding 4.5 g NaCl to 500 ml Tris-water. Tris-water was made by the addition of concentrated HCl to a 0.5M solution of Trizma base until a pH of 7.6 was obtained. In the original protocol (Pickel, 1981), the sections were next exposed to the detergent Triton X-100. This detergent, which dissolves membranes, enhances the penetration of the antibody but is deleterious to the tissue morphology (Pickel, 1982). Sections were, therefore, not exposed to the detergent. In order to block unspecific antigenic sites (Oertel et al., 1982), the sections were then incubated for 30 minutes in normal goat serum (n.g.s.) diluted 1:30 with Tris-saline. This incubation was followed by two 8 minute rinses with Tris-saline. The sections were then incubated overnight at 4°C with the TH antibody diluted 1:750 with Tris-saline containing 1% n.g.s.. During the overnight incubation, the sections were constantly agitated as they were for all steps involving an antibody in the procedure.

The following morning, the sections were rinsed twice, 8 minutes each time, with Tris-saline containing 1% n.g.s., and incubated for 30 minutes with a goat anti-rabbit immunoglobulin diluted 1:50 with Tris-saline containing 1% n.g.s.. This was followed by two 8 minute rinses with Tris-saline containing 1% n.g.s. and a 30 minute incubation with the peroxidase-antiperoxidase (PAP) complex (Cedarlane Laboratories Ltd.) diluted 1:50 with Tris-saline containing 1% n.g.s.. Although in the original protocol, a 1:10 dilution of the anti-IgG and a 1:30 dilution of the PAP were used, dilutions as high as 1:50 and 1:100, respectively, do not appreciably alter immunostaining (Pickel, 1981). The sections were then submitted to two 8

minute rinses with Tris-saline alone, incubated 10 minutes with $CoCl_2$ 0.5% in Tris-saline and rinsed twice (8 minutes) with Tris-saline. The $CoCl_2$ step is not found in Pickel's methodology but is used here because it enhanced the electron density of the immunoprecipitate, permitting an improved visualization with the electron microscope (Adams, 1977; Silverman, 1983). Finally, the sections were reacted (in the dark) for 6 minutes with 0.05% 3-3' diaminobenzidine and 0.01% hydrogen peroxide in Tris-buffer, rapidly rinsed in distilled water and transferred in phosphate buffer 0.1M. Higher concentrations of diaminobenzidine (0.05% vs 0.013%) and hydrogen peroxide (0.01% vs 0.003%) were used than those in the original protocol (Pickel, 1981).

VII- Tissue Processing for Light and Electron Microscopic Observations

Immediately after the immunocytochemical staining, some sections were processed for electron microscopy in the following manner: one out of every four sections cut along the rostro-caudal axis of the mid-portion of the arcuate nucleus was selected and post-fixed for one hour in a 2% solution of osmium tetroxide. The sections were then stained with uranyl acetate for one hour and dehydrated in a graded series of ethanols. Each section was then cut in half with a scalpel blade under the dissecting microscope. A drop of fresh epon was put on a plastic coverslip, one half-section was deposited on the drop, covered by another drop, and a second coverslip was placed on top, forming a "sandwich". The "sandwiches" were put in the oven at $60^{\circ}C$ for 16-17 hours. Once the epon had polymerized, they were taken out of the oven and trimmed with a pair of scissors in order to fit at the

bottom of Beem capsules. The "sandwiches" were then reembedded in the capsules which were filled with epon and put in the oven at 60°C for 16-17 hours. Once out of the oven, the epon blocks were trimmed in the shape of a truncated pyramid (the base of which was lined up with the edge of the third ventricle) including mainly the arcuate nucleus region, and the top cover slip of the sandwich was carefully removed with a razor blade. Thin ultramicrotome sections (silver) were then cut from the epon blocks, put on Formvar-coated grids and stained with lead citrate for 2 1/2 minutes. Sections suitable for ultrastructural study must be selected with care. Indeed, the heavy labeling of the first few sections makes it difficult to identify underlying structures and sections deeper than 1 µm from the surface have very faint labeling due to the limited penetration of the antibody.

For light microscopy, the sections (not selected for electron microscopy) including those of rostral and caudal arcuate nucleus, were exposed to osmium tetroxide vapors for about 1/2 hour, in order to increase the staining intensity of the reaction product. These sections were then placed directly on gelatin-coated glass slides (three sections per slide), and dried at 37°C overnight. The following morning, they were dehydrated in a graded series of ethanols and mounted with permount.

VIII- Light and Electron Microscopy

The immunocytochemically stained sections (mounted on slides) from 3 intact adult males and from both control and EV-treated females (3 per age group) were examined with a Wild light microscope and photographed in

series, or mapped using a camera lucida that could be adapted to the microscope.

The sections embedded in epon for electron microscopy were also examined under the light microscope before the blocks were trimmed for thin sectionning. The shape of the trimmed blocks could then be outlined on the camera lucida drawings. Using a Siemens 101 Electron Microscope, coronal sections from the mid-arcuate nucleus region of neonatal, 15 day old, 30 day old, control adult and EV-treated adult female rats, as well as of adult male rats, were scanned. The number of sections examined in individual animals and the number of blocks cut to obtain these sections are shown in Table I. Each section examined was scanned entirely, and pictures of every TH positive element encountered were taken. The resulting electronmicrographs were then analyzed.

TABLE I: NUMBER AND SOURCE OF SECTIONS EXAMINED AT THE ULTRASTRUCTURAL LEVEL

Strain	Animals	#Blocks Cut	#Sections Examined
S.D.	CI	3	3
W	CII	1	12
W	CIII	2	3
S.D.	EVI	3	3
W	EVII	2	3
W	EVIII	2	4
W	C1	2	4
W	C2	1	3
W	C3	1	4
W	D1-1	2	4
W	D1-2	2	6
W	D1-3	3	8
W	D15-1	1	4
W	D15-2	1	2
W	D15-3	1	2
W	D30-1	1	3
W	D30-2	1	2
W	D30-3	1	3

Legend:

S.D.= Sprague-Dawley; W= Wistar; C= control adults (CI-III= normally cycling females and C1-3= intact males); EV= EV-treated females; D1= neonatal females; D15= 15 day old females; D30= 30 day old females.

RESULTS

I- THE ADULT TIDA SYSTEM

A. Light Microscopic Observations

a) Normally Cycling Females

According to the description of Walsh and Brawer (1979), five levels of the arcuate nucleus may be easily identified : 1) level A or the mid-anterior arcuate region, where the nucleus consists of a single cell mass just below the floor of the third ventricle 2) level B which is approximately midway between level A and the point at which the ventricular floor expands to form the lateral recesses (at this and the following levels, two distinct arcuate nuclei are seen, one on either side of the third ventricle) 3) level C or the middle portion of the ventricular expansion region 4) level D where the pituitary stalk originates 5) level E or posterior arcuate region, which is just behind the pituitary stalk's posterior attachment point.

Levels B to E of the adult arcuate nucleus of 3 normally cycling female rats were examined (Plate 1a-g). As was previously reported (Hökfelt et al., 1976; 1984b; Chan-Palay et al., 1984; van den Pol et al., 1984), TH positive nerve cell bodies were found both in the dorso-medial and lateral regions of the nucleus in all animals. These immunoreactive cells, at level B (Plate 1a), were distributed on either side of a slightly convex imaginary line connecting the medio-dorsal and the ventro-lateral arcuate areas. Level C (Plate 1b-d) was characterized by numerous TH posi-

tive perikarya in the medio-dorsal arcuate region, immediately next to the third ventricle. Most of the remaining immunoreactive cells were scattered within the lateral region of the nucleus, appearing almost as a distinct ventro-lateral cell cluster. The most ventral TH positive cells of the ventro-lateral arcuate region usually stained less intensely than those more dorsally. Furthermore, a few slightly immunoreactive cells extended beyond the arcuate region, laterally, just above the ventral surface of the diencephalon. Pale staining perikarya were also found throughout the arcuate nucleus. The distinct ventro-lateral cluster seen at level C was no longer present at level D (Plate 1e-f), where numerous labeled nerve cell bodies were distributed in an apparently random manner through the nucleus. At level E (Plate 1g), the arcuate nucleus contained only a few scattered labeled perikarya.

In addition to labeled nerve cell bodies, a complex network of immunoreactive processes, some of which could be seen to originate from TH positive perikarya, and small punctate elements, were present at all levels of the arcuate nucleus (Fig. 1). The punctate elements were particularly numerous in the external layer of the median eminence. Furthermore, both the immunolabeled processes and punctate elements extended into the ependymal layer of the ventricular wall.

b) EV-treated Females

In each of the 3 EV-treated female rats, both the immunocytochemical labeling patterns and numbers of labeled cells within the arcuate nucleus were similar to those of the normally cycling animals (Plate 2a-d). The medio-dorsal cluster of the mid-portion of the nucleus (level C) was more distinct in the EV-treated than in the control animals (compare Plates 2b-c

and 1b-d). Furthermore, the arcuate ventro-lateral cell cluster (of level C) could not be easily delineated in control animals whereas in EV-treated rats, a distinct ventro-lateral aggregation of immunoreactive perikarya was clearly separated from the obvious medio-dorsal cluster.

c) Intact Males

No obvious difference was seen between the distributional pattern of the male and female TH positive perikarya, processes, and punctate elements. In each of the 3 male rats examined, however, the medio-dorsal and ventro-lateral clusters seen at level C were not as distinct (Plate 3d-e) as they were in the females (both control and EV-treated). Furthermore, under our experimental conditions, the staining intensity of the immunoreactive nerve cell bodies and processes of the male arcuate nucleus appeared to be significantly less than that of the females.

B. Electron Microscopic Observations

a) Normally Cycling Female Rats

1. Perikarya

Twenty-two TH positive perikarya from control female rats were examined. These polygonal or ovoid nerve cell bodies were small, averaging approximately 8 µm in short diameter and 12 µm in long diameter. In most cases, each immunoreactive cell profile was occupied by a large indented nucleus containing, in some fortuitous sections, a large nucleolus. The rest of the cell exhibited a scant peripheral cytoplasm containing numerous mitochondria, randomly scattered short cisternae of endoplasmic reticulum, and one to several small Golgi apparatus (Fig. 2). Lysosomes (membrane-bound accumulations of dark homogeneous dense material) were also present in

many neuronal cell bodies in significant numbers. A single perikaryal profile could contain from one up to 15 lysosomes. On the other hand, multivesicular bodies (membrane-bound clusters of small vesicles) were only occasionally encountered, and no more than 3 multivesicular bodies were seen in any single perikaryon. The granulated black immunoprecipitate appeared relatively uniformly distributed throughout the cytoplasm. It was not associated with any particular organelle but appeared to accumulate mostly on membranous surfaces (Fig. 2).

The TH immunoreactive nerve cell bodies were extensively ensheathed by glial lamellae directly applied to the neuronal plasmalemma. Where the glial sheath was interrupted, labeled and unlabeled axon terminals and/or TH positive dendrites (but not TH negative dendrites) abutted the plasmalemma (Fig. 2). One instance of somato-somatic apposition was also observed. In this case, the plasmalemmas of a TH positive and a TH negative perikaryon were in direct apposition for some distance.

The morphological characteristics of most unlabeled perikarya were similar to those of labeled cell bodies. The absence of black immunoprecipitate within unlabeled perikarya allowed for visualization of ribosomes that were associated with the cisternae of endoplasmic reticulum (rER), as well as scattered throughout the cytoplasm.

2. Dendrites

The large majority of the immunoreactive processes observed were dendritic profiles. These were easily identified on the basis of shape, size, and internal framework of regularly spaced microtubules. The latter were seen in linear array in longitudinally sectioned profiles (Fig. 3) and appeared as small evenly distributed circles in transversely cut profiles

(Fig. 4). Axon terminals often were seen in synaptic contact with immunoreactive dendrites (Figs. 3 and 5). Mitochondria were frequently encountered within these dendrites. In addition, short, often distended, cisternae of endoplasmic reticulum, and occasional multivesicular bodies similar to those found in labeled perikarya, also occurred within dendrites.

The cytoplasm of TH positive dendrites contained a black immunoprecipitate which preferentially accumulated below the inner leaflet of the dendritic plasmalemma, around the outer mitochondrial and endoplasmic reticular membranes, as well as around the microtubules. Thus, as in the case of perikarya, the immunoprecipitate in dendrites was most densely distributed at membranous, filamentous or microtubular surfaces.

TH positive dendrites abutted on labeled and unlabeled perikarya, other dendrites, axon terminals and tanycytes. Table II summarizes the number of each of these relationships observed in normally cycling female rats. The most common type of relationship encountered in our material involved unlabeled axon terminals which formed predominantly asymmetrical axo-dendritic synapses with labeled dendritic profiles (Fig. 5). These axon terminals were filled with small round vesicles of homogeneous content. At the point of contact, vesicles formed an obvious cluster and membrane specializations could be seen. In contrast, labeled nerve terminals were never seen in contact with labeled dendrites.

The next most frequently encountered relationship consisted of direct appositions involving labeled dendritic profiles and tanycytic processes. However, in contrast to the axo-dendritic synapse, neither vesicles nor membrane specializations were present at the contact point. Numerous TH positive dendritic profiles were frequently encountered along the length of a single tanycytic process (Fig. 6). Favorable planes of section clearly

TABLE II: TYPES OF RELATIONSHIPS OBSERVED BETWEEN TH POSITIVE DENDRITES AND OTHER ELEMENTS OF THE ARCUATE NEUROPIL OF NORMALLY CYCLING FEMALES

	Animals			
	CI	CII	CIII	Total
Total #TH+ dendrites observed :	237	106	424	767
#axo(TH-)dendritic(TH+)synapses :	26 (11%)*	12 (11%)	93 (22%)	131 (17%)
#TH+ dendrites apposed to:				
Tanycytic processes :	26 (11%)	9 (8%)	28 (7%)	63 (8%)
TH+ dendrites :	6 (3%)	6 (6%)	12 (3%)	24 (3%)
TH- dendrites :	7 (3%)	1 (1%)	9 (2%)	17 (2%)
TH+ perikarya :	3 (1%)	2 (2%)	1 (.2%)	6 (1%)
TH- perikarya :	4 (2%)	1 (1%)	0 (0%)	5 (1%)

* % = $\frac{\text{\#TH+ dendrites involved in a given type of contact}}{\text{Total number of TH+ dendrites observed}}$

demonstrated thin sheets and processes emerging from tanycytic processes, and partially or completely enveloping TH positive dendritic profiles.

Immunolabeled dendrites were also seen in direct apposition to other dendrites, both labeled and unlabeled, as well as to both labeled and unlabeled perikarya. As in the case of dendro-tanycytic appositions, no vesicle nor membrane specializations occurred at the contact points. Although less common than axo-dendritic synapses or even dendro-tanycytic appositions (Table II), dendro-dendritic and dendro-somatic appositions occurred fairly often. The size range of the dendritic profiles examined indicated that these dendro-dendritic appositions occur mainly between dendritic shafts. There were fewer TH positive dendrites in direct apposition to unlabeled dendrites (Fig. 7) than to labeled dendrites (Fig. 8). On the other hand, TH positive dendrites contacted both labeled (Fig. 9) and unlabeled (Fig. 10) perikarya in more or less equal proportions. The contact sites of these dendro-somatic appositions were also devoid of vesicular clusters or membrane specializations.

Even though TH positive dendrites directly apposed both labeled and unlabeled perikarya, unlabeled dendrites were never seen in direct apposition to labeled nerve cell bodies. In contrast, TH positive and TH negative dendrites both came in direct apposition to unlabeled nerve cell bodies in roughly equal proportions. The examination of 52 unlabeled perikaryal profiles revealed 5 TH positive and 5 TH negative dendrites involved in dendro-somatic appositions.

As in the case of TH positive perikarya, labeled dendrites throughout the arcuate neuropil were encapsulated over much of their surface by glial sheaths. These sheaths were often multilamellar, consisting of concentric gyres in close apposition. Although these sheaths appeared similar to the

astrocytic sheaths found throughout the central nervous system, some undoubtedly originate from tanycytic processes as described above. Such thin glial sheaths, whether astrocytic or tanycytic in origin, were occasionally intercalated between a labeled dendrite and an identified tanycytic process. Similarly, a thin glial leaflet was occasionally seen intercalated between an immunoreactive dendrite and a nerve cell body (Fig. 11).

3. Axon Terminals

In our material, TH positive terminals were filled with round, densely packed, clear vesicles of somewhat variable size, surrounded by the immunoprecipitate. A few large dense core vesicles were sometimes present, as well as mitochondria and profiles of smooth endoplasmic reticulum (Fig. 12).

Only 27 immunoreactive axon terminals were observed, and these were mostly located in the lateral arcuate region. Table III shows the different types of contacts established by these terminals within the arcuate neuropil. Labeled nerve terminals were most commonly found in direct apposition to unlabeled dendritic profiles (Fig. 12). In contrast to synaptic contacts, membrane specializations and vesicular clusters at these points of contact were rare. In fact, only one instance of such a synaptic specialization occurred, involving one labeled axon terminal and one unlabeled dendrite (Fig. 13a).

Labeled axon terminals were also often seen directly apposed to both unlabeled axon terminals (Fig. 13b) and tanycytic processes (Fig. 13c), but they never contacted TH positive dendrites or other labeled terminals. Although they occasionally came in direct apposition to both labeled and unlabeled perikarya (Fig. 13d,e), labeled axon terminals never formed synap-

TABLE III: TYPES OF RELATIONSHIPS SEEN BETWEEN LABELED AXON TERMINALS AND OTHER ELEMENTS OF THE ARCUATE NEUROPIL OF NORMALLY CYCLING FEMALES

	Animals			
	CI	CII	CIII	Total
Total #TH+ terminals observed :	7	9	11	27
#TH+ terminals apposed to:				
TH- dendrites :	1 (14%)*	3 (33%)	3 (27%)	7 (26%)
TH- axon terminals :	2 (29%)	2 (22%)	1 (9%)	5 (19%)
Tanycytic processes :	1 (14%)	1 (11%)	2 (18%)	4 (15%)
TH+ perikarya :	2 (29%)	0 (0%)	0 (0%)	2 (7%)
TH- perikarya :	0 (0%)	0 (0%)	1 (9%)	1 (4%)
#axo(TH+)dendritic(TH-)synapses:	0 (0%)	1 (11%)	0 (0%)	1 (4%)

* $\% = \frac{\#\text{TH+ dendrites involved in a given type of contact}}{\text{Total number of TH+ dendrites observed}}$

tic relationships with these nerve cell bodies. Thus, they differ from unlabeled axon terminals which were commonly observed directly apposed to, or even synapsing on, both labeled and unlabeled perikarya (Figs. 2 and 14; Table IV).

b) EV-treated Females

1. Perikarya

The ultrastructural features of the 27 TH positive nerve cell bodies examined in the EV-treated female rats were indistinguishable from those described in normal controls (Fig. 2). TH immunoreactive perikarya were partially ensheathed by glial lamellae and contacted by various elements of the neuropil at points where the sheath was absent, as will be described below. However, no somato-somatic apposition such as the one seen in control animals was encountered.

2. Dendrites

Most of the immunoreactive processes observed in the EV-treated female rats were dendrites. These formed a variety of relationships with other elements in the neuropil as shown in Table V. As in normal females, the most common type of connection observed was the axo-dendritic asymmetrical synapse involving unlabeled axon terminals and TH positive dendritic profiles. Such axo-dendritic synapses never occurred between labeled axon terminals and labeled dendrites.

Although the other types of relationships previously described in the normal female rat also occurred in EV-treated animals, the relative proportions of each type of contact differed slightly (compare Tables II and V). For instance, while the second most common type of relationship was the

TABLE IV: NUMBER OF AXO-SOMATIC APPOSITIONS AND SYNAPSES INVOLVING UNLABELED AXON TERMINALS AND BOTH LABELED AND UNLABELED PERIKARYA OF NORMALLY CYCLING FEMALES

	Animals			
	CI	CII	CIII	Total
# TH+ perikarya observed :	4	7	11	22
#axo(TH-)somatic(TH+) appositions:	7	17	32	56
#axo(TH-)somatic(TH+) synapses :	1	5	22	28
# TH- perikarya observed :	9	6	37	52
#axo(TH-)somatic(TH-)appositions :	4	8	10	22
#axo(TH-)somatic(TH-)synapses :	3	3	9	15

TABLE V: TYPES OF RELATIONSHIPS OBSERVED BETWEEN TH POSITIVE DENDRITES AND OTHER ELEMENTS OF THE ARCUATE NEUROPIL IN EV-TREATED FEMALES

	Animals			
	EVI	EVII	EVIII	Total
Total #TH+ dendrites observed :	58	111	59	228
#axo(TH-)dendritic(TH+)synapses :	8 (14%)*	17 (15%)	4 (7%)	29 (13%)
#TH+ dendrites apposed to:				
Tanycytic processes :	3 (5%)	5 (5%)	3 (5%)	11 (5%)
TH+ dendrites :	0 (0%)	7 (6%)	4 (7%)	11 (5%)
TH- dendrites :	0 (0%)	5 (5%)	6 (10%)	11 (5%)
TH+ perikarya :	7 (12%)	7 (6%)	4 (7%)	18 (8%)
TH- perikarya :	2 (3%)	0 (0%)	0 (0%)	2 (1%)

* % = #TH+ dendrites involved in a given type of contact / Total number of TH+ dendrites observed

dendro-tanycytic apposition in normally cycling females, it was the dendro-somatic apposition involving two labeled elements in the EV-treated animals. Consequently, in the EV-treated females, the dendro-tanycytic appositions were third in frequency of occurrence, being ex equo with the dendro-dendritic apposition. In EV-treated rats, but not in controls (Table II), there were as many TH positive dendrites directly apposed to unlabeled dendrites as to labeled dendrites. The small proportion of dendro-somatic appositions involving labeled dendrites and unlabeled perikarya was the same in EV-treated and control animals. The greatest difference between the EV-treated and control groups occurred in the number of dendro-somatic appositions involving labeled dendrites and labeled perikarya. The percentage of these appositions was markedly higher in EV-treated animals than in controls (Tables II and V).

Finally, although TH negative dendrites never came in direct apposition to labeled nerve cell bodies in control animals, unlabeled dendrites closely apposed to both labeled (in 2 instances) and unlabeled perikarya (in one instance) have been seen in the EV-treated animals.

3. Axon Terminals

Only 8 immunoreactive axon terminals were observed, two of which were seen in synaptic contact with unlabeled nerve cell bodies, and one with an unlabeled dendrite. Three labeled terminals were apposed to TH negative dendrites, and one to a tanycytic process. The remaining terminal was simply surrounded by glia. Labeled axon terminals were never seen synapsing on, or even coming in close apposition to, TH positive perikarya.

c) Intact Males

1. Perikarya

The ultrastructural features of the 20 immunoreactive perikarya observed in intact male rats were similar to those described in the female. The male arcuate nucleus, however, contained slightly smaller nerve cell bodies, averaging about 7 μm in short diameter and 11 μm in long diameter. At points where there was no glial sheath adjacent to the perikarya, various elements of the neuropil contacted the cells (Fig. 15). Note that no somato-somatic apposition, such as the one seen in control females, was encountered in the males.

2. Dendrites

As in the case of the female, the majority of TH positive processes within the intact male arcuate nucleus consisted of dendritic profiles, most of which were contacted by unlabeled axon terminals, predominantly forming asymmetrical synapses (Table VI). As in the normally cycling female, the second most common type of contact was the dendro-tanycytic apposition, followed by appositions involving either 2 labeled dendrites, or one labeled and one unlabeled dendrite. Appositions involving labeled dendrites and both labeled and unlabeled nerve cell bodies occurred in equal proportions in the male and in the normally cycling female. However, unlabeled dendrites were seen directly apposed to labeled perikarya (in two instances) in the male rat whereas such relationship was not found in the normally cycling female. Such appositions were also present in EV-treated females.

The examination of 24 unlabeled perikaryal profiles also revealed the presence of 2 dendro-somatic appositions involving TH positive den-

TABLE VI: TYPES OF RELATIONSHIPS OBSERVED BETWEEN TH POSITIVE DENDRITES AND OTHER ELEMENTS OF THE INTACT MALE ARCUATE NEUROPIL

	Animals			
	C1	C2	C3	Total
Total #TH+ dendrites observed :	261	152	74	487
#axo(TH-)dendritic(TH+)synapses :	69 (26%)*	24 (16%)	24 (32%)	117 (24%)
#TH+ dendrites apposed to:				
Tanycytic processes :	20 (8%)	11 (7%)	8 (11%)	39 (8%)
TH+ dendrites :	13 (5%)	4 (3%)	2 (3%)	19 (4%)
TH- dendrites :	11 (4%)	3 (2%)	4 (5%)	18 (4%)
TH+ perikarya :	1 (.4%)	0 (0%)	1 (1%)	2 (.4%)
TH- perikarya :	1 (.4%)	1 (.7%)	0 (0%)	2 (.4%)
TH+ axon terminals :	0 (0%)	3 (2%)	0 (0%)	3 (1%)

* $\% = \frac{\text{\#TH+ dendrites involved in a given type of contact}}{\text{Total number of TH+ dendrites observed}}$

drites. TH negative dendrites, however, were not seen contacting unlabeled nerve cell bodies.

As in all other groups, dendritic appositions in the male generally lacked any specializations. However, there was one instance of a dendro-dendritic apposition, involving 2 labeled elements, where prominent membrane specializations were present at the contact site, although vesicles were absent (Fig. 16). Finally, 3 of the TH positive dendrites were in direct apposition to a labeled axon terminal. Such appositions were never encountered in normally cycling nor EV-treated females.

3. Axon Terminals

A total of 30 labeled axon terminals, which were morphologically similar to those encountered in the adult female, were observed. Nine of these terminals were directly apposed to unlabeled dendrites, 6 to tanycytic processes, 3 to labeled dendrites, and one synapsed on a TH positive dendrite. The remainder of the observed terminals were surrounded by glia.

II- ONTOGENY OF THE TIDA SYSTEM

A. Light Microscopic Observations

a) Neonatal Females

Levels A through D of the female neonatal arcuate nucleus were examined (Plate 4a-e). At all levels, the labeled neurons were morphologically similar to adult arcuate neurons as demonstrated by Golgi studies (van den Pol and Cassidy, 1982), showing one to several dendritic processes

emerging from a fusiform nerve cell body. At level A (Plate 4a), immunoreactive nerve cell bodies and processes were seen directly beneath the ventricular floor. These labeled cells and processes extended extensively beyond the arcuate nucleus area, laterally, just above the ventral surface of the hypothalamus. At level B (Plate 4b), the TH positive perikarya and processes were mostly located in the ventro-lateral region of the arcuate nucleus, on either side of the third ventricle. These labeled elements again extended beyond the arcuate nucleus, laterally, just above the ventral hypothalamus. Lightly stained perikarya and processes, however, were also occasionally encountered in the medio-dorsal arcuate region. At levels C and D (Plate 4c-e), the distributional pattern of labeled cells and processes resembled that of the adult with 2 exceptions: the small number of TH positive perikarya and processes present in the medio-dorsal portion of the nucleus, and the abundance of immunoreactive neurons in the ventro-lateral region extending laterally, just above the ventral surface of the hypothalamus. TH positive perikarya occasionally occurred within the median eminence (Plate 4c).

The small TH positive punctate elements seen in the adult were very scarce within the neonatal arcuate nucleus. However, the external layer of the median eminence contained numerous labeled punctate elements.

b) 15 Day Old Females

Levels A to E of the arcuate nucleus of 15 day old female rats were examined (Plate 5a-f). At level A (Plate 5a), a few immunoreactive nerve cell bodies and processes were present directly beneath the third ventricle and more laterally, just above the ventral surface of the diencephalon. At level B, the distribution of the TH positive nerve cells and processes of

the 15 day old female rat appeared intermediate between the adult and neonatal patterns (Plate 5b): the medio-dorsal cluster of labeled cells (seen in the adult) was present, but there was also an abundance of labeled cells in the ventro-lateral arcuate nucleus and laterally, just above the ventral hypothalamic border as seen in the neonatal animal. However, the TH positive cells of the medio-dorsal cluster generally stained more intensely than the immunoreactive cells of the ventro-lateral arcuate or lateral hypothalamic areas.

At level C (Plate 5c-e), prominent dark staining medio-dorsal and ventro-lateral clusters were present, together with numerous pale staining cells in the ventral most lateral arcuate regions as well as laterally, just above the ventral hypothalamic surface. Although level D (Plate 5f) resembled level C, it contained progressively fewer labeled cells within both the arcuate and lateral diencephalic regions, and immunoreactive cells became increasingly scattered throughout the arcuate nucleus. At level E (not illustrated), the arcuate nucleus contained very few dispersed immunoreactive perikarya.

c) 30 Day Old Females

The distributional pattern of the TH positive perikarya, processes, and punctate elements within the antero-posterior extent of the arcuate nucleus (levels B-E) of 30 day old female rats, was similar to that of the adult female rat.

B. Electron Microscopic Observations

a) Neonatal Females

1. Perikarya

Most of the 30 TH positive perikarya observed were ovoid to polygonal in shape, although fusiform and teardrop shaped cell bodies were also encountered. These somata were considerably smaller than those encountered in the adult, averaging about 5 μm in short diameter and 8 μm in long diameter. Each of these small immunoreactive nerve cell bodies contained a large nucleus, generally indented, conforming to the cell's shape and taking up most of the cytoplasmic space (Fig. 17). The majority of these nuclear profiles exhibited a single nucleolus, although 4 profiles each had 2 nucleoli.

The thin rim of cytoplasm was filled by a black, granular, immunoprecipitate which tended to associate with membranous structures as in the adult. Also as in the adult, neonatal perikarya contained mitochondria and short, sometimes distended, scattered strands of endoplasmic reticulum. However, long individual strands of endoplasmic reticulum could sometimes be followed for some distance along the cell's circumference. The Golgi apparatus were small and poorly developed. Multivesicular bodies similar to those seen in the adult were occasionally encountered (Fig. 18) but lysosomes, which were frequently seen in the adult, occurred in only one perikaryal profile. Few profiles showed only a thin rim of cytoplasm which was filled with reaction product but completely devoid of organelles.

The labeled neonatal perikarya were sometimes contacted by tanycytic processes for some distance (Fig. 18). In addition, unlabeled nerve terminals and/or TH positive dendrites contacted the neonatal labeled peri-

karya in a manner similar to that described in the adult. There were also 5 somato-somatic appositions similar to the one described in the adult arcuate nucleus. Whereas no TH negative dendrite was ever seen directly apposed to labeled perikarya in adult animals, 10 such dendro-somatic appositions occurred in the neonates (Fig. 19). On the other hand, labeled terminals, which occasionally contacted adult immunoreactive perikarya, never contacted neonatal labeled nerve cell bodies.

2. Dendrites

The types of relationships established by TH positive dendrites were examined in the neonatal arcuate nucleus. The results are shown in Table VII. Except for the presence of one neonatal axo-dendritic synapse involving 2 labeled elements, and the absence of this type of contact in the adult female (and in any other age group), the types of relationships involving TH positive dendrites observed in the neonate were identical to those seen in the adult. However, the proportions of the different types of contacts markedly differed in the two age groups (compare Tables II and VII). Thus, in the neonate, the most commonly encountered type of relationship was the dendro-dendritic apposition involving one labeled and one unlabeled dendrite (Fig. 20a). The second most common type of contact was the dendro-tanycytic apposition (Fig. 21), followed by the axo-dendritic synapse with unlabeled axon terminals (Fig 20c). Then, came the dendro-somatic apposition involving unlabeled and labeled perikarya respectively (Figs. 22 and 23), as well as dendro-dendritic appositions involving two labeled elements (Fig. 20b). One of these dendro-dendritic appositions showed a membrane specialization at the contact point (Fig. 20c).

TABLE VII: TYPES OF RELATIONSHIPS OBSERVED BETWEEN TH POSITIVE DENDRITES AND OTHER ELEMENTS OF THE NEONATAL ARCUATE NEUROPIL

	Animals			
	D1-1	D1-2	D1-3	Total
Total #TH+ dendrites observed :	52	43	97	192
#axo(TH-)dendritic(TH+)synapses :	7 (13%)*	3 (7%)	9 (9%)	19 (10%)
#TH+ dendrites apposed to:				
Tanycytic processes :	8 (15%)	3 (7%)	10 (10%)	21 (11%)
TH+ dendrites :	3 (6%)	0 (0%)	1 (1%)	4 (2%)
TH- dendrites :	11 (21%)	10 (23%)	26 (27%)	47 (24%)
TH+ perikarya :	2 (4%)	0 (0%)	2 (2%)	4 (2%)
TH- perikarya :	3 (6%)	1 (2%)	12 (12%)	16 (8%)
#axo(TH+)dendritic(TH+)synapses :	1 (2%)	0 (0%)	0 (0%)	1 (1%)

* $\% = \frac{\#\text{TH+ dendrites involved in a given type of contact}}{\text{Total number of TH+ dendrites observed}}$

3. Axon Terminals

Immunoreactive axon terminals filled with small, round, densely packed, clear vesicles, were encountered in the neonatal arcuate nucleus (Fig. 24) far more frequently than in the adult. Forty-eight such terminals were observed, many of which formed direct appositions with unlabeled dendritic profiles or tanycytic processes. A few labeled terminals also formed synapses with TH negative dendrites. There was one instance in which one synapsed on a TH positive dendrite, and another where one labeled terminal was apposed to another labeled terminal (Table VIII).

Although, in our material, labeled terminals never synapsed or even contacted TH positive perikarya, one of these was seen synapsing on a TH negative perikaryon, and 5 were directly apposed to TH negative nerve cell bodies. In contrast, unlabeled terminals were frequently encountered directly apposed to, or synapsing on, both labeled and unlabeled perikarya (Table IX).

b) 15 Day Old Females

1. Perikarya

The TH positive nerve cell profiles of 15 day old female rats were ovoid or fusiform, and sometimes polygonal in shape. The size range of the 34 labeled perikarya observed was approximately 6 μm in short diameter and 10 μm in long diameter. Thus, these cells were slightly smaller than the adult TH positive perikarya, but larger than the neonatal labeled nerve cell bodies. In favorable planes of section, one nucleolus was often seen in the large indented nucleus, although 2 nuclei each contained 2 nucleoli. The nucleus took up most of the cytoplasmic space, leaving only a thin rim of cytoplasm filled with the black immunoprecipitate.

TABLE VIII: TYPES OF RELATIONSHIPS OBSERVED BETWEEN LABELED AXON TERMINALS AND OTHER ELEMENTS OF THE NEONATAL ARCUATE NEUROPIL

	Animals			
	D1-1	D1-2	D1-3	Total
Total #TH+ terminals observed :	19	17	12	48
#TH+ terminals apposed to:				
TH- dendrites :	2 (11%)*	4 (24%)	3 (25%)	9 (19%)
TH- axon terminals :	1 (5%)	0 (0%)	0 (0%)	1 (2%)
TH+ axon terminals :	1 (5%)	0 (0%)	0 (0%)	1 (2%)
Tanycytic processes :	5 (26%)	3 (18%)	0 (0%)	8 (17%)
TH- perikarya :	2 (11%)	1 (6%)	2 (17%)	5 (10%)
#axo(TH+)dendritic(TH-)synapses :	2 (11%)	2 (12%)	0 (0%)	4 (8%)
#axo(TH+)dendritic(TH+)synapses :	1 (5%)	0 (0%)	0 (0%)	1 (2%)
#axo(TH+)somatic(TH-)synapses :	1 (5%)	0 (0%)	0 (0%)	1 (2%)

* % = $\frac{\text{\#TH+ dendrites involved in a given type of contact}}{\text{Total number of TH+ dendrites observed}}$

TABLE IX: NUMBER OF AXO-SOMATIC APPOSITIONS AND SYNAPSES INVOLVING UNLABELED AXON TERMINALS AND BOTH LABELED AND UNLABELED PERIKARYA OF NEONATAL FEMALES

	Animals			
	D1-1	D1-2	D1-3	Total
# TH+ perikarya observed :	10	4	16	30
#axo(TH-)somatic(TH+) appositions :	14	4	34	52
#axo(TH-)somatic(TH+) synapses :	1	0	11	12
# TH- perikarya observed :	10	11	21	42
#axo(TH-)somatic(TH-)appositions :	2	10	20	32
#axo(TH-)somatic(TH-)synapses :	2	0	6	8

As in the adult, there were numerous mitochondria, well developed Golgi apparatus, and short strands of endoplasmic reticulum dispersed throughout the cytoplasm of these perikarya (Fig. 25). A couple of lysosomes were observed in one of the labeled cells examined, and multivesicular bodies were occasionally encountered. In contrast to what was seen in the adult, 15 day old labeled arcuate perikarya did not exhibit any obvious glial ensheathment. Also pertaining to this age group were numerous (17) dendro-somatic appositions involving unlabeled dendrites and labeled perikarya. Such contacts were not observed in the adult female. However, 15 day old labeled perikarya were contacted by labeled dendrites and unlabeled axon terminals as in the adult. Moreover, these 15 day old labeled perikarya formed somato-somatic appositions with unlabeled perikarya in 3 instances, and with other labeled perikarya in 2 instances.

2. Dendrites

The types of relationships involving TH positive dendrites of the 15 day old arcuate nucleus are shown in Table X. As in the neonate, the most common type of relationship was the dendro-dendritic apposition involving one labeled and one unlabeled dendrite. However, in view of the total number of dendrites observed in each case (compare Tables VII and X), these dendro-dendritic appositions occurred much more frequently in the neonate. Furthermore, the frequency of occurrence of axo-dendritic synapses involving unlabeled axon terminals and labeled dendrites was almost as high as that of the dendro-dendritic appositions. The dendro-tanycytic appositions were the third most frequent association, followed by dendro-dendritic appositions between 2 labeled dendrites, and the dendro-somatic appositions involving both labeled and unlabeled perikarya. The two latter types of appositions

TABLE X: TYPES OF RELATIONSHIPS OBSERVED BETWEEN TH POSITIVE DENDRITES AND OTHER ELEMENTS OF THE ARCUATE NEUROPIL OF 15 DAY OLD FEMALES

	Animals			
	D15-1	D15-2	D15-3	Total
Total #TH+ dendrites observed :	87	172	94	353
#axo(TH-)dendritic(TH+)synapses :	10 (11%)*	15 (9%)	8 (9%)	33 (9%)
#TH+ dendrites apposed to:				
Tanycytic processes :	7 (8%)	14 (8%)	5 (5%)	26 (7%)
TH+ dendrites :	3 (3%)	5 (3%)	3 (3%)	11 (3%)
TH- dendrites :	15 (17%)	12 (7%)	10 (11%)	37 (10%)
TH+ perikarya :	3 (3%)	1 (1%)	1 (1%)	5 (1%)
TH- perikarya :	1 (1%)	4 (2%)	1 (1%)	6 (2%)
TH+ axon terminals :	0 (0%)	0 (0%)	1 (1%)	1 (.3%)

* $\% = \frac{\#TH+ \text{ dendrites involved in a given type of contact}}{\text{Total number of TH+ dendrites observed}}$

occurred in practically equal proportions.

Finally, there was one instance of an apposition between a TH positive dendrite and a TH positive axon terminal. This type of contact was not observed in the neonatal or normally cycling female rat, but it was seen in the adult male rat (Table VI) and, as will be mentioned below, in the 30 day old female (Table XI).

3. Axon Terminals

Only eleven labeled axon terminals, morphologically similar to those described in the adult, were observed in the 15 day old female rat. Ten of these terminals were directly apposed to unlabeled dendrites, and one to a TH positive dendrite. Furthermore, 3 of the labeled terminals apposed to unlabeled dendrites were also in direct apposition to other axon terminals: 2 to an unlabeled and one to a labeled axon terminal.

c) 30 Day Old Females

1. Perikarya

Twenty immunoreactive perikaryal profiles from 30 day old female rats were observed and found to be small, ranging from about 7 μm in short diameter and 9 μm in long diameter. These cells were in the size range of the 15 day old labeled perikarya. Their general morphological appearance was similar to that of the perikarya from adult rats, and as in the adult, were ensheathed by glial processes. In contrast to the adult, however, many more multivesicular bodies were seen. One 30 day old TH positive soma was in direct contact with an unlabeled cell body, and two other labeled perikarya were directly apposed to one another. Labeled perikarya were also contacted by both labeled (Table XI) and unlabeled dendrites in equal proportions.

TABLE XI: TYPES OF RELATIONSHIPS OBSERVED BETWEEN TH POSITIVE DENDRITES AND OTHER ELEMENTS OF THE ARCUATE NEUROPIL OF 30 DAY OLD FEMALES

	Animals			
	D30-1	D30-2	D30-3	Total
Total #TH+ dendrites observed :	161	130	110	401
#axo(TH-)dendritic(TH+)synapses :	26 (16%)*	30 (23%)	23 (21%)	79 (20%)
#TH+ dendrites apposed to:				
Tanycytic processes :	7 (4%)	7 (5%)	5 (5%)	19 (5%)
TH+ dendrites :	8 (5%)	3 (2%)	3 (3%)	14 (3%)
TH- dendrites :	15 (9%)	8 (6%)	3 (3%)	26 (6%)
TH+ perikarya :	2 (1%)	2 (2%)	0 (0%)	4 (1%)
TH- perikarya :	3 (2%)	1 (1%)	1 (1%)	5 (1%)
TH+ axon terminals :	0 (0%)	1 (1%)	0 (0%)	1 (.2%)

* $\% = \frac{\#TH+ \text{ dendrites involved in a given type of contact}}{\text{Total number of TH+ dendrites observed}}$

2. Dendrites

A total of 401 immunoreactive dendritic profiles from the 30 day old female rat arcuate nucleus were examined, and the type of relationships observed were detailed in Table XI. All the relationships present in the adult were also seen in the 30 day old rats. As in the adult, the most common type of relationship encountered was the axo-dendritic synapse involving unlabeled axon terminals. In the 30 day old animals, however, dendro-dendritic appositions involving one labeled and one unlabeled dendrite occurred more frequently than dendro-dendritic appositions involving 2 labeled elements, which was not the case in the adult (compare Tables II and XI). Dendro-somatic appositions involving both labeled and unlabeled perikarya occurred in equal proportions in 30 day old and adult animals.

In addition to the adult type of relationships, there was one instance of an axo-dendritic apposition where both elements involved were labeled. This type of contact was also present in the adult male rats but not in adult females (normally cycling and EV-treated).

3. Axon Terminals

We encountered only 19 labeled axon terminals in the 30 day old animals. These terminals were morphologically similar to those seen in the adult. Three were apposed to unlabeled terminals, two to unlabeled dendrites, and one to a TH positive dendrite. Three of these terminals synapsed on TH negative dendrites, but none ever contacted tanycytic processes, labeled perikarya or unlabeled perikarya.

DISCUSSION

I- THE ADULT TIDA SYSTEM

A. Topography

The distribution of TH positive perikarya was similar in both male and female rats, and generally corresponded to that described by other investigators (Pickel et al., 1975; Bosler et al., 1984; Chan-Palay et al., 1984; van den Pol et al., 1984). Immunolabeled nerve cell bodies were found in both the medio-dorsal and ventro-lateral regions of the arcuate nucleus. Previous studies, however, did not delineate the medio-dorsal cell group as being distinct from the less clearly defined ventro-lateral cluster of immunoreactive neurons, in the mid-portion of the arcuate nucleus. Both cell groups were rather described as a single continuum. This discrepancy, between our results and those of others, may have resulted from either the thickness of the sections, or the way in which maps were constructed. Chan-Palay et al. (1984), for example, worked with 100 µm thick coronal sections of the arcuate region. Although van den Pol et al. (1984) used 30 µm thick sections, as we did, each of their topographical drawings combined all the immunoreactive neurons seen in 3 consecutive sections. It is possible that the sharp delineation between the two cell clusters observed in the present study occurs in a restricted portion of the nucleus' antero-posterior axis. Thus, thin sections, at frequent intervals, would be required to identify it. Alternatively, TH containing neurons may exist in the zone between the two demarcated clusters, but the level of the enzyme may be too low for detection by our antibody. Subsets of immunoreactive neurons with different concentrations of TH have been identified in the

arcuate nucleus (Brawer et al., in press).

The two cell groups, dorso-medial and ventro-lateral, could represent two biochemically distinct populations of TIDA neurons. Everitt et al. (1984b), for example, demonstrated the coexistence of glutamic acid decarboxylase (GAD), and TH positive immunoreactivities, in most neurons of the medio-dorsal arcuate nucleus of male rats. However, TH positive neurons of the ventral arcuate nucleus region did not contain GAD. In view of the similarity of TIDA cell distribution in male and female, such a biochemical parcellation may also apply to the female.

B. Ultrastructural Organization

The arcuate neuronal cell population has previously been described as consisting of small, unremarkable perikarya, containing the usual array of cytoplasmic organelles and inclusions, that is, mitochondria, Golgi apparatus, endoplasmic reticulum, lysosomes, and multivesicular bodies (Kobayashi et al., 1967; Jaim-Etcheverry and Pellegrino de Iraldi, 1968; Brawer and van Houten, 1976). The TH positive perikarya observed in this study conform to this general morphological description. In addition, male and female TIDA nerve cell bodies were ultrastructurally identical, although male TH positive perikarya tended to be slightly smaller than those of the female. This latter observation may be of significance, in view of the possible inhibitory role of testosterone (T) upon the TIDA cells, in the male (see section I-C).

The present results indicated that TH immunoreactive neurons make extensive contacts with each other, as well as with other elements of the arcuate neuropil. Unexpectedly, and as far as TH positive terminals are

concerned, axo-dendritic and axo-somatic connections are infrequently observed. In contrast, dendro-dendritic and dendro-somatic contacts are numerous. However, the interpretation of relationships established by TH positive axon terminals is complicated by the fact that noradrenergic (NA) and adrenergic (A) terminals, which also contain TH (for review see Záborszky, 1982), are present in the arcuate nucleus. The majority of noradrenergic fibers to the arcuate nucleus were shown to originate in the A1 cell group and locus ceruleus (Palkovits et al., 1980b; Záborszky et al., 1977), while most of the adrenergic innervation is derived from the lateral reticular nucleus (C1 cell group) (Palkovits et al., 1980a). Brownstein et al. (1976) also demonstrated, by means of deafferentation experiments, that most of the arcuate dopaminergic innervation originated from within the hypothalamus, while Záborszky (1982) indicated that a fraction of these terminals came from extrahypothalamic sources such as the A8 cell group, as well as from the supramamillary and caudal periventricular nuclei (A10 and A11 cell groups respectively). Thus, the arcuate nucleus contains the three types of catecholaminergic nerve terminals. Although the TH antibody used in the present study labels dopaminergic nerve terminals (Pickel et al., 1981), it can not be considered as selective in a region also containing other catecholaminergic nerve endings, in as much as this same antibody has been shown to stain noradrenergic terminals as well (Pickel, 1982).

Since the TH antibody should theoretically recognize both NA and DA nerve terminals, it is surprising that so few labeled terminals were observed within the arcuate region. This may be due, in part, to the preferential staining of DA terminals over NA terminals (Pickel et al., 1975; Hökfelt et al. 1976). There is, presumably, either a higher TH content in DA than in NA neurons, or a TH form in DA neurons which is more accessible

to antibodies than in NA neurons (Pickel et al., 1975). In either case, DA terminals of the arcuate nucleus may not be stained. Those few terminals that were labeled, however, showed strong immunoreactivity.

The presence in the fixative of a relatively high concentration of glutaraldehyde (0.5%), which has been shown to significantly reduce hypothalamic TH immunostaining (van den Pol et al., 1984), may also partially account for the paucity of stained terminals. Paradoxically, good immunoreactivity was obtained in the dopaminergic nerve terminals of the striatum, with concentrations of glutaraldehyde varying between 0.5 and 1% (Arluison et al., 1984). Some areas of the CNS, therefore, may be more sensitive to glutaraldehyde than others, possibly due to different TH molecular weight (MW) forms with different affinities for antibodies (Joh and Reis, 1975). Both the present results and those of van den Pol et al. (1984), indicate that hypothalamic areas, including the arcuate nucleus, are especially sensitive to glutaraldehyde. Consequently, in order to study the arcuate nucleus using TH immunostaining, perfusing solutions containing low concentrations of glutaraldehyde should be used, and perfusion time should not be unduly extended. Furthermore, the temperature of the fixative should be closely monitored (17-20°C) since, at higher temperatures, better tissue preservation is obtained, but loss of antigenicity increases.

Using low glutaraldehyde concentrations (0.08%), Léranth et al. (1985b) successfully detected TH posftive axon terminals within the rat arcuate nucleus. Although the number of TH positive axon terminals observed was not mentioned by the authors, their description suggests that these terminals were commonly encountered. Furthermore, they reported the presence of numerous axo-dendritic synapses involving immunoreactive terminals and dendrites. In contrast, we rarely observed this type of relationship

(once in the adult male and once in the neonate). Similarly, only few axo-dendritic appositions, involving 2 labeled elements, occurred in our material (3 in adult males, 1 in 15 day old female, and 1 in 30 day old females). Our results indicate that, failure in detecting many of the TH positive terminals, for reasons discussed above, prevented the detection of several connections involving these labeled terminals. For example, the paucity of axo-dendritic synapses between labeled terminals and unlabeled dendrites (Fig. 13a), may be explained by the fact that the majority of axon terminals remained unlabeled.

Glutaraldehyde concentration is not the only factor responsible for good immunostaining of axon terminals. Léranth et al. (1985b) used the avidin-biotin-peroxidase complex (ABC), instead of the PAP complex, as an immunoperoxidase technique. The ABC method is based on the strong affinity of the glycoprotein avidin, for the small vitamin biotin. The immunocytochemical steps for the ABC method are the same as those described for the PAP method (see Materials and Methods), but in the former method, the secondary (or link) antibody is labeled with biotin.

The ABC technique has been shown to be more sensitive than the PAP method (Hsu et al., 1981). This higher sensitivity is thought to result from the numerous peroxidase molecules present in the ABC. Indeed, the PAP complex contains only 3 peroxidase molecules, and 2 immunoglobulin molecules (Sternberger, 1979b). During formation of the ABC, however, avidin can act as a bridge to biotin-peroxidase which, in turn, contains several biotin moieties which link avidin molecules. Consequently, the ABC has more than 3 peroxidase molecules and, since a greater number of peroxidase molecules increases staining intensity, sensitivity is improved.

Despite the few TH positive terminals observed using the PAP method, strong immunoreactivity was obtained in many nerve cell bodies and dendrites. The TH positive perikarya of the arcuate nucleus appeared ultrastructurally similar to those shown in a recently published study (van den Pol et al., 1984). These labeled perikarya were frequently apposed by unlabeled nerve terminals, but because of the inherent difficulty in staining catecholaminergic nerve endings using TH immunocytochemistry (see above), the non-dopaminergic nature of all such terminals is doubtful. TH positive dendrites were often seen in direct apposition to labeled nerve cell bodies and, for reasons outlined above, these TH positive elements are clearly dopaminergic. Immunoreactive dendrites were also seen in direct apposition to other dendrites, both labeled and unlabeled, and to unlabeled perikarya. Léránth et al. (1985b), however, did not report such dendro-dendritic and dendro-somatic connections. It is not clear whether their immunostaining method (ABC) failed to demonstrate such relationships, or whether these investigators focused their attention exclusively on contacts involving immunoreactive axon terminals.

Although dendro-somatic appositions involving dopaminergic dendritic processes have, to our knowledge, never been reported, dendro-dendritic appositions, similar to those observed in the present study, have been described in the pars reticulata of the substantia nigra (Wassef et al., 1981). Dopamine, which can be synthesized and stored in dendrites (Pickel et al., 1975; Björklund and Lindvall, 1975; Hattori et al., 1979; Mercer et al., 1979), has been shown to be released by dendrites in substantia nigra, both in vitro (Geffen et al., 1976; Tagerud and Cuello, 1979), and in vivo (Korf et al., 1976; Nieoullon et al., 1977a,b). To date, the mechanism through which this dendritic release occurs is not well understood. However,

the concept of dendrites acting solely as passive receptive neuronal appendages was abandoned many years ago, following the demonstration of presynaptic dendrites in several regions of the CNS (Sloper, 1971; Gobel et al., 1980; Ellis and Rustioni, 1981; Groves and Wilson, 1980; Romansky et al., 1980). Based on some observations, in the substantia nigra, of vesicular clusters in the presynaptic dendritic structures (Hajdu et al., 1973; Wilson et al., 1977), vesicular exocytosis was proposed as a mechanism of dendritic release. Many investigators, however, failed to observe vesicular clusters, or membrane specializations, at the dendro-dendritic contact sites within the substantia nigra (Cuello and Iversen, 1978; Mercer et al., 1979; Reubi and Sandri, 1979; Wassef et al., 1981), indicating that dopamine release may occur through a non-vesicular mechanism. The smooth endoplasmic reticulum has been proposed as a possible storage site for dendritic dopamine (Mercer et al., 1979), although the mode of release of dopamine stored in endoplasmic reticulum cisternae, is a matter of pure speculation.

Although dendritic release still remains to be demonstrated within the arcuate nucleus, the presence of numerous dendro-dendritic appositions, similar to those found in the substantia nigra (Wassef et al., 1981), suggests that dendritic release may also occur in this nucleus. Furthermore, the proportions of labeled dendrites contacting other dendrites, both labeled and unlabeled, were higher in the arcuate nucleus [100 (7%) out of 1482 observed labeled dendrites in all our adult animals] than in the substantia nigra [22 (4%) out of 580 observed labeled dendrites in adult rats (Wassef et al., 1981)]. This high incidence of dendro-dendritic appositions within the arcuate nucleus, suggests that these contacts do not occur by chance, but rather represent biologically significant relation-

ships. Similarly, although the dendro-somatic appositions are less frequently encountered [except in the estradiol valerate (EV)-treated animals as discussed below], the absence in the normally cycling female, and the paucity in both EV-treated females and in intact males, of unlabeled dendrites apposed to labeled perikarya, indicates that appositions between dopaminergic dendrites and arcuate perikarya are not fortuitous and may, in fact, be functional points of communication. Although infrequent, neuronal-perikaryal appositions could be functionally highly significant, since the closer an input is to the perikaryon, the greater is its influence over the cell's activity. Finally, the absence of any vesicular clusters, or membrane specializations, at the dendro-somatic and dendro-dendritic contact points, is consistent with the view of a non-vesicular dendritic release of dopamine, as previously proposed for the substantia nigra (Cuello and Iversen, 1978; Mercer et al., 1979; Reubi and Sandri, 1979; Wassef et al., 1981). Even though there were two instances, one in the neonate and the other in the adult male, of a membrane specialization at the site of apposition between two immunoreactive dendrites, no vesicular clusters were present (Fig. 16).

In view of the ability of dendrites in the substantia nigra to release dopamine (Geffen et al., 1976; Korf et al., 1976; Nieoullon et al., 1977a,b; Tagerud and Cuello, 1979), dendro-dendritic appositions involving two TH positive elements in the substantia nigra (Wassef et al., 1981), are probably functionally significant. It has been proposed (Groves et al., 1975) that, within the substantia nigra, dopamine is autoinhibitory. This was based on the observed effects of amphetamine, a drug which causes dopamine release (Fuxe and Ungerstedt, 1968), and haloperidol, a dopamine antagonist (Anden et al., 1970), on the discharge rate of substantia nigra

neurons. The intravenous administration of amphetamine caused a decrease in neuronal activity, and this effect could either be blocked, or reversed, by the administration of haloperidol (Bunney, 1974). Haloperidol, when given alone, produced an increase in neuronal firing. Furthermore, dopamine itself, applied iontophoretically directly onto putative dopaminergic cell bodies, diminished the discharge rate of the cells. More recently, Eriksson et al. (1985) showed that the activity of nigral dopaminergic neurons was reduced, in a dose-dependent manner, after the intravenous administration of B-HT 920, an azepine derivative that was proposed as a potent dopamine agonist, with selectivity for autoreceptors (Anden et al., 1983). The inhibitory effect of B-HT 920 was reversed by haloperidol. Thus, dendritic release may play a role in self-inhibition by the substantia nigra dopaminergic neurons.

In view of the similarity between the dendro-dendritic appositions of the substantia nigra, and those of the arcuate nucleus, it is tempting to propose that TIDA cells may also be self-inhibitory, by way of a dendro-dendritic, or dendro-somatic mechanism. Biochemical evidence supports this possibility (Kizer et al., 1978). Following the administration of the TH inhibitor alpha-methyl-p-tyrosine, to haloperidol-treated rats, a significant decrease was observed in dopamine, but not in noradrenaline concentration, within the median eminence. In addition, there was an increased rate of dopamine depletion, accompanied by an increase in TH activity, within the median eminence, as indicated by the increase in Vmax, but an unchanged affinity of the enzyme for its substrate, or cofactor. The experimentally induced increase in dopamine turnover rate, and in synthetic capacity of TIDA cells, led the authors to suggest an increased electrical activity in TIDA neurons. Thus, in addition to blocking the post-synaptic

dopaminergic receptors within the median eminence, haloperidol may inhibit self-inhibitory receptors located on TIDA neurons. It has been suggested (Kizer et al., 1978) that this self-inhibition may occur through the action of recurrent axon collaterals, identified using electrophysiological criteria (Yagi and Sawaki, 1975). Such electrophysiological methods, however, would most likely be inadequate to distinguish between axon collaterals or dendritic transmission. Furthermore, it is unlikely that Yagi and Sawaki (1975) would have even considered the possibility of a dendritic mechanism, since the concept is a fairly recent one.

Although the paucity of TH positive axon terminals would seem to favor dendritic release as the major self-inhibitory mechanism, the many inconsistencies and problems surrounding the staining of catecholaminergic terminals, render negative findings difficult to interpret. Furthermore, as previously mentioned, Léránth et al. (1985b), using the ABC method, observed numerous TH positive axon terminals, many of which synapsing on TH positive dendrites. The lack of detection of this type of relationship in the present study, may merely reflect the inadequacy of our method in detecting catecholaminergic terminals. A proportion of the numerous unlabeled axon terminals, observed synapsing on TH positive dendrites, may in fact contain TH. Furthermore, recent radioautographic (Bosler et al., 1982) and immunocytochemical (Chan-Palay et al., 1984) studies, suggest that the arcuate nucleus contains an abundance of catecholaminergic axon terminals. In any case, recurrent collateral, and dendritic release self-inhibition, need not be mutually exclusive operative mechanisms.

In addition to its self-regulation, the TIDA neuronal system may also be regulating other non-dopaminergic neurons, through dendritic release of dopamine. Dendro-dendritic appositions, involving two labeled dendrites,

occurred in similar proportions to those appositions involving one labeled, and one unlabeled dendrite. Furthermore, the proportions of TH immunoreactive dendrites directly apposed to unlabeled perikarya, were similar to the proportions of labeled dendrites in direct apposition to labeled nerve cell bodies, in both males and females.

EV-treated females exhibited the same range of dendritic contacts as the other groups, with one important exception: there were significantly more TH positive dendrites apposed to labeled than to unlabeled perikarya, in EV-treated animals. The proportions of dendro-somatic appositions involving TH immunoreactive dendrites, on both labeled, and unlabeled perikarya, were uniformly low in all adult groups, the only exception being the high proportion of TH positive dendrites apposed to labeled perikarya in EV-treated animals. Thus, the EV treatment seems to preferentially affect these latter contact sites. Why EV treatment should have such a selective effect is not clear, and requires further study. It would also be important to determine whether this phenomenon is sex, and/or steroid specific. In any case, the detection of an increased number of labeled dendro-somatic appositions, following EV- treatment, is most probably due to an increase in dendritic content of TH within already existing connections, rather than to the formation of new connections. EV was injected in adult females, that is, at a time when all arcuate synaptic connections have been established (Matsumoto and Arai, 1976), and when estradiol (E_2) does not stimulate synaptogenesis within the arcuate nucleus (Matsumoto and Arai, 1979). An increase in TH activity has also been reported following the injection of estradiol benzoate in adult rats (Tobias et al., 1981). Although these observations do not explain why EV enhancement of TH content should be restricted to specific dendrites, one possibility emerges from

discussion of neonatal material (see section II-A). The shift in TH content away from dendrites, as development progresses, suggests that dendritic TH may normally be quite low in adults. Enhancement of TH levels throughout the cell would thus be most appreciable in dendrites, in which the amount of TH might then be sufficient to detect immunocytochemically.

The sites where labeled dendrites come in direct apposition to tanycytic processes may also be functional points of contact. Two main arguments can be brought forward in favor of this hypothesis. First, such dendro-tanycytic appositions do not seem to occur by chance since, in both male and female controls, they were the second most frequently encountered type of contact involving labeled dendrites (the most common type of contact was the axo-dendritic synapse). Second, tanycytes were recently shown to be strongly immunoreactive for DARPP-32 (dopamine- and adenosine 3':5'-monophosphate-regulated phosphoprotein), a protein whose phosphorylation is regulated by dopamine and cAMP (Ouimet et al., 1984). Furthermore, the cellular localization of DARPP-32 indicated that this protein is not found in dopaminergic neurons, but rather in dopamine receptive cells. Dendro-tanycytic apposition may thus provide the basis for dopamine action at the level of the tanycytes. The biological significance of dopamine interaction with tanycytes is unknown.

C. Effects of Sex Steroids on Male and female TIDA Neurons

The adult rat TIDA system has been extensively studied at the light microscopic level, by means of fluorescence, immunofluorescence, and immunocytochemical techniques (Carlsson et al., 1962; Fuxe, 1964; Dahlström and Fuxe, 1964; Fuxe and Hökfelt, 1969; Hökfelt et al., 1976; 1984b; Pickel et

al., 1975; Bosler et al., 1984; Chan-Palay et al., 1984; van den Pol et al., 1984; Piotte et al., 1985). These studies, however, did not address the question of possible sex differences. In fact, two recent immunocytochemical studies, providing extensive topographical mapping of this system, did not even report the sex of the animals used (Chan-Palay et al., 1984; van den Pol et al., 1984). Although the present investigation revealed a similarity in the distribution of TH immunoreactive nerve cell bodies within the hypothalamic arcuate nuclei of male and female (both normally cycling and EV-treated) rats, the immunostaining intensity of the male nerve cell bodies and processes was markedly less than that seen in the females (Plates 1, 2 and 3). This may be accounted for by a putative inhibitory effect of testosterone (T) upon TH expression in TIDA neurons (Brawer et al., in press). Castration enhanced the staining intensity of individual neurons in the male, but had no effect in the female, suggesting that T, but not E_2 , suppressed enzyme expression. The castration enhancement in TH staining was reversed by replacement with T, but not with E_2. Thus sex-specific differences in TH expression are probably due to the androgenic status of the male. Interestingly, the most intensely stained neurons occurred in EV-treated females. This may relate to a reported stimulatory effect of E_2 on TH activity in both the hypothalamus and median eminence (Tobias et al., 1981; Löfström et al., 1977; Wiesel et al., 1978).

The observation that both TH positive cell clusters were best delineated in the mid-portion of the arcuate nucleus of EV-treated females (in comparison to intact males and normally cycling females), is suggestive of an action of E_2 upon the TIDA neurons. E_2 receptors have been demonstrated within TH immunoreactive neurons (Grant and Stumpf, 1973; 1981; Heritage et al., 1980; Sar, 1984). Furthermore, following the subcutaneous

injection of estradiol benzoate (EB) in ovariectomized rats, DA turnover was found to be higher in the lateral palisade zone of the median eminence (Löfström et al., 1977; Wiesel et al., 1978), and TH activity was increased in medial basal hypothalamus (MBH) (Tobias et al., 1981). In contrast, Luine et al. (1977) reported a decrease in MBH TH activity after EB administration in ovariectomized rats. The source of this discrepancy may reside in the composition of the tissue samples, which included the median eminence, part of the pituitary stalk, and arcuate nucleus in Tobias et al. (1981), but also comprised ventromedial and periventricular nuclei, in Luine et al. (1977). Both the ventromedial and periventricular nuclei contain dopaminergic perikarya (van den Pol et al., 1984). In both these nuclei, cell bodies containing E_2 receptors have also been demonstrated (Stumpf, 1968). Thus, E_2 may affect the DA-containing neurons of the ventromedial and periventricular nuclei, but not necessarily in a way similar to that observed for TIDA neurons. Such differential effect of E_2 may explain, at least in part, the contradictory results obtained in the two studies mentioned above.

II- ONTOGENY OF THE TIDA SYSTEM

A. Topography

In the rat, which has a gestation period of 21 days, arcuate neurons form late in the prenatal developmental period [between the 16th and 19th days of gestation, and beyond (Altman and Bayer, 1978a,b)]. It has also been shown that 1% of the arcuate neurons were labeled in animals injected

with [^{3}H] thymidine on the 3rd or 5th postnatal day. No labeled cells were seen when the injection was given 10 days after birth (László, 1985). Further differentiation of the nucleus, including synaptogenesis, occurs for as long as 45 days postnatally (Matsumoto and Arai, 1976). Immature neuronal profiles are even seen in the adult (Brawer, 1971; Walsh et al., 1982). The arcuate nucleus, therefore, develops very late in the life of the animal. In light of this, the most surprising and striking feature of the neonatal TIDA system, was its similarity to that of the adult. This is not to say that neonatal TIDA neurons were identical to their adult counterparts in all respects. Neonatal dendritic profiles, for instance, were generally stained for longer distances than those of the adult. One possible explanation for this phenomenon is a better antibody penetration of neonatal tissue, although there may also be changes in the amount of dendritic TH during development. Coyle and Axelrod (1972) reported a considerable increase in TH specific activity within whole rat brain, between the 15th gestational day and adulthood. During this developmental period, a shift in the distribution of TH activity, from regions containing catecholaminergic perikarya (e.g. midbrain-hypothalamus), to regions containing only nerve terminals (e.g. corpus striatum), was also reported. In a recent study, Jimenez et al. (1984) demonstrated that the TH activity was low within the median eminence of 10 day old female rats, but progressively increased until it peaked at 20 days of age, and remained high up until day 39 (the last time point they considered). Since the median eminence contains primarily axons, and axon terminals, this maturational shift in TH activity corroborates Coyle and Axelrod's (1972) findings. A progressive age dependent decrease in the TH activity of the TIDA neurons is, therefore, not unexpected, since these neurons project extensively to the median eminence.

This decrease in enzymatic activity may be due to lower amounts of TH within TIDA neurons. Since synthesizing enzymes are produced in the nerve cell bodies, and are thus present there in high concentrations (Hökfelt et al., 1984a), a small decrease in the amount of perikaryal TH may go unnoticed. On the other hand, a decrease in the dendritic content of TH, which is generally lower than in perikaryon, may result in loss of immunocytochemical detection of this enzyme within adult dendrites. Indeed, although most of the adult dopaminergic dendrites did not stain as well as those of the neonate, intense staining was observed in most of the adult TIDA perikarya.

Our finding of mature-looking TH positive arcuate neurons in the neonate, is consistent with the study of Specht et al. (1981b) who reported arcuate TH positive neurons that were morphologically similar to those of the adult, as early as the 18th embryonic day. These investigators also described the distribution of TH immunoreactive nerve cell bodies in fetal arcuate nucleus (embryonic day 21), as being similar to that of the adult. However, they reported on the location of TH positive cells within the whole brain, and the arcuate nucleus was, therefore, not studied in great detail. The present study of the topography of TIDA neurons revealed that, in the neonate, most TH positive cells were located in the ventro-lateral region of the nucleus, whereas in the adult, these cells occurred predominantly in the medio-dorsal region. Since the characteristic adult distribution pattern was still not present in 15 day old rats, but was seen in the 30 day old animals, it is conceivable that cell migration occurs until at least the third postnatal week. Furthermore, in the 15 day old animals, numerous TH positive perikarya were found both in the medio-dorsal and ventro-lateral areas of the arcuate nucleus, suggesting that cell migration is not yet completed at this time. However, the medio-lateral and dorso-ventral expan-

sion of the arcuate nucleus during development should also be considered as a determining factor of the final adult cell distribution.

In both neonates and adults, TH positive neurons were consistently located in the vicinity of a slightly convex imaginary line, joining the medio-dorsal and ventro-lateral arcuate regions. This slightly curved medio-lateral axis is also the course taken by the tanycytic processes. One can speculate that young TH positive cells may follow the course of tanycytic processes during migration. The concept of glial processes guiding migrating cells during development was proposed by Rakic (1971), following his observation, within the monkey cerebellar cortex, of a close association between migrating granule cells, and highly oriented fibers originating from a type of protoplasmic astrocyte. Similarly, it was suggested that glial radial fibers served as guidelines for migrating cells within the cerebrum of fetal monkeys (Rakic, 1972). In order to guide migrating TH positive neurons, however, tanycytic processes must appear early in development. Tanycytic cytogenesis has been reported to be in progress for many days after birth (Altman and Bayer, 1978c). Thus, it is possible that the similarity of orientation between the course of the tanycytic processes, and the distribution of TH positive neurons, is merely a fortuitous event.

B. Ultrastructural Organization

The finding, in the neonate, of adult-type connections, came as a surprise since the arcuate nucleus has been shown to be relatively undeveloped at birth. This is indicated by the presence of numerous growth cones, abundant immature-looking perikarya, and a paucity of synapses (Walsh

and Brawer, 1979). Previous evidence suggesting the early maturity of the TIDA system came from histochemical and pharmacological studies. Catecholamine fluorescence was detected as early as the 3rd postnatal day within the external layer of the median eminence (Hyyppä, 1969), a region that receives abundant DA terminals originating from arcuate neurons (Fuxe and Hökfelt, 1966). In addition, the catecholamine-containing neurons of newborn rats have been shown to take up amine precursors, and to be affected by reserpine (a drug which blocks the uptake-storage mechanism), and nialamide (a drug which inhibits monoamine oxidase), just like adult catecholaminergic neurons (Loizou, 1972). Furthermore, physiological evidence suggests that the prolactin inhibitory function of the TIDA system is operative at birth. Ojeda and McCann (1974) reported a significant increase in prolactin plasma levels, following the subcutaneous injection of pimozide [a drug that selectively blocks DA receptors (Janssen and Allewijn, 1968)] in 3 or 6 day old female rats. This drug, however, did not have any effect when administered on the day of birth. It appears, therefore, that the TIDA system becomes functional sometime during the 72 hours following birth. As early as the 3rd postnatal day, TIDA neurons seem to be able to regulate prolactin secretion through the release of dopamine at the level of the median eminence.

The morphological findings of the present study conform very well to evidence indicating an early onset of TIDA function. Adult-type connections, as well as adult cell morphology, were observed in 2 day old animals. Furthermore, the changes occurring during development appear to be of a quantitative rather than a qualitative nature. The proportions of both dendro-dendritic and dendro-somatic appositions (each type involving 2 labeled elements) did not significantly vary throughout development. The

number of TH positive dendrites directly apposed to other immunoreactive dendrites constituted 2% of the total number of labeled dendrites observed in the neonate, and 3% in all other age groups examined. The corresponding respective proportions for dendro-somatic appositions involving 2 labeled elements were 2% and 1%. Therefore, the connections necessary for the putative self-inhibitory control described for adult TIDA neurons, may already be established and functional in newborn rats. The apparent stability of these connections throughout development reinforces the idea that they are functional contact sites. In contrast, there were obvious quantitative changes in the relative number of connections made by TIDA cells with other non-dopaminergic neurons. Twenty-four percent of the TH positive dendrites of the neonate were in direct apposition to unlabeled dendrites. This percentage fell to 10% in the 15 day old animal, and 6% in the 30 day old animal, reaching 2% in the adult. However, the proportions of immunoreactive dendrites directly apposed to unlabeled perikarya, reached adult values earlier, falling from 8% in the neonate, to 2% in the 15 day old animal, and 1% in both the 30 day old and the adult. This decrease in the proportion of TH positive dendrites in apposition to non-dopaminergic elements, may be due to the development of new connections by other maturing neuronal systems within the arcuate neuropil. The formation of these new connections probably results in a dilution of the number of contacts involving the early established TIDA system. For example, the frequency of unlabeled axon terminals, in synaptic contact with immunoreactive perikarya, was found to be 3 times higher in the adult than in the neonate.

Thus, TIDA neurons make extensive contacts with one another very early in postnatal development. These intrinsic connections, which are potentially functional at birth, are probably retained until adulthood. The

quantitative maturational changes that take place among contacts involving labeled and unlabeled elements, however, suggest that there is a reorganization, in time, of the connections between the TIDA neurons and other non-dopaminergic nerve cells of the arcuate neuropil.

SUMMARY AND CONCLUSIONS

The topography and ultrastructural connection patterns of the TIDA system were studied by means of the peroxidase-antiperoxidase (PAP) method, using an antibody against tyrosine hydroxylase (TH). Neonatal, 15 and 30 day old females, normally cycling and EV-treated adult females, and intact adult male rats were examined.

Light microscopic results indicated a similar distribution of TH positive neurons within the hypothalamic arcuate nucleus of adult male and female rats. This pattern was observed as early as postnatal day 30, indicating that by the first month after birth, TIDA neurons have probably reached their final positions within the nucleus.

The electron microscopic examination of the TIDA neuronal patterns of connections, revealed that TH positive dendritic profiles frequently occurred in direct apposition to one another, to unlabeled dendrites, to perikarya, both labeled and unlabeled, and to tanycytic processes. The extensive contacts made by the immunoreactive dendritic profiles with both labeled perikarya and dendrites, suggests that TIDA cells may communicate with each other by means of dendritic release of dopamine. The presence of appositions between TH positive dendrites and both unlabeled perikarya and dendrites, suggests that the TIDA system may influence other neuronal populations through its dendrites. Finally, in view of the recent finding of a dopamine-regulated protein (DARPP-32) within tanycytes (Ouimet et al, 1984), the dendro-tanycytic relationship is suggestive of a regulation of tanycytic function by the dendrites of TIDA neurons.

All types of connections (involving TH positive dendrites) seen in the adult, were also observed in the neonate. Thus dendritic release, which has been proposed as a mechanism of action for the adult TIDA system, may also be effective in early postnatal development. However, postnatal maturation of different types of TIDA neuronal connections, occurs well into the postnatal period and involves quantitative changes. For example, the percentage of labeled dendrites in direct apposition to unlabeled dendrites was found to be 24% in the neonate, 10% in the 15 day old, 6% in the 30 day old, and only 2% in the adult. It seems that although dendritic release probably takes place early in neonatal life, complete maturity of the TIDA system may not be attained before adulthood.

ORIGINAL CONTRIBUTIONS

The purpose of the present study was to examine, at both the light and electron microscopic levels, the postnatal development of the rat TIDA system. This work also included a comparison between the TIDA systems of adult male and female rats, and evaluation of a possible effect of E_2 upon the latter. We have shown:

1. The existence within the hypothalamic arcuate nucleus of extensive contacts involving TH positive dendritic profiles that is, labeled dendrites in direct apposition to one another, to unlabeled dendrites, to perikarya, both labeled and unlabeled, and to tanycytic processes.

2. The presence within the neonatal female rat of the same types of contacts (involving TH positive dendrites) encountered in the adult.

3. The similarity of the male and female TIDA systems, in both topography and ultrastructural pattern of connections.

4. An increase within the female arcuate nucleus, following chronic E_2 exposure, of the relative proportion of dendro-somatic appositions between TH positive dendrites and perikarya.

BIBLIOGRAPHY

Adams, J.C. (1977). Technical considerations on the use of horseradish peroxidase as a neuronal marker. Neuroscience 2: 141-145.

Ajika, K., Arai, K. and Okinaga, S. (1982). Localization of dopamine in the prolactin cell of the rat anterior pituitary gland: a fluorescence and immuno-electron microscopical study. Prog. 64th Ann. Meet. Endocr. Soc. San Francisco, Calif. (Abstr. #367).

Ajika, K. and Hökfelt, T. (1973). Ultrastructural identification of catecholamine neurones in the hypothalamic periventricular-arcuate nucleus-median eminence complex with special reference to quantitative aspect. Brain Res. 57: 97-117.

Altman, J. and Bayer, S.A. (1978a). Development of the diencephalon in the rat. I. Autoradiographic study of the time of origin and settling patterns of neurons of the hypothalamus. J. Comp. Neurol. 182: 945-972.

Altman, J. and Bayer, S.A. (1978b). Development of the diencephalon in the rat. II. Correlation of the embryonic development of the hypothalamus with the time of origin of its neurons. J. Comp. Neurol. 182: 973-994.

Altman, J. and Bayer, S.A. (1978c). Development of the diencephalon in the rat. III. Ontogeny of the specialized ventricular linings of the hypothalamic third ventricle. J. Comp. Neurol. 182: 995-1016.

Andén, N.-E., Butcher, S.G., Corrodi, H., Fuxe, K. and Ungerstedt, U. (1970). Receptor activity and turnover of dopamine and noradrenaline after neuroleptics. Eur. J. Pharmacol. 11: 303-314.

Andén, N.-E., Nilsson, H., Ros, E. and Thornström, U. (1983). Effects of B-HT 920 and B-HT 933 on dopamine and noradrenaline autoreceptors in the rat brain. Acta Pharmacol. et Toxicol. 52: 51-56.

Arluison, M., Dietl, M. and Thibault, J. (1984). Ultrastructural morphology of dopaminergic nerve terminals and synapses in the striatum of the rat using tyrosine hydroxylase immunocytochemistry: A topographical study. Brain Res. Bull. 13: 269-285.

Barraclough, C.A. (1983). The role of catecholamines in the regulation of gonadotropin secretion. Acta Morphol. Hung. 31: 101-116.

Ben-Jonathan, N., Oliver, C., Mical, R.S. and Porter, J.C. (1976). Hypothalamic secretion of dopamine into hypophysial portal blood. Fed. Proc. 35: 305 (Abstr. #547).

Ben-Jonathan, N., Oliver, C., Weiner, H.J., Mical, R.S. and Porter, J. (1977). Dopamine in hypophysial portal plasma of the rat during the estrous cycle and throughout pregancy. Endocrinology 100: 452-458.

Berger, B. and Glowinski, J. (1978). Dopamine uptake in serotoninergic terminals in vitro. A valuable tool for the histochemical differentiation of catecholaminergic and serotoninergic terminals in rat cerebral structures. Brain Res. 147: 29-45.

Björklund, A., Ehinger, B. and Falck, B. (1972). Analysis of fluorescence excitation peak ratios for the cellular identification of noradrenaline, dopamine or their mixtures. J. Histochem. Cytochem. 20: 56-64.

Björklund, A. and Lindvall, O. (1975). Dopamine in dendrites of substantia nigra neurons: suggestions for a role in dendritic terminals. Brain Res. 83: 531-537.

Björklund, A., Moore, R.Y., Nobin, A. and Stenevi, U. (1973). The organization of tubero-hypophyseal and reticulo-infundibular catecholamine neuron systems in the rat brain. Brain Res. 51: 171-191.

Björlklund, A. and Nobin, A. (1973). Fluorescence histochemical and microspectrofluorometric mapping of dopamine and noradrenaline cell groups in the rat diencephalon. Brain Res. 51: 193-205.

Bleier, R., Cohn, P. and Siggelkow, I.R. (1979). A cytoarchitectonic atlas of the hypothalamus and hypothalamic third ventricle of the rat. In: Handbook of the Hypothalamus, Vol.I: Anatomy of the Hypothalamus. P.J. Morgane and J. Panksepp (eds.), New York, M. Dekker, pp. 137-219.

Bloch, B., Bugnon, C., Fellmann, D., Lenys, D. and Gouget, A. (1979). Neurons of the rat hypothalamus reactive with antisera against endorphins, ACTH, MSH and β-LPH. Cell Tiss. Res. 204: 1-15.

Bodoky, M. and Réthelyi, M. (1977). Dendritic arborization and axon trajectory of neurons in the hypothalamic arcuate nucleus of the rat. Exp. Brain Res. 28: 543-555.

Bosler, O. and Beaudet, A. (1985). Relations ultrastructurales entre systèmes monoaminergiques et peptidergiques dans l'hypothalamus. Approche radioautographique et immunocytochimique couplée dans le noyau arqué et le noyau suprachiasmatique du rat. Ann. Endocrinol. (Paris) 46: 19-26.

Bosler, O., Bloch, B., Bugnon, C. et Calas, A. (1982). Bases morphologiques des interactions monoamines-peptides dans l'hypothalamus neuroendocrine du rat. Données radioautographiques et immunocytochimiques. Les colloques de l'INSERM. Régulations cellulaires multihormonales en neuroendocrinologie. INSERM 110: 17-36.

Bosler, O. and Calas, A. (1982). Radioautographic investigation of monoaminergic neurons. An evaluation. Brain Res. Bull. 9: 151-169.

Bosler, O., Joh, T.H. and Beaudet, A. (1984). Ultrastructural relationships between serotonin and dopamine neurons in the rat arcuate nucleus and medial zona incerta: a combined radioautographic and immunocytochemical study. Neurosci. Lett. 48: 279-285.

Brawer, J., Bertley, J. and Beaudet, A. Testosterone inhibition of tyrosine hydroxylase expression in the hypothalamic arcuate nucleus (in press).

Brawer, J.R. (1971). The role of the arcuate nucleus in the brain-pituitary-gonad axis. J. Comp. Neurol. 143: 411-445.

Brawer, J.R. and van Houten, M. (1976). Cellular organization of luteinizing hormone-releasing factor delivery systems. In: Subcellular Mechanisms in Reproductive Neuroendocrinology, F. Naftolin, K.J. Ryan and I.J. Davies (eds.), Elsevier, Amsterdam, The Netherlands, pp. 1-31.

Brownstein, M.J., Palkovits, M., Tappaz, M.L., Saavedra, J.M. and Kizer, J.S. (1976). Effect of surgical isolation of the hypothalamus on its neurotransmitter content. Brain Res. 117: 287-295.

Bunney, B.S. (1974). Dopaminergic blocking effects of antipsychotic drugs. J. Psychiatr. Res. 11: 72-73.

Carlsson, A. (1959). The occurrence, distribution and physiological role of catecholamines in the nervous system. Pharmacol. Rev. 11: 490-493.

Carlsson, A., Falck, B. and Hillarp, N.-Å. (1962). Cellular localization of brain monoamines. Acta Physiol. Scand. 56, Suppl. 196: 1-27.

Carlsson, A. and Waldeck, B. (1958). A fluorimetric method for the determination of dopamine (3-hydroxytyramine). Acta Physiol. Scand. 44: 293-298.

Chan-Palay, V., Záborszky, L., Kohler, C., Goldstein, M. and Palay, S.L. (1984). Distribution of tyrosine-hydroxylase-immunoreactive neurons in the hypothalamus of rats. J. Comp. Neurol. 227: 467-496.

Corrodi, H. and Jonsson, G. (1967). The formaldehyde fluorescence method for the histochemical demonstration of biogenic monoamines. A review on the methodology. J. Histochem. Cytochem. 15: 65-78.

Coyle, J.T. and Axelrod, J. (1972). Tyrosine hydroxylase in rat brain: developmental characteristics. J. Neurochem. 19: 1117-1123.

Crawford, T.B.B. and Outschoorn, A.S. (1951). The quantitative separation of adrenaline and noradrenaline in biological fluids and tissue extracts. Brit. J. Pharmacol. 6: 8-20.

Cuello, A.C. and Iversen, L.L. (1978). Interactions of dopamine with other neurotransmitters in the rat substantia nigra: a possible functional role of dendritic dopamine. In: Interactions between Putative Neurotransmitters in the Brain, S. Garattini, J.F. Pujol and R. Samanin (eds.), Raven Press, New York, pp.127-149.

Cuello, A.C. and Sofroniew, M.V. (1984). The anatomy of the CNS cholinergic neurons. Trends Neurosci. 7: 74-78.

Dahlström, A. and Fuxe, K. (1964). Evidence for the existence of monoamine containing neurons in the central nervous system. I. Demonstration of monoamines in the cell bodies of brainstem neurons. Acta Physiol. Scand. 62, Suppl. 232: 1-55.

Descarries, L. and Beaudet, A. (1983). The use of radioautography for investigating transmitter-specific neurons. In: Handbook of Chemical Neuroanatomy, Vol. I: Methods in Chemical Neuroanatomy, A. Björklund and T. Hökfelt (eds.), Elsevier, pp. 286-364.

Dierickx, K. and Vandesande, F. (1979). Immunocytochemical localization of somatostatin-containing neurons in the rat hypothalamus. Cell Tiss. Res. 201: 349-359.

Ellar, D.J., Nuñoz, E. and Salton, M.R.J. (1971). The effects of low concentrations of glutaraldehyde on Micrococcus lysodeikticus: changes in the release of membrane associated enzymes and membrane structure. Biochim. Biophys. Acta 225: 140-150.

Ellis, L.C. Jr. and Rustioni, A. (1981). A correlative HRP, Golgi, and EM study of the intrinsic organization of the feline dorsal column nuclei. J. Comp. Neurol. 197: 341-367.

Eriksson, E., Svensson, K. and Clark, D. (1985). The putative dopamine autoreceptor agonist B-HT 920 decreases nigral dopamine cell firing rate and prolactin release in rat. Life Sci. 36: 1819-1827.

Everett, J.W. (1954). Luteotropic function of autografts of the rat hypophysis. Endocrinology 54: 685-690.

Everitt, B.J., Hökfelt, T., Wu, J.-Y. and Goldstein, M. (1984). Coexistence of tyrosine hydroxylase-like and gamma-aminobutyric acid-like immunoreactivities in neurons of the arcuate nucleus. Neuroendocrinology 39: 189-191.

Falck, B. (1962). Observations on the possibilities of the cellular localization of monoamines by a fluorescence method. Acta Physiol. Scand. 56, Suppl. 197: 1-25.

Falck, B., Hillarp, N.-Å., Thieme, G. and Torp, A. (1962). Fluorescence of catecholamines and related compounds with formaldehyde. J. Histochem. Cytochem. 10: 348-354.

Fuxe, K. (1964). Cellular localization of monoamines in the median eminence and infundibular stem of some mammals. Z. Zellforsch. 61: 710-724.

Fuxe, K. and Hökfelt, T. (1966). Further evidence for the existence of tubero-infundibular dopamine neurons. Acta Physiol. Scand. 66: 245-246.

Fuxe, K. and Hökfelt, T. (1969). Catecholamines in the hypothalamus and the pituitary gland. In: Frontiers in Neuroendocrinology, W.F. Ganong and L. Martini (eds.), Oxford University Press, Oxford, pp. 47-96.

Fuxe, K., Hökfelt, T., Agnati, L.F., Johansson, O., Goldstein, M., Perez de la Mora, M., Possani, L., Tapia, R., Teran, L. and Palacios, R. (1978). Mapping out central catecholamine neurons: immunocytochemical studies on catecholamine-synthesizing enzymes. In: Psychopharmacology: A Generation of Progress, M.A. Lipton, A. DiMascio and K.F. Killam (eds.), New York: Raven Press, pp. 67-94.

Fuxe, K., Hökfelt, T., Agnati, L., Löfström, A., Everitt, B.J., Johansson, O., Jonsson, G., Wuttke, W. and Goldstein, M. (1976a). Role of monoamines in the control of gonadotropin secretion. In: Neuroendocrine Regulation of Fertility, A. Kumar (ed.), Karger, Basel, pp. 124-140.

Fuxe, K., Hökfelt, T. and Ungerstedt, U. (1969). Distribution of monoamines in the mammalian central nervous system by histochemical studies. In: Metabolism of Amines in the Brain, G. Hooper (ed.), Macmillan, London, pp. 10-22.

Fuxe, K., Löfström, A., Eneroth, P., Gustafsson, J.A., Hökfelt, T., Skett, P., Wuttke, W., Fraser, H. and Jeffcoate, S. (1976b). Interactions between hypothalamic catecholamine nerve terminals and LRF containing neurons. Further evidence for an inhibitory dopaminergic and a facilitatory noradrenergic influence. Excerpta Medica International Congress Series, No. 374.

Fuxe, K., Löfström, A., Eneroth, P., Gustafsson, J.-Å., Skett, P., Hökfelt, T., Wiesel, F.-A. and Agnati, L. (1977). Involvement of central catecholamines in the feedback actions of 17β-estradiolbenzoate on luteinizing hormone secretion in the ovariectomized rat. Psychoneuroendocrinology 2: 203-225.

Fuxe, K. and Ungerstedt, U. (1968). Histochemical studies on the effect of (+)-amphetamine, drugs of the impramine group and tryptamine on central catecholamine and 5-hydroxytryptamine neurons after intraventricular injection of catecholamines and 5-hydroxytryptamine. Eur. J. Pharmacol. 4: 135-144.

Geffen, L.B., Jessell, T.M., Cuello, A.C. and Iversen, L.L. (1976). Release of dopamine from dendrites in rat substantia nigra. Nature 260: 258-260.

Gibbs, D.M. and Neill, J.D. (1978). Dopamine levels in hypophysial stalk blood in the rat are sufficient to inhibit prolactin secretion in vivo. Encocrinology 102: 1895-1900.

Gobel, S., Falls, W.M., Bennet, G.J., Abdelmoumene, M., Hayashi, H. and Humphrey, E. (1980). An EM analysis of the synaptic connections of horseradish peroxidase-filled stalked cells and islet cells in the substantia gelatinosa of adult cat spinal cord. J. Comp. Neurol. 194: 781-807.

Goldsmith, P.C., Cronin, M.J. and Weiner, R.I. (1979). Dopamine receptor sites in the anterior pituitary. J. Histochem. Cytochem. 27: 1205-1207.

Graham, R.C. Jr. and Karnovsky, M.J. (1966). The early stages of absorption of injected horseradish peroxidase in the proximal tubules of mouse kidney: ultrastructural cytochemistry by a new technique. J. Histochem. Cytochem. 14: 291-302.

Grant, L.D. and Stumpf, W.E. (1973). Localization of ^{3}H-estradiol and catecholamines in identical neurons in the hypothalamus. Abstracts of the Histochemical Society 21:404(6).

Grant, L.D. and Stumpf, W.E. (1981). Combined autoradiography and formaldehyde-induced fluorescence methods for localization of radioactively labeled substances in relation to monoamine neurons. J. Histochem. Cytochem. 29: 175-180.

Groves, P.M. and Wilson, C.J. (1980). Monoaminergic presynaptic axons and dendrites in locus coeruleus as seen in reconstructions of serial sections. J. Comp. Neurol. 193: 853-862.

Groves, P.M., Wilson, C.J., Young, S.J. and Rebec, G.V. (1975). Self-inhibition by dopaminergic neurons. Science 190: 522-529.

Hajdu, F., Hassler, R. and Bak, I.J. (1973). Electron microscopic study of the substantia nigra and the strio-nigral projection in the rat. Z. Zellforsch. 146: 207-221.

Hattori, T., McGeer, P.L. and McGeer, E.G. (1979). Dendro-axonic neurotransmission: II. Morphological sites for the synthesis, binding and release of neurotransmitters in dopaminergic dendrites in the substantia nigra and cholinergic dendrites in the neostriatum. Brain Res. 170: 71-83.

Heritage, A.S., Stumpf, W.E., Sar, M. and Grant, L.D. (1980). Brainstem catecholamine neurons are target sites for sex steroid hormones. Science 207: 1377-1379.

Hisano, S., Kawano, H., Nishiyama, T. and Daikoku, S. (1982). Immunoreactive ACTH/β-endorphin neurons in the tubero-infundibular hypothalamus of rats. Cell Tiss. Res. 224: 303-314.

Hodges, G.M., Smolira, M.A. and Livingston, D.C. (1984). Scanning electron microscope immunocytochemistry in practice. In: Immunolabelling for Electron Microscopy, J.M. Polak and I.M. Varndell (eds.), Elsevier, New York, pp. 189-233.

Hökfelt, T. and Fuxe, K. (1971). On the morphology and the neuroendocrine role of the hypothalamus catecholamine neurons. In: Brain-Endocrine Interaction. Median Eminence: Structure and Function, K.M. Knigge, D.E. Scott and A. Weindl (eds.), Karger, Basel, pp. 181-223.

Hökfelt, T., Fuxe, K., Goldstein, M. and Joh, T.H. (1973). Immunohistochemical localization of three catecholamine synthesizing enzymes: aspects on methodology. Histochemie 33: 231-254.

Hökfelt, T., Johansson, O., Fuxe, K., Goldstein, M. and Park, D. (1976). Immunohistochemical studies on the localization and distribution of monoamine neuron systems in the rat brain. I. Tyrosine hydroxylase in the mes- and diencephalon. Med. Biol. 54: 427-453.

Hökfelt, T., Johansson, O. and Goldstein, M. (1984a). Central catecholamine neurons are revealed by immunohistochemistry with special reference to adrenaline neurons. In: Handbook of Chemical Neuroanatomy, A. Bjorklund and T. Hokfelt (eds.), Vol. 2, Part I: Classical Transmitters in the CNS, Elsevier, New York, pp. 157-276.

Hökfelt, T., Mårtensson, R., Björklund, A., Kleinau, S. and Goldstein, M. (1984b). Distributional maps of tyrosine-hydroxylase-immunoreactive neurons in the rat brain. In: Handbook of Chemical Neuroanatomy, A. Björklund and T. Hökfelt (eds.), Vol. 2, Part I: Classical Transmitters in the CNS, Elsevier, New York, pp. 277-379.

Hsu, S.M., Raine, L. and Fanger, H. (1981). The use of avidin-biotin-peroxidase complex (ABC) in immunoperoxidase techniques: a comparison between ABC and unlabeled antibody (PAP) procedures. J. Histochem. Cytochem. 29: 577-590.

Hyyppä, M. (1969). A histochemical study of the primary catecholamines in the hypothalamic neurons of the rat in relation to the ontogenic and sexual differentiation. Z. Zellforsch. 98: 550-560.

Jaim-Etcheverry, G. and Pellegrino de Iraldi, A. (1968). Ultrastructure of neurons in the arcuate nucleus of the rat. Anat. Rec. 160: 239-254.

Janssen, P.A.J. and Allewijn, F.T.N. (1968). Pimozide, a chemically novel, highly potent and orally long-acting neuroleptic drug. Part II: Kinetic study of the distribution of pimozide and metabolites in brain, liver, and blood of the Wistar rat. Arzneim.-Forsch. 18: 279-282.

Jimenez, A.E., Meyer, D.C. and Murphy, P.J. (1984). Developmental patterns of tyrosine hydroxylase activity in discrete central nervous system regions and serum LH and prolactin in the prepubertal rat. Neuroendocrinology 38: 134-138.

Joh, T.H., Gegham, C. and Reis, D.H. (1973). Immunochemical demonstration of increased tyrosine hydroxylase protein in sympathetic ganglia and adrenal medulla elicited by reserpine. Proc. Natl. Acad. Sci. U.S.A. 70: 2767-2771.

Joh, T.H. and Reis, D.J. (1974). Different forms of tyrosine hydroxylase in noradrenergic and dopaminergic systems in brain. Fed. Proc. 33: 535 (Abstr. #1828).

Joh, T.H. and Reis, D.J. (1975). Different forms of tyrosine hydroxylase in central dopaminergic and noradrenergic neurons and sympathetic ganglia. Brain Res. 85: 146-151.

Joh, T.H. and Ross, M.E. (1983). Preparation of catecholamine-synthesizing enzymes as immunogens for immunohistochemistry. In: Immunohistochemistry, A.C. Cuello (ed.), Ibro Handbook Series: Methods in the Neurosciences, Vol. 3, John Wiley and Sons, Chichester, pp. 121-138.

Johansson, O. and Hökfelt, T. (1980). Thyrotropin releasing hormone, somatostatin, and enkephalin: distribution studies using immunohistochemical techniques. J. Histochem. Cytochem. 28: 364-366.

Jonsson, G., Fuxe, K. and Hökfelt, T. (1972). On the catecholamine innervation of the hypothalamus, with special reference to the median eminence. Brain Res. 40: 271-281.

Kamberi, I.A., Mical, R.S. and Porter, J.C. (1970a). Effect of anterior pituitary perfusion and intraventricular injection of catecholamines and indolamines on LH release. Endocrinology 87: 1-12.

Kamberi, I.A., Mical, R.S. and Porter, J.C. (1970b). Effect of anterior pituitary perfusion and intraventricular injection of catecholamines on FSH release. Endocrinology 88: 1003-1011.

Kamberi, I.A., Mical, R.S. and Porter, J.C. (1971). Pituitary portal vessel infusion of hypothalamic extract and release of LH, FSH and prolactin. Endocrinology 88: 1294-1299.

Kamberi, I.A., Schneider, H.P.G. and McCann, S.M. (1970c). Action of dopamine to induce release of FSH-releasing factor (FRF) from hypothalamic tissue in vitro. Endocrinology 86: 278-284.

Kizer, J.S., Humm, J., Nicholson, G., Greeley, G. and Youngblood, W. (1978). The effect of castration, thyroidectomy and haloperidol upon the turnover rates of dopamine and norepinephrine and the kinetic properties of tyrosine hydroxylase in discrete hypothalamic nuclei of the male rat. Brain Res. 146: 95-107.

Kobayashi, T., Kobayashi, T., Yamamoto, K. and Kaibara, M. (1967). Electron microscopic observation on the hypothalamo-hypophyseal system in the rat. II. Ultrafine structure of the median eminence and of the nerve cells of the arcuate nucleus. Endocrinol. Jpn. 14: 158-177.

Kordon, C. and Glowinski, J. (1972). Role of hypothalamic monoaminergic neurones in the gonadotrophin release-regulating mechanisms. Neuropharmacology 11: 153-162.

Korf, J., Zieleman, M. and Westerink, B.H. (1976). Dopamine release in substantia nigra. Nature 260: 257-258.

László, S. (1985). Postnatal neurogenesis in the rat hypothalamus. Develop. Brain Res. 22: 156-160.

Leong, D.A., Frawley. L.S. and Neill, J.D. (1983). Neuroendocrine control of prolactin secretion. Ann. Rev. Physiol. 45: 109-127.

Léránth, C., Sakamoto, H., Maclusky, N.J., Shanabrough, M. and Naftolin, F. (1985a). Application of avidin-ferritin and peroxidase as contrasting electron-dense markers for simultaneous electron microscopic immunocytochemical labelling of glutamic acid decarboxylase and tyrosine hydroxylase in the rat arcuate nucleus. Histochemistry 82: 165-168.

Léránth, C., Sakamoto, H., Maclusky, N.J., Shanabrough, M. and Naftolin, F. (1985b). Intrinsic tyrosine hydroxylase (TH) immunoreactive axons synapse with TH immunopositive neurons in the rat arcuate nucleus. Brain Res. 331: 371-375.

Levitt, M., Spector, S., Sjoerdsma, A. and Udenfriend, S. (1965). Elucidation of the rate-limiting step in norepinephrine biosynthesis in the perfused guinea-pig heart. J. Pharmacol. Exp. Ther. 148: 1-8.

Lichtensteiger, W. and Langemann, H. (1966). Uptake of exogenous catecholamines by monoamine-containing neurons of the central nervous system. Uptake of catecholamines by arcuato-infundibular neurons. J. Pharmacol. Exp. Ther. 151: 400-408.

Löfström, A. (1977). Catecholamine turnover alterations in discrete areas of the median eminence of the 4- and 5-day cyclic rat. Brain Res. 120: 113-131.

Löfström, A., Eneroth, P., Gustafsson, J.-Å. and Skett, P. (1977). Effects of estradiol benzoate on catecholamine levels and turnover in discrete areas of the median eminence and the limbic forebrain, and on serum luteinizing hormone, follicle stimulating hormone and prolactin concentrations in the ovariectomized female rat, Endocrinology 101: 1559-1569.

Loizou, L.A. (1969). The development of monoamine-containing neurones in the brain of the albino rat. J. Anat. (Lond.) 104: 588 (Abstr.).

Loizou, L.A. (1971a). Effects of inhibition of catecholamine synthesis on central catecholamine-containing neurones in the developing albino rat. Brit. J. Pharmacol. 41: 41-48.

Loizou, L.A. (1971b). The postnatal development of monoamine-containing structures in the hypothalamo-hypophyseal system of the albino rat. Z. Zellforsch. 114: 234-252.

Loizou, L.A. (1972). The postnatal ontogeny of monoamine-containing neurones in the central nervous system of the albino rat. Brain Res. 40: 395-418.

Luine, V.N., McEwen, B. and Black, I.B. (1977). Effect of 17β-estradiol on hypothalamic tyrosine hydroxylase activity. Brain Res. 120: 188-192.

MacLeod, R.M. and Lehmeyer, J.E. (1974). Studies on the mechanism of the dopamine-mediated inhibition of prolactin secretion. Endocrinology 94: 1077-1085.

Matsumoto, A. and Arai, Y. (1976). Developmental changes in synaptic formation in the hypothalamic arcuate nucleus of female rats. Cell Tiss. Res. 169: 143-156.

Matsumoto, A. and Arai, Y. (1979). Synaptogenic effect of estrogen on the hypothalamic arcuate nucleus of the adult female rat. Cell. Tiss. Res. 198: 427-433.

McCann, S.M., Kalra, P.S., Donoso, A.O., Bishop, W., Schneider, H.P.G., Fawcett, C.P. and Krulich, L. (1971). The role of monoamines in the control of gonadotropin and prolactin secretion. In: Brain-Endocrine Interaction. Median Eminence: Structure and Function. K.M. Knigge, D.E. Scott and A. Weindl (eds.), Karger, Basel, pp. 221-235.

McCann, S.M. and Moss, R.L. (1975). Putative neurotransmitters involved in discharging gonadotropin-releasing neurohormones and the action of LH-releasing hormone on the CNS. Life Sci. 16: 833-852.

Mercer, L., del Fiacco, M. and Cuello, A.C. (1979). The smooth endoplasmic reticulum as a possible storage site for dendritic dopamine in substantia nigra neurons. Experientia 35: 101-103.

Merchenthaler, I., Vigh, S., Schally, A.V. and Petrusz (1984). Immunocytochemical localization of growth hormone-releasing factor in the rat hypothalamus. Endocrinology 114: 1082-1085.

Millhouse, O.E. (1979). A Golgi anatomy of the rodent hypothalamus. In: Handbook of the Hypothalamus, Vol. I: Anatomy of the Hypothalamus. P.J. Morgane and J. Panksepp (eds.), New York: M. Dekker, pp. 221-265.

Miyachi, Y., Mecklenburg, R.S. and Lipsett, M.B. (1973). In vitro studies of pituitary-median eminence unit. Endocrinology 93: 492-496.

Nadler, N.J. (1979). Quantitation and resolution in electron microscope radioautography. J. Histochem. Cytochem. 27: 1531-1533.

Nagatsu, T., Levitt, M. and Udenfriend, S. (1964). The initial step in norepinephrine biosynthesis. J. Biol. Chem. 239: 2910-2917.

Nieoullon, A., Cheramy, A. and Glowinski, J. (1977a). Release of dopamine in vivo from cat substantia nigra. Nature 266: 357-377.

Nieoullon, A., Cheramy, A. and Glowinski, J. (1977b). Release of dopamine from terminals and dendrites of the two nigro-striatal dopaminergic pathways in response to unilateral sensory stimuli in the cat. Nature 269: 340-342.

Oertel, W.H., Mugnaini, E., Schmechel, D.E., Tappaz, M.L. and Kopin, I.J. (1982). The immunocytochemical demonstration of gamma-aminobutyric acid-ergic neurons --- Methods and application. In: Neurology and Neurobiology, Vol. I: Cytochemical Methods in Neuroanatomy. V. Chan-Palay and S.L. Palay (eds.), Alan R. Liss, New York, pp. 297-329.

Ojeda, S.R., Harms, P.G. and McCann, S.M. (1974). Possible role of cyclic AMP and prostaglandin E, in the dopaminergic control of prolactin release. Endocrinology 95: 1694-1703.

Ojeda, S.R. and McCann, S.M. (1974). Development of dopaminergic and estrogenic control of prolactin release in the female rat. Endocrinology 95: 1499-1505.

Ouimet, C.C., Miller, P.E., Hemmings, H.C. Jr., Walaas, S.I. and Greengard, P. (1984). DARPP-32, a dopamine- and adenosine 3':5'-monophosphate-regulated phosphoprotein enriched in dopamine-innervated brain regions. III. Immunocytochemical localization. J. Neurosci. 4: 111-124.

Palkovits, M., Mezey, E., Záborszky, L., Feminger, A., Versteeg, D.H.G., Wijnen, H.L.J.M., De Jong, W., Fekéte, M.I.K., Herman, J.P. and Kanyicska, B. (1980a). Adrenergic innervation of the rat hypothalamus. Neurosci. Lett. 18: 237-243.

Palkovits, M., Záborszky, L., Feminger, A., Mezey, E., Fekete, M.I.K., Herman, J.P., Kanyicska, B. and Szabó, D. (1980b). Noradrenergic innervation of the rat hypothalamus: experimental biochemical and electron microscopic studies. Brain Res. 191: 161-171.

Paton, D.M. (1980). Neuronal transport of noradrenaline and dopamine. Pharmacology 21: 85-92.

Peters, A., Palay, S.L. and Webster, H.deF. (1976). The fine structure of the nervous system: the neurons and supporting cells. W.B. Saunders Co., Philadelphia.

Petrusz, P., Sar, M., Ordronneau, P. and DiMeo, P. (1976). Specificity in immunocytochemical staining. J. Histochem. Cytochem. 24: 1110-1112.

Pickel, V.M. (1981). Immunocytochemical methods. In: Neuroanatomical Tract-Tracing Methods. L. Heimer and M.J. Robards (eds.), pp. 483-509.

Pickel, V.M. (1982). Immunocytochemical methodology for the ultrastructural idendification of neurotransmitter-specific neurons. In: Cytochemical Methods in Neuroanatomy. V. Chan-Palay and S.L Palay (eds.), Alan R. Liss, New York, pp. 229-240.

Pickel, V.M., Beckley, S.C., Joh, T.H. and Reis, D.J. (1981). Ultrastructural immunocytochemical localization of tyrosine hydroxylase in the neostriatum. Brain Res. 225: 373-385.

Pickel, V.M., Joh, T.H., Field, P.M., Becker, C.C. and Reis, D. J. (1975). Cellular localization of tyrosine hydroxylase by immunohistochemistry. J. Histochem. Cytochem. 23: 1-12.

Pickel, V.M., Joh, T.H. and Reis, D.J. (1976). Monoamine-synthesizing enzymes in central dopaminergic, noradrenergic and serotonergic neurons. Immunocytochemical localization by light and electron microscopy. J. Histochem. Cytochem. 24: 792-806.

Piotte, M., Beaudet, A., Joh, T.H. and Brawer, J.R. (1985). The fine structural organization of tyrosine hydroxylase immunoreactive neurons in rat arcuate nucleus. J. Comp. Neurol. 239: 44-53.

Plotsky, P.M., Gibbs, D.M. and Neill, J.D. (1978). Liquid chromatographic-electrochemical measurement of dopamine in hypophysial stalk blood of rats. Endocrinology 102: 1887-1894.

Rakic, P. (1971). Neuron-glia relationship during granule cell migration in developing cerebellar cortex. A Golgi and electronmicroscopic study in Macacus Rhesus. J. Comp. Neurol. 141: 283-312.

Rakic, P. (1972). Mode of cell migration to the superficial layers of fetal monkey neocortex. J. Comp. Neurol. 145: 61-84.

Rees, T.S. and Karnovsky, M.J. (1967). Fine structural localization of blood-brain barrier to exogenous peroxidase. J. Cell. Biol. 34: 207-217.

Reubi, J.C. and Sandri, C. (1979). Ultrastructural observations on intercellular contacts of nigral dendrites. Neurosci. Lett. 13: 183-188.

Richards, G. (1983). Ultrastructural visualization of biogenic monoamines. In: Handbook of Chemical Neuroanatomy, Vol. I: Methods in Chemical Neuroanatomy, A. Björklund and T. Hökfelt (eds.), Elsevier, pp. 122-146.

Romansky, K.V., Usunoff, K.G. and Ivanov, D.P. (1980). Vesicle containing dendrites in the subthalamic nucleus of the cat. J. Hirnforsch 21: 515-521.

Rubinstein, L. and Sawyer, C.H. (1970). Role of catecholamines in the release of pituitary ovulating hormone(s) in rat. Endocrinol. 86: 988-995.

Ruggiero, D.A., Ross, C.A., Anwar, M., Park, D.H., Joh, T.H. and Reis, D.J. (1985). Distribution of neurons containing phenylethanolamine-N-methyltransferase in medulla and hypothalamus of rat. J. Comp. Neurol. 239: 127-154.

Salpeter, M.M., McHenry, F.A. and Salpeter, E.E. (1978). Resolution in electron microscope autoradiography. IV. Application to analysis of autoradiographs. J. Cell. Biol. 76: 127-145.

Sar, M. (1984). Estradiol is concentrated in tyrosine hydroxylase-containing neurons of the hypothalamus. Science 223: 938-940.

Schneider, H.P.G. and McCann, M. (1969). Possible role of dopamine as transmitter to promote discharge of LH-releasing factor. Endocrinology 85: 121-132.

Schneider, H.P.G. and McCann, S.M. (1970). Mono- and indolamines and control of LH secretion. Endocrinology 86: 1127-1133.

Scott, D.E., McNeill, T.H., Krobisch-Dudley, G. (1978a). Fine structural localization of radiolabelled L-Dopa in the mammalian hypothalamus. In: Brain Endocrine Interaction. III. Neural Hormones and Reproduction, D.E. Scott, G.P. Kozlowski and A. Weindl (eds.), Karger, Basel, pp. 228-237.

Scott, D.E., Scott, P.M. and Krobisch-Dudley, G. (1978b). Ultrastructural localization of radiolabelled L-Dopa in the endocrine hypothalamus of the rat. Cell Tiss. Res. 195: 29-43.

Scott, D.E., Sladek, J.R., Knigge, K.M., Krobish-Dudley, G., Kent, D.L. and Sladek, C.D. (1976). Localization of dopamine in the endocrine hypothalamus of the rat. Cell Tiss. Res. 166: 461-473.

Seiger, Å. and Olson, L. (1973). Late prenatal ontogeny of central monoamine neurons in the rat: fluorescence histochemical observations. Z. Anat. Entwickl.-Gesch. 140: 281-318.

Shaar, C.J. and Clemens, J.A. (1974). The role of catecholamines in the release of anterior pituitary prolactin in vitro. Endocrinology 95: 1202-1212.

Silverman, A.-J., Hou-Yu, A. and Oldfield, B.J. (1983). Ultrastructural identification of noradrenergic nerve terminals and vasopressin-containing neurons of the paraventricular nucleus in the same thin section. J. Histochem. Cytochem. 31: 1151-1156.

Sloper, J.J. (1971). Dendro-dendritic synapses in the primate motor cortex. Brain Res. 34: 186-192.

Smith, G.C. and Fink, G. (1972). Experimental studies on the origin of monoamine-containig fibres in the hypothalamo-hypophysial complex of the rat. Brain Res. 43: 37-51.

Sofroniew, M.V. (1979). Immunoreactive β-endorphin and ACTH in the same neurons of the hypothalamic arcuate nucleus in the rat. Am. J. Anat. 154: 283-289.

Somogyi, P. and Takagi, H. (1982). A note on the use of picric acid-paraformaldehyde-glutaraldehyde fixation for correlated light and electron microscopic immunocytochemistry. Neuroscience 7: 1779-1783.

Specht, L.A., Pickel, V.M., Joh, T.H. and Reis, D.J. (1981a). Light-microscopic immunocytochemical localization of tyrosine hydroxylase in prenatal rat brain. I. Early ontogeny. J. Comp. Neurol. 199: 233-253.

Specht, L.A., Pickel, V.M., Joh, T.H. and Reis, D.J. (1981b). Light-microscopic immunocytochemical localization of tyrosine hydroxylase in prenatal rat brain. II. Late ontogeny. J. Comp. Neurol. 199: 255-276.

Sternberger, L.A. (1974). Immunocytochemistry. Englewood Cliffs, New Jersey, Prentice-Hall.

Sternberger, L.A. (1979a). Neurocytochemistry. In: Immunocytochemistry, 2nd ed., Wiley Medical Publication, New York, pp. 193-261.

Sternberger, L.A. (1979b). The unlabeled antibody peroxidase-antiperoxidase (PAP) method. In: Immunocytochemistry, 2nd ed., Wiley Medical Publication, New York, pp. 104-169.

Stumpf, W.E. (1968). Estradiol-concentrating neurons: topography in the hypothalamus by dry-mount autoradiography. Science 162: 1001-1003.

Swanson, L.W. and Hartman, B.K. (1975). The central adrenergic system. An immunofluorescence study of the location of cell bodies and their efferent connections in the rat utilizing dopamine-β-hydroxylase as a marker. J. Comp. Neurol. 163: 467-506.

Szentágothai, J., Flerkó, B., Mess, B. and Halász, B. (eds.) (1972). Hypothalamic control of the anterior pituitary, Akademia Kiado, Budapest.

Tagerud, S.E.O. and Cuello, A.C. (1979). Dopamine release from the rat substantia nigra in vitro. Effect of raphe lesions and veratridine stimulation. Neuroscience 4: 2021-2029.

Takahara, J., Arimura, A. and Schally, V. (1974). Suppression of prolactin release by a purified porcine PIF preparation and catecholamines infused into a rat hypophysial portal vessel. Endocrinology 95: 462-465.

Tobias, H., Carr, L.A. and Voogt, J.L. (1981). Effect of estradiol benzoate and clomiphene on tyrosine hydroxylase activity and on luteinizing hormone and prolactin levels in ovariectomized rats. Life Sci. 29: 711-716.

Tobias, H., Carr, L.A. and Voogt, J.L. (1983). Catecholamine mechanisms in the feedback effects of estradiol benzoate on the release of LH and prolactin. Proc. Soc. Expt. Biol. Med. 174: 284-290.

Tranzer, J.P. and Richards, J.G. (1976). Ultrastructural cytochemistry of biogenic amines in nervous tissue: methodologic improvements. J. Histochem. Cytochem. 24: 1178-1193.

Tranzer, J.P. and Thoenen, H. (1968). An electron miocroscopic study of selective, acute degeneration of sympathetic nerve terminals after administration of 6-hydroxydopamine. Experientia 24: 155-156.

van den Pol, A.N. and Cassidy, J.R. (1982). The hypothalamic arcuate nucleus of rat --- A quantitative Golgi analysis. J. Comp. Neurol. 204: 65-98.

van den Pol, A.N., Herbst, R.S. and Powell, J.F. (1984). Tyrosine hydroxylase-immunoreactive neurons of the hypothalamus: a light and electron microspic study. Neuroscience 13: 1117-1156.

van Maanen, J.H. and Smelik, P.G. (1968). Induction of pseudopregnancy in rats following local depletion of monoamines in the median eminence of the hypothalamus. Neuroendocrinology 3: 177-186.

Vijayan, E. and McCann, S.M. (1978). Re-evaluation of the role of catecholamines in control of gonadotropin and prolactin release. Neuroendocrinology 25: 150-165.

Vogt, M. (1954). The concentration of sympathin in different parts of the central nervous system under normal conditions and after the administration of drugs. J. Physiol. (Lond.) 123: 451-481.

Walsh, R.J. and Brawer, J.R. (1979). Cytology of the arcuate nucleus in newborn male and female rats. J. Anat. 128: 121-133.

Walsh, R.J., Brawer, J.R. and Naftolin, F. (1982). Early postnatal development of the arcuate nucleus in normal and sexually reversed male and female rats. J. Anat. 135: 733-744.

Wassef, M., Berod, A. and Sotelo, C. (1981). Dopaminergic dendrites in the pars reticulata of the rat substantia nigra and their striatal input. Combined immunocytochemical localization of tyrosine hydroxylase and anterograde degeneration. Neuroscience 6: 2125-2139.

Weiner, N. (1970). Regulation of norepinephrine biosynthesis. Annu. Rev. Pharmacol. 10: 273-290.

Weiner, N., R.I., Blake, A. and Sawyer, C.H.(1971). Effects of deafferentation on hypothalamic catecholamine content. Fed. Proc. 30: 253 (Abstr. #336)

Weiner, R.I. and Ganong, W.F. (1978). Role of brain monoamines and histamine in the regulation of anterior pituitary secretion. Physiol. Rev. 58: 905-976.

Wiesel, F.-A., Fuxe, K., Hökfelt, T. and Agnati, L.F. (1978). Studies on dopamine turnover in ovariectomized or hypophysectomized female rats. Effects of 17β-estradiol benzoate, ethynodioldiacetate and ovine prolactin. Brain Res. 148: 399-411.

Wilson, C.J., Groves, P.M. and Fifková, E. (1977). Monoaminergic synapses, including dendro-dendritic synapses in the rat substantia nigra. Exp. Brain Res. 30: 161-174.

Wood, J.G. (1966). Electron microscopic localization of amines in central nervous tissue. Nature (Lond.) 209: 1131-1133.

Wood, J.G. and Barrnett, R.J. (1964). Histochemical demonstration of norepinephrine at a fine structural level. J. Histochem. Cytochem. 12: 197-209.

Yagi, K. and Sawaki, Y. (1975). Recurrent inhibition and facilitation: demonstration in the tubero-infundibular system and effects of strychnine and picrotoxin. Brain Res. 84: 155-159.

Záborszky, L. (1982). Afferent connections of the medial basal hypothalamus. Adv. Anat. Embryol. Cell Biol. 69: 1-107.

Záborszky, L., Brownstein, M.J. and Palkovits, M. (1977). Ascending projections to the hypothalamus and limbic nuclei from the dorsolateral pontine tegmentum: a biochemical and electron microscopic study. Acta Morphol. Acad. Sci. Hung. 25: 175-189.

Plate 1

TH positive nerve cell bodies from representative coronal sections taken from 4 different levels of the arcuate nucleus of a normally cycling female rat (CII). A range of staining intensity is observed. The intensely immunoreactive perikarya are totally black while the lightly stained cells are empty-looking. la is more rostral and lg is more caudal. Scale: 100 μm

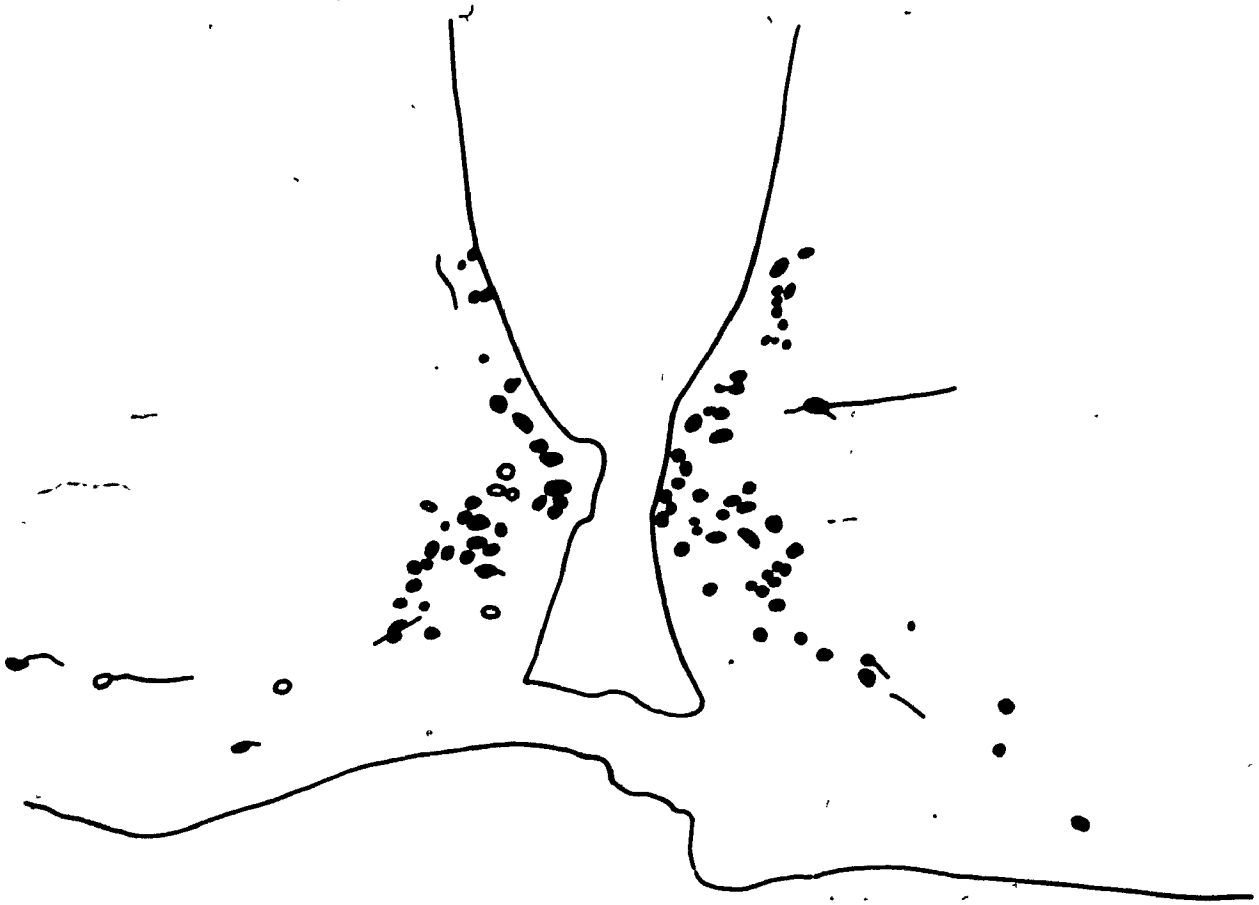

Plate 1a (level B)

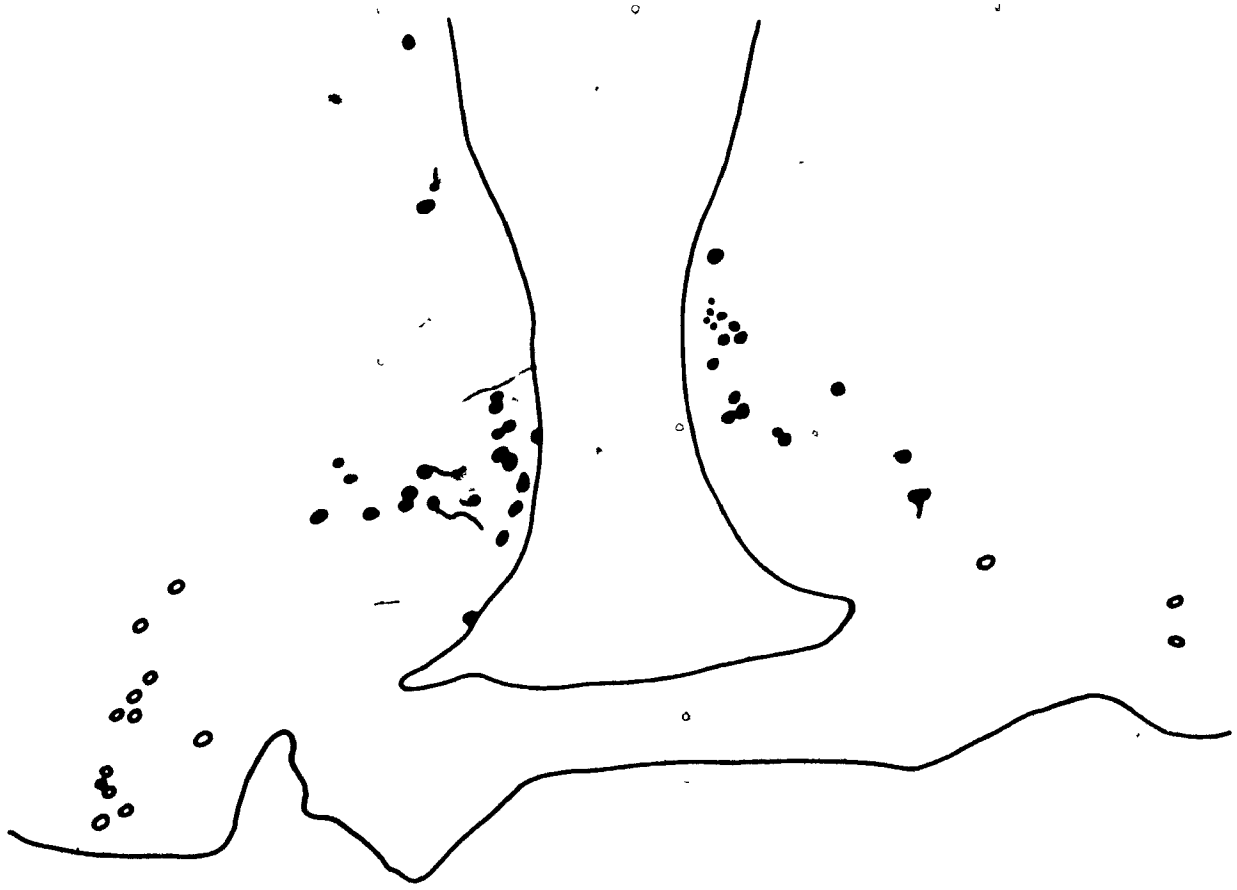

Plate 1b (level C)

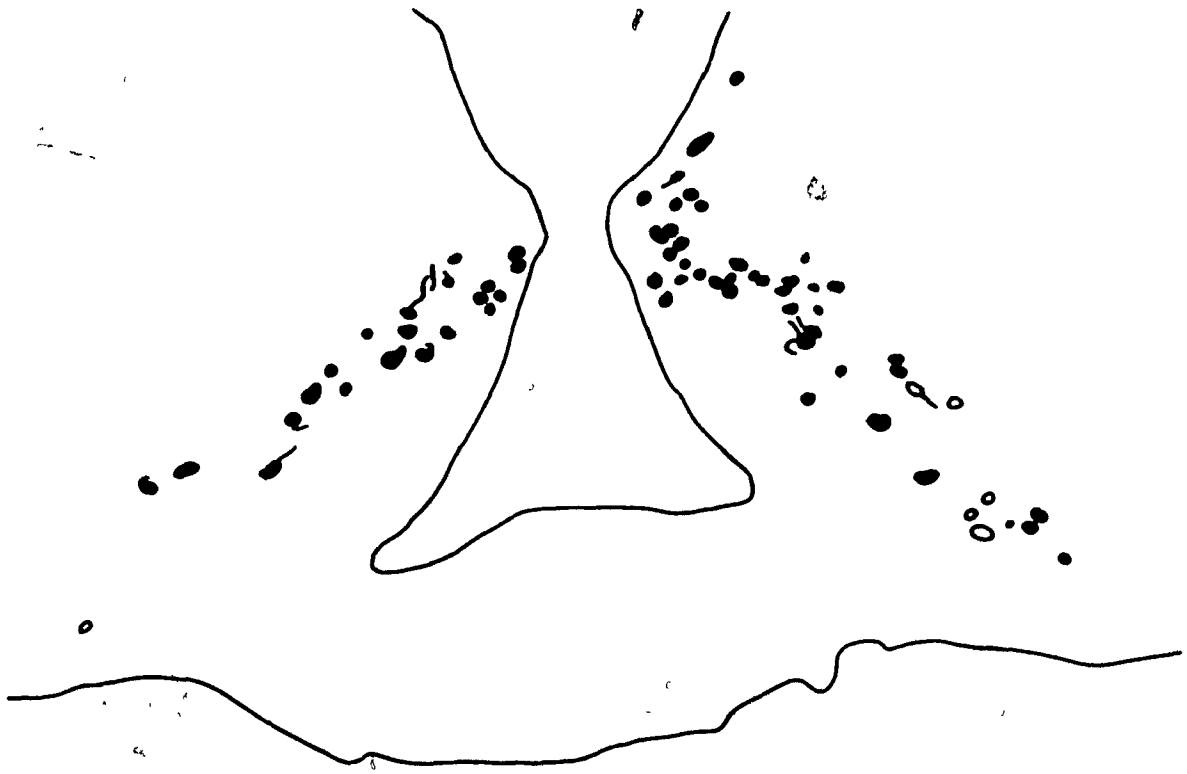

Plate 1c (level C)

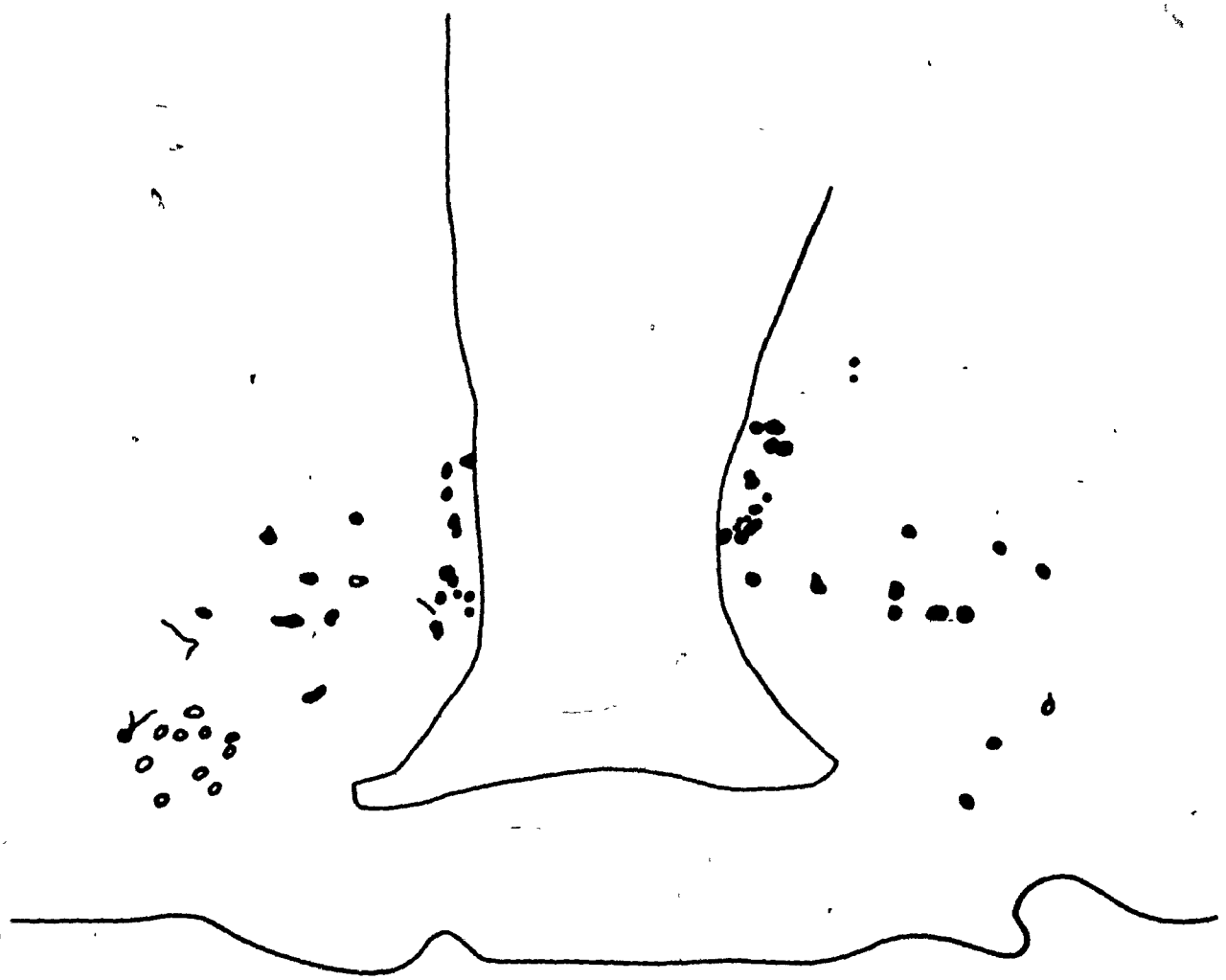

Plate 1d (level C)

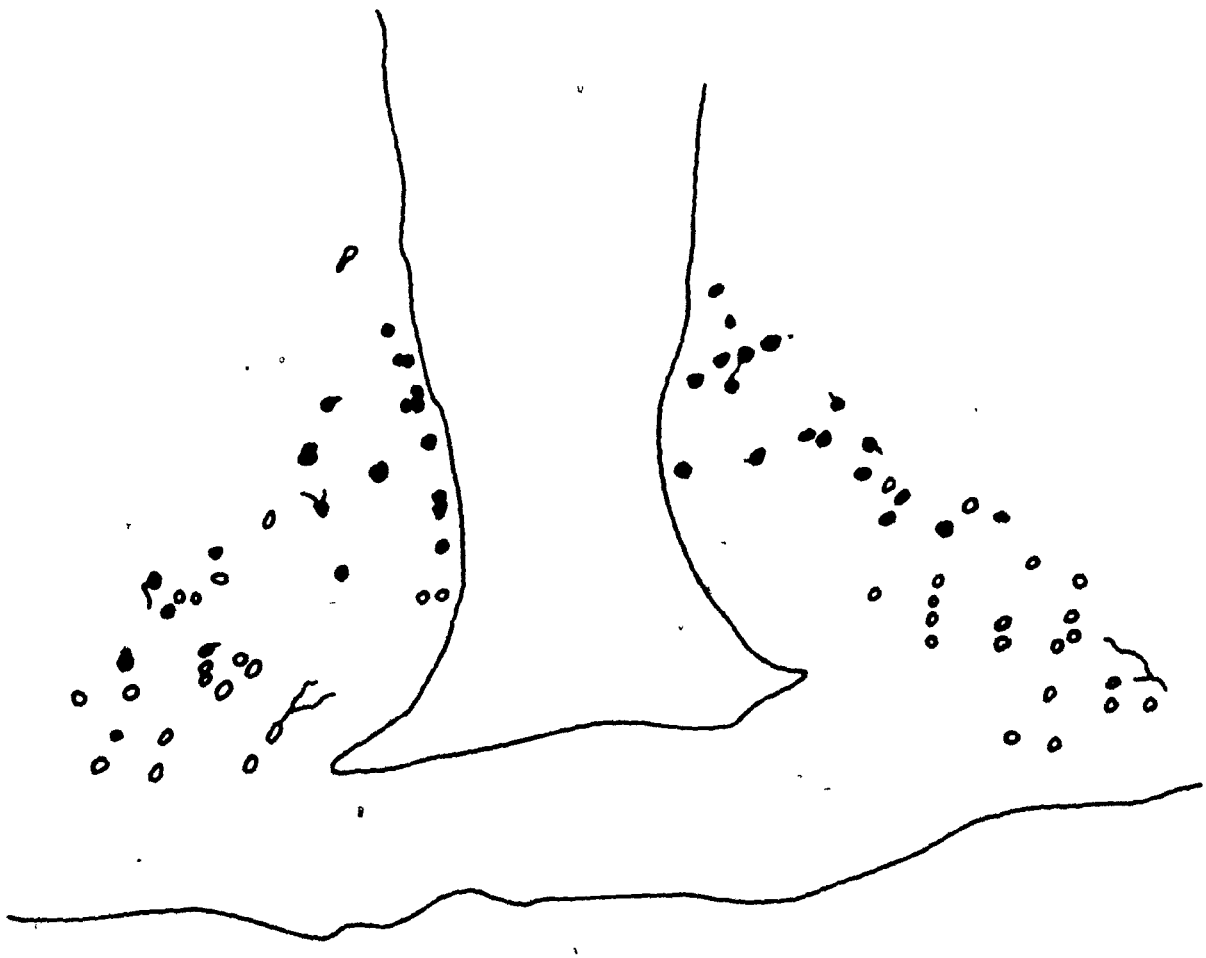

Plate 1e (level D)

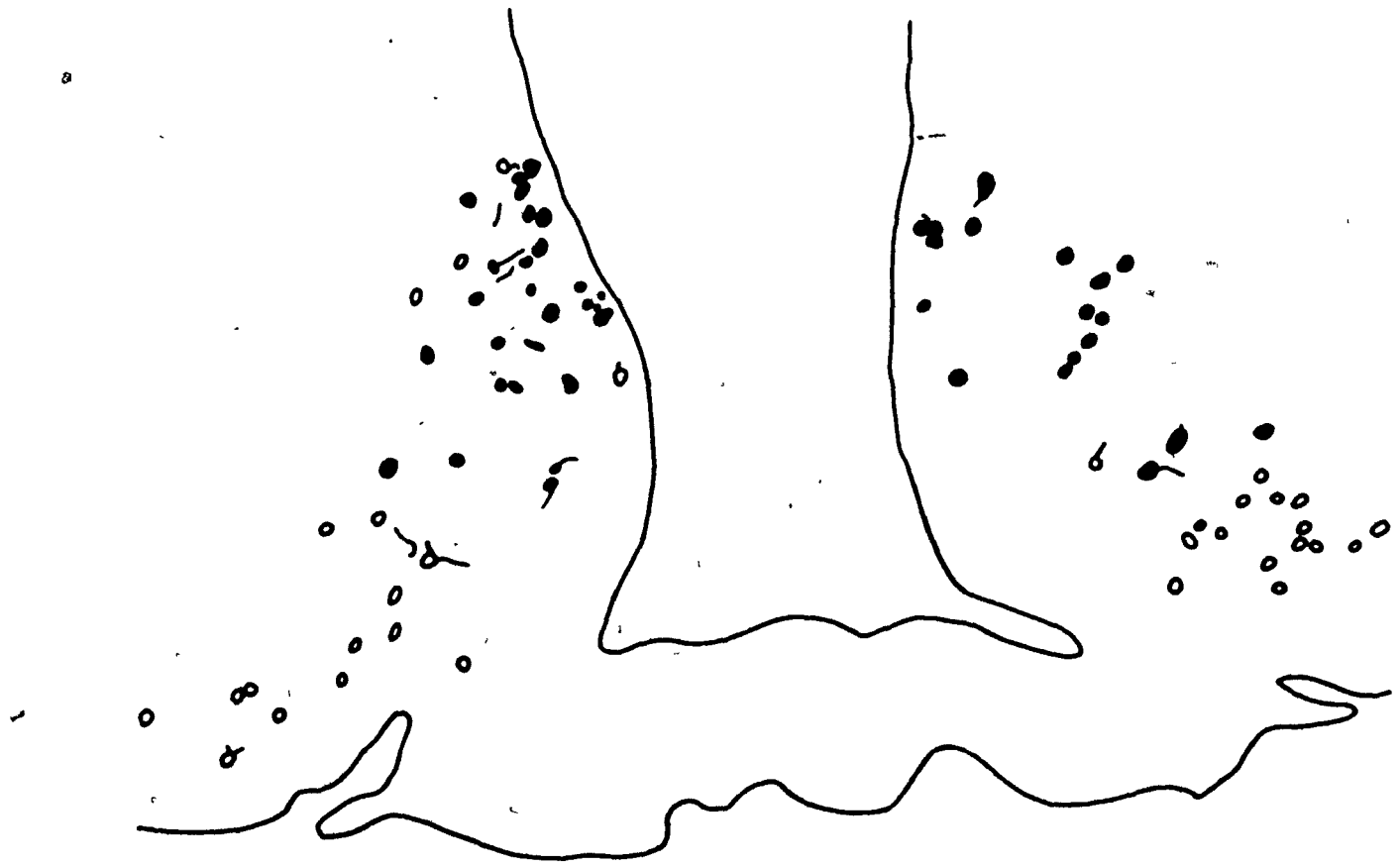

Plate 1f (level D)

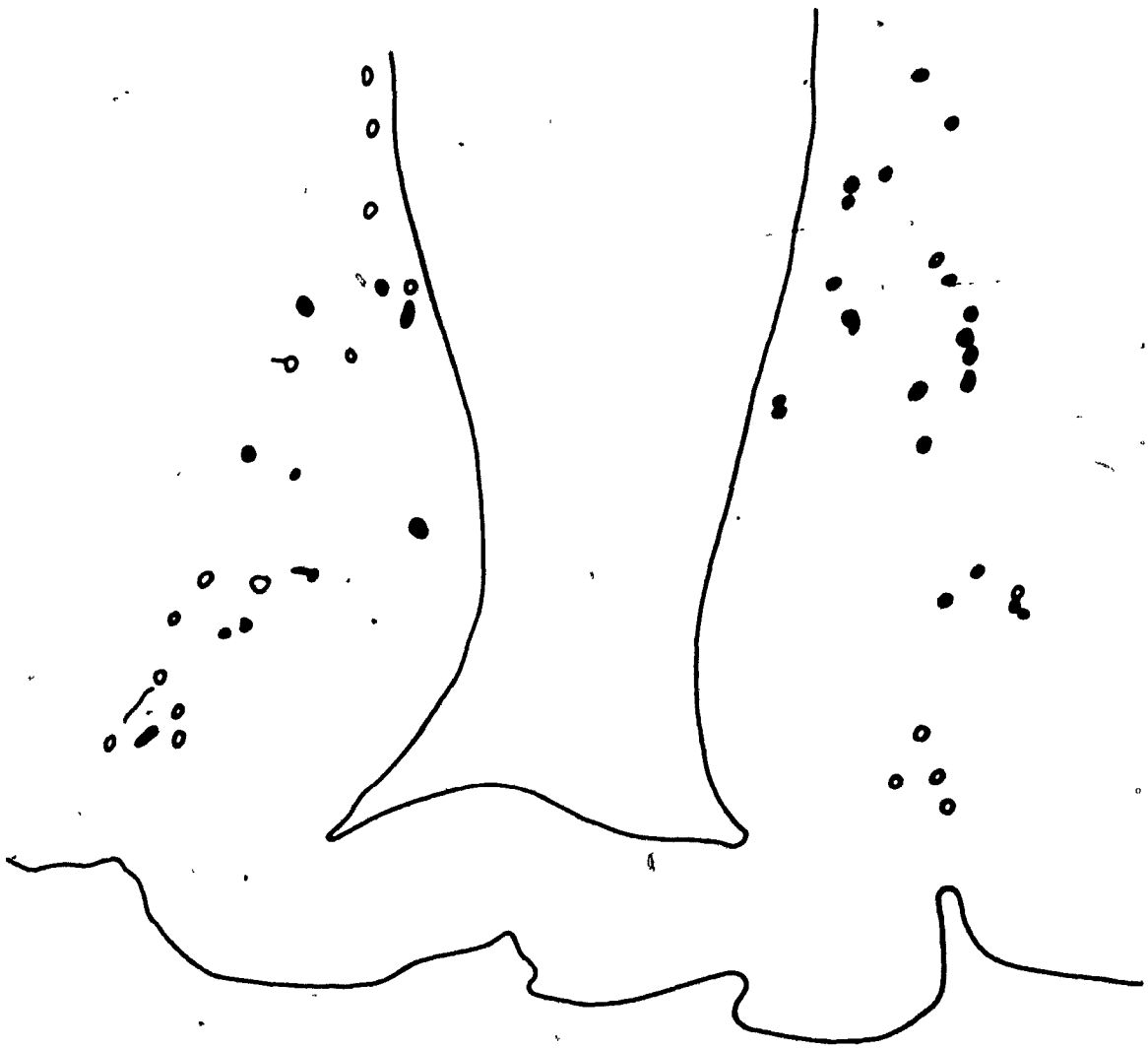

Plate 1g (level E)

Figure 1

Transverse section of mid-arcuate nucleus, from which Plate 1d was obtained (the extent of the nucleus is indicated by the overlay tracing). In addition to TH positive nerve cell bodies, a complex network of immunoreactive processes, as well as small punctate elements, can be seen within the nucleus. The punctate elements are particularly abundant in the external layer of the median eminence. Scale: 100 μm

Plate 2

TH positive nerve cell bodies from representative coronal sections taken from 3 different levels of the arcuate nucleus of an EV-treated female rat (EV-II). 2a is more rostral and 2d is more caudal. Scale: 100 µm

Plate 2a (level B)

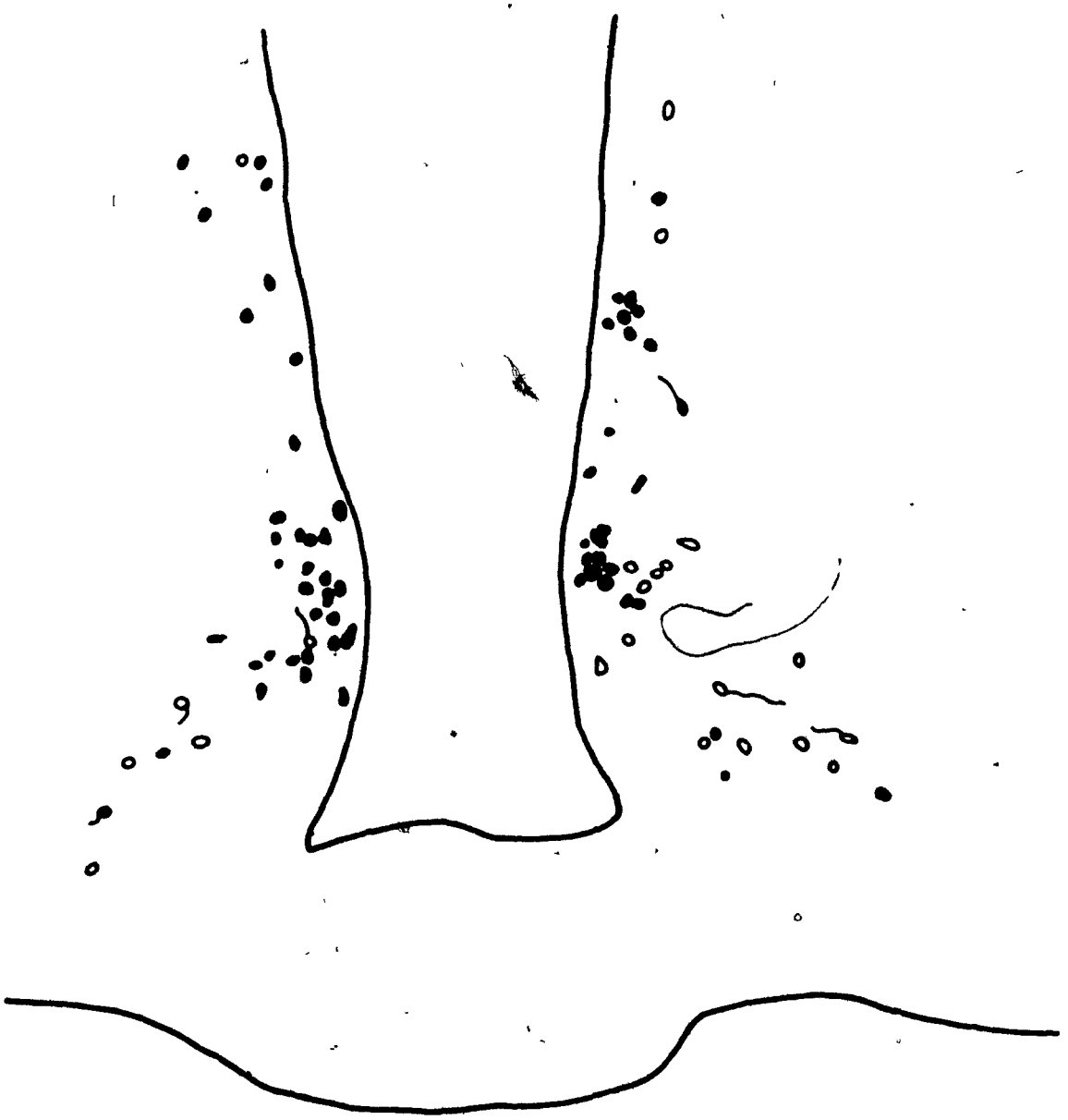

Plate 2b (level C)

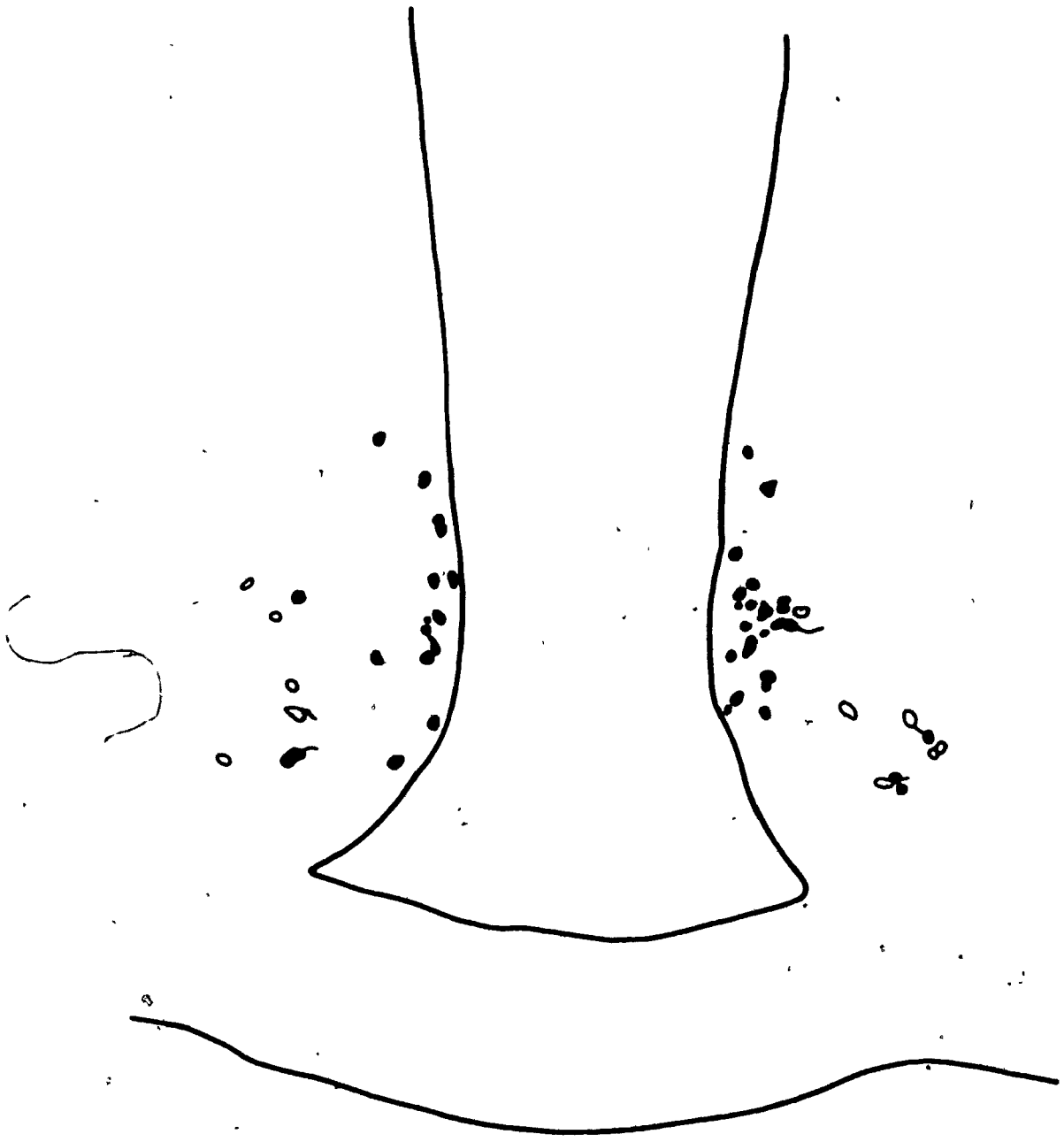

Plate 2c (level C)

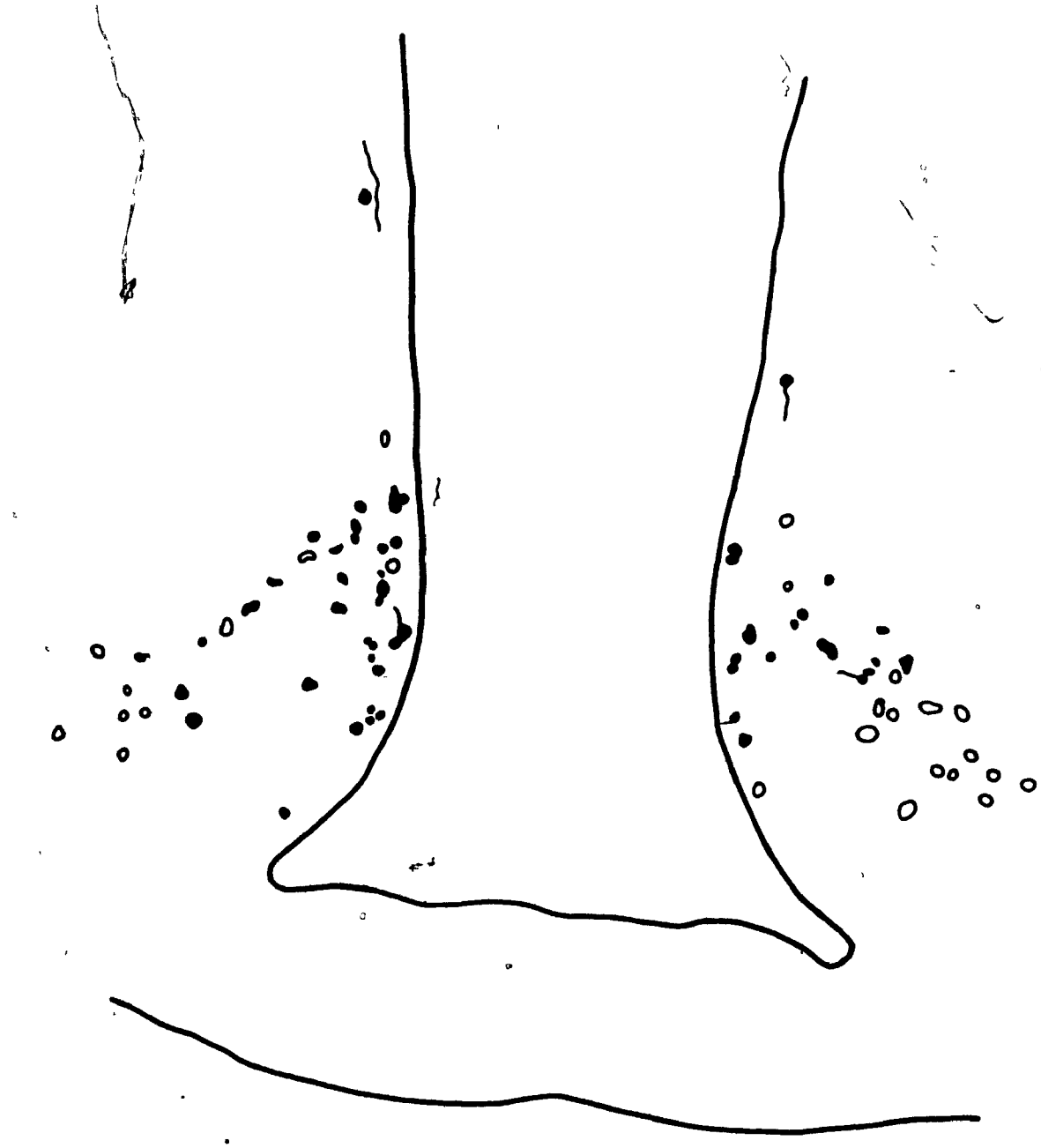

Plate 2d (level D)

Plate 3

TH positive perikarya from representative coronal sections taken from 3 different levels of the male arcuate nucleus (animal C3). 3a is more rostral and 3e is more caudal. Scale: 100 µm

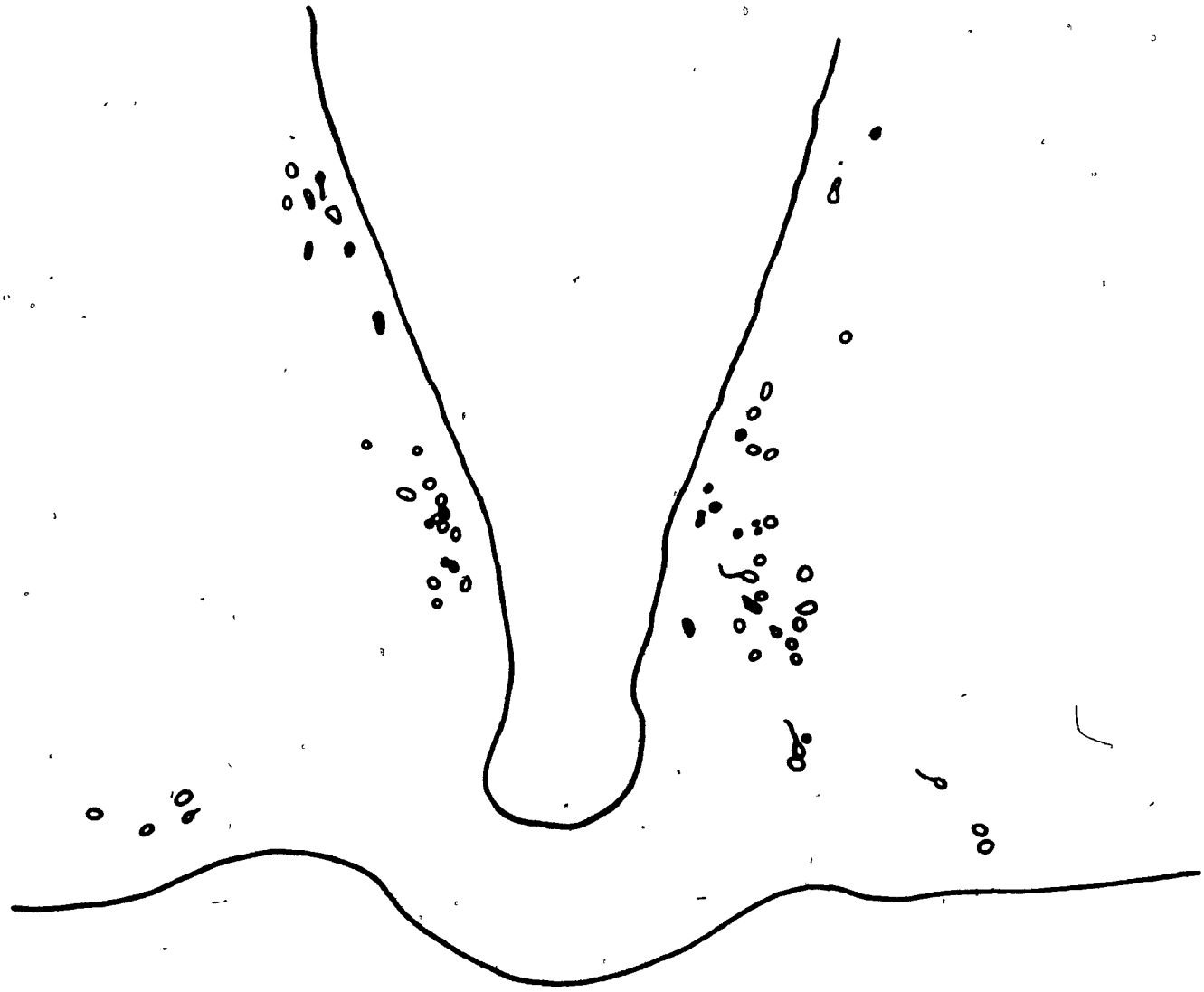

Plate 3a (level B)

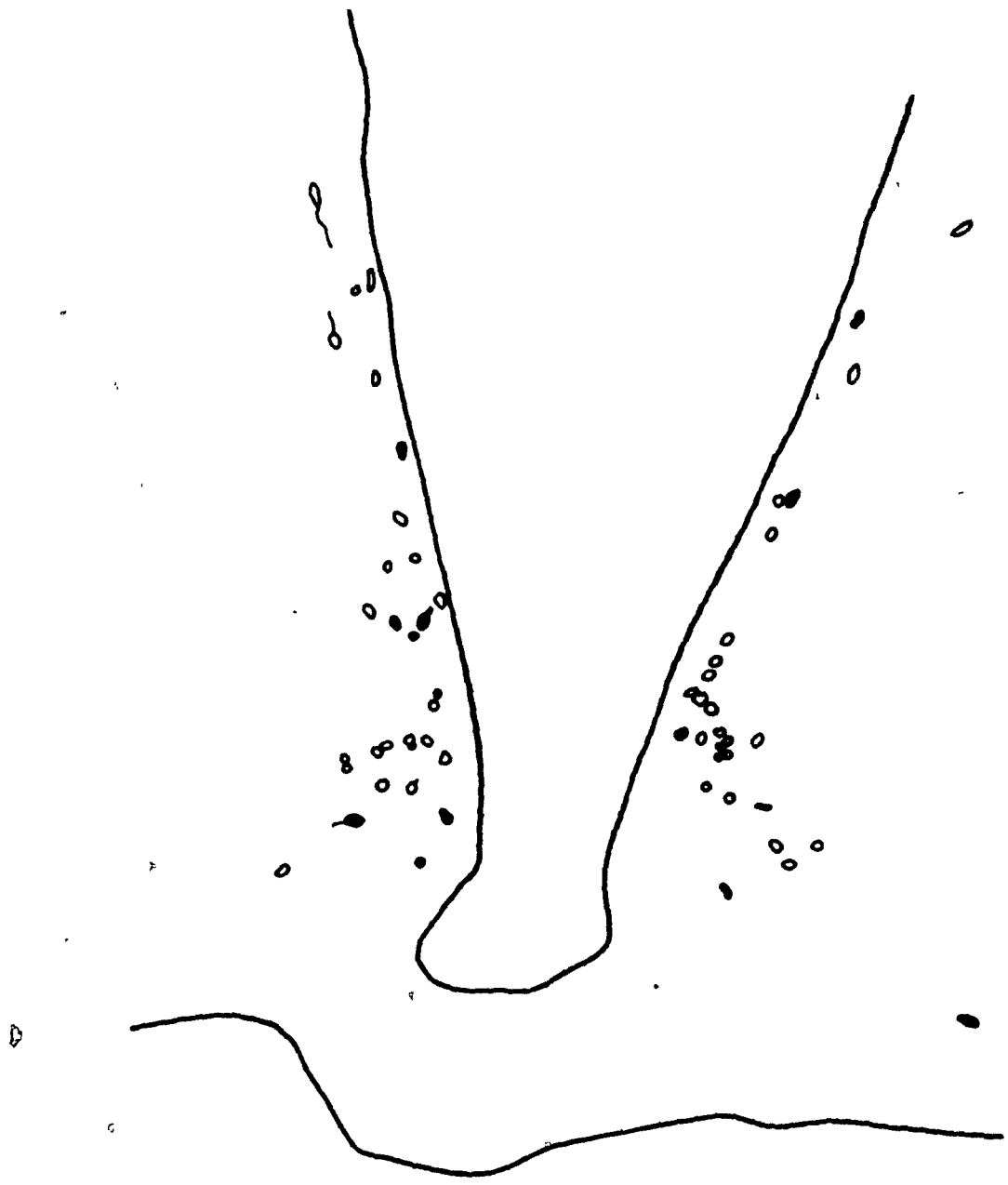

Plate 3b (level B)

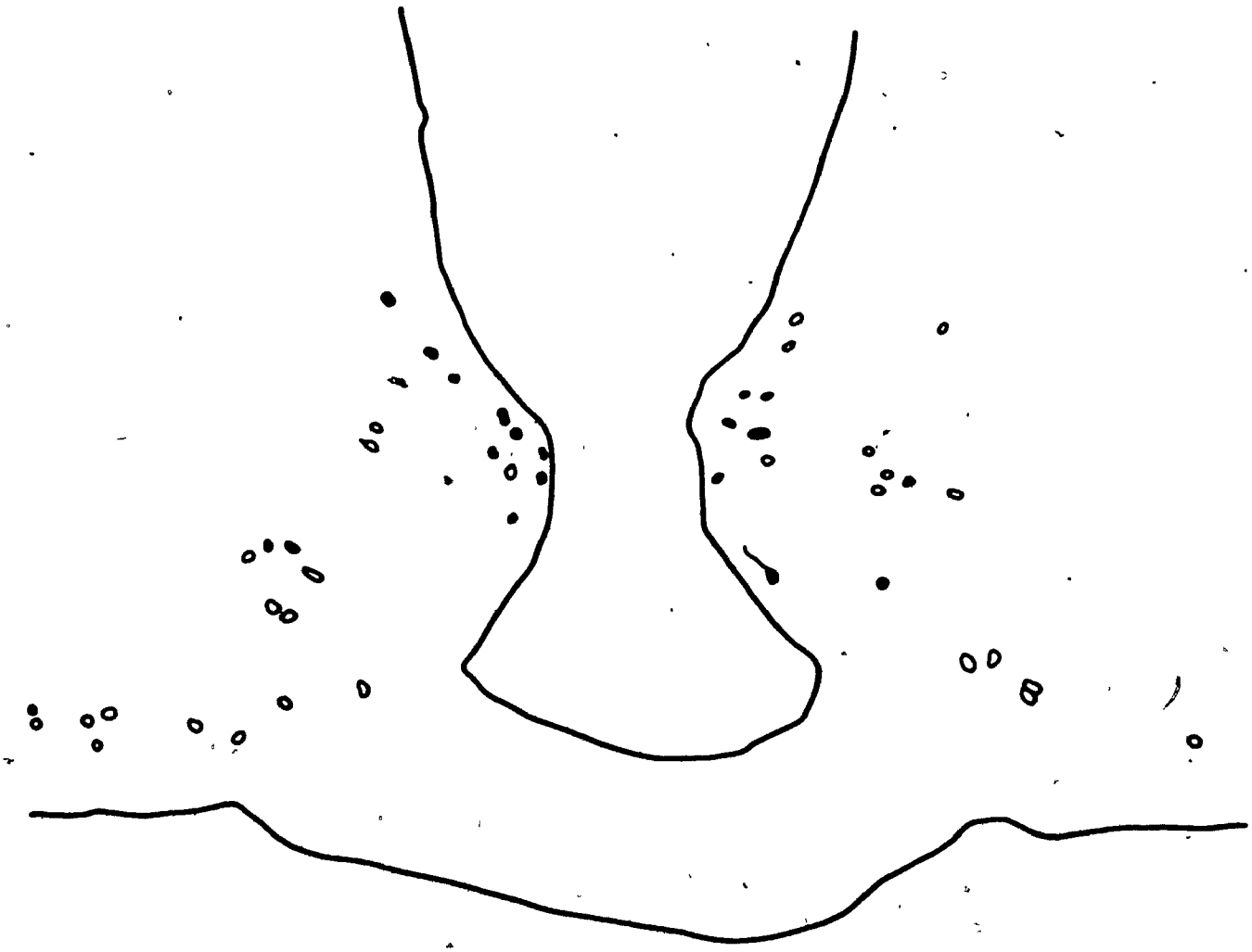

Plate 3c (level C)

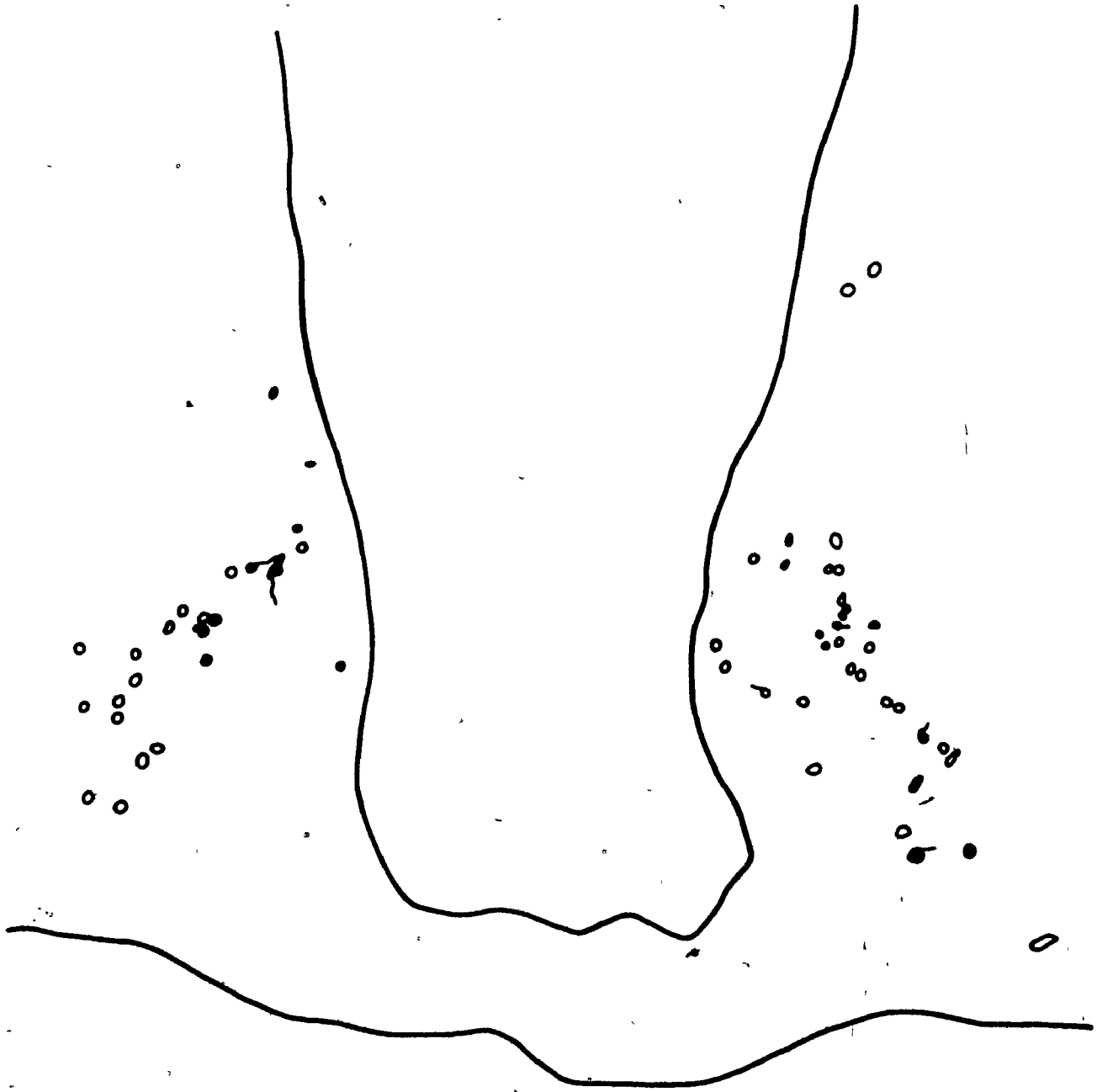

Plate 3d (level C)

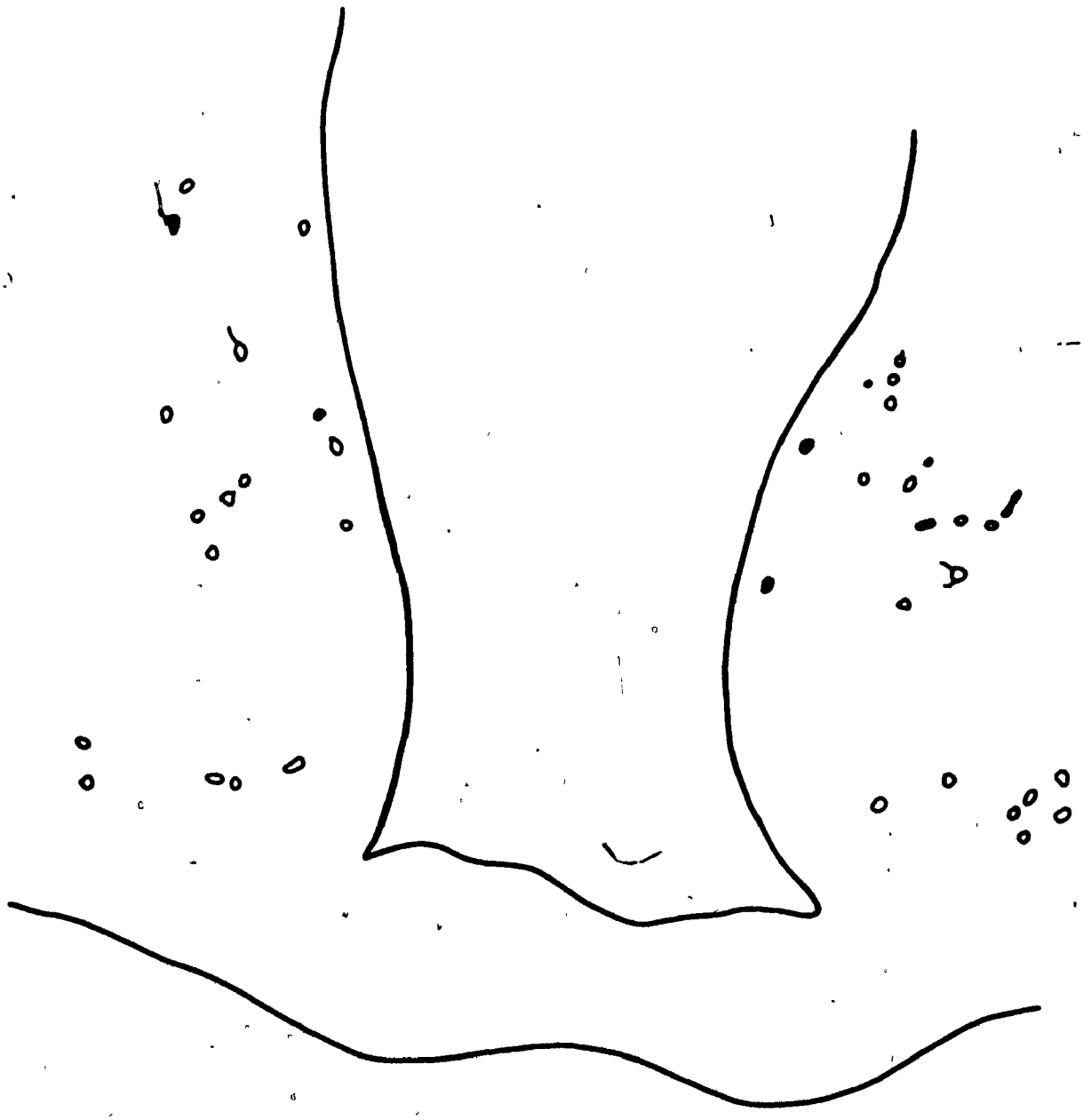

Plate 3e (level D)

Figure 2

TH immunoreactive perikaryon. Typically, a large indented nucleus containing a nucleolus, occupies most of the volume of the cell. The densely stained scant peripheral cytoplasm contains: mitochondria, endoplasmic reticulum, Golgi apparatus, lysosomes and multivesicular bodies. Three immunoreactive dendrites (arrowheads) are directly apposed to the perikaryon. At points where its surrounding glial sheath is interrupted, the cell is also contacted by unlabeled axon terminals. Scale: 1 µm

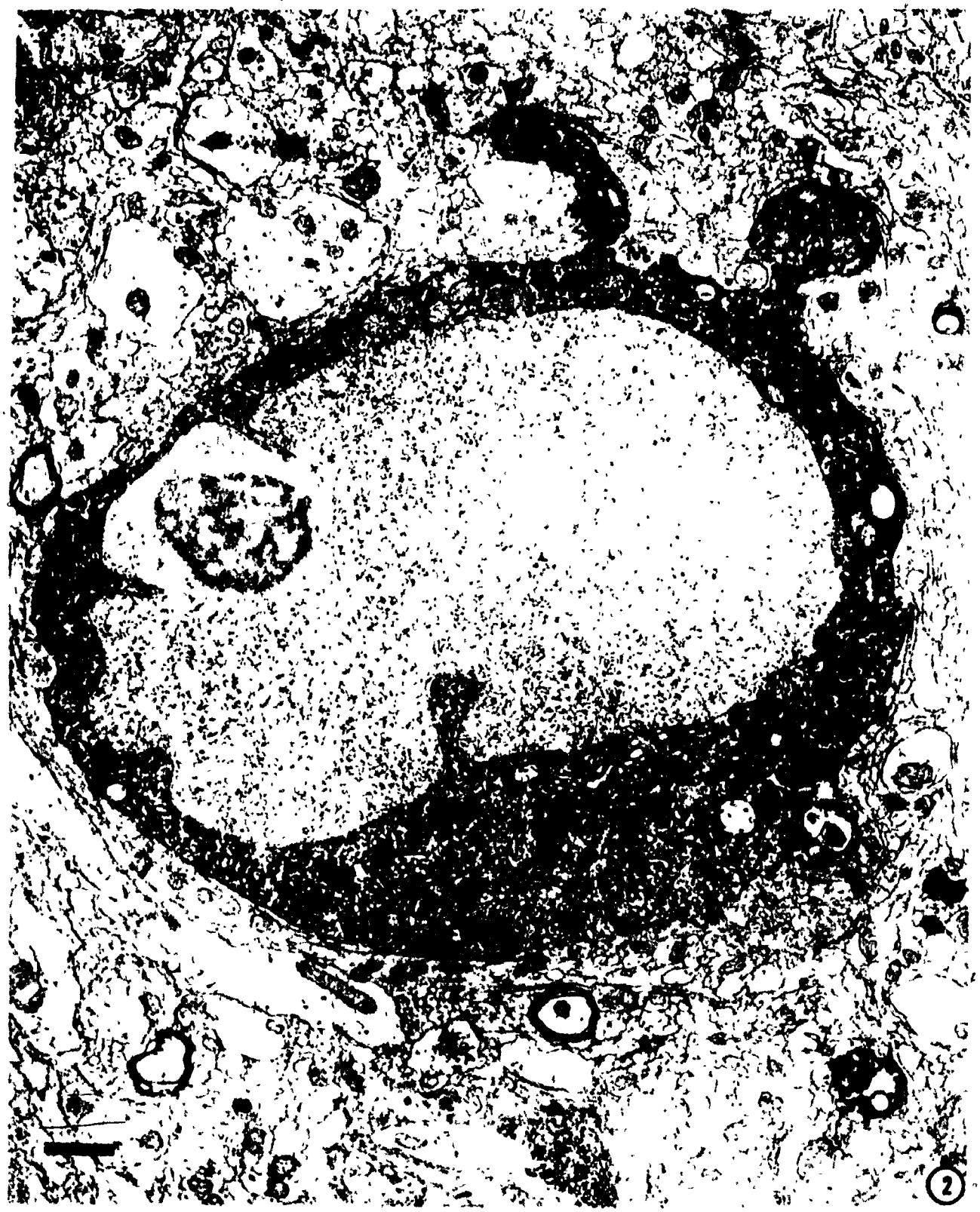
2

Figure 3

Immunolabeled dendrite in longitudinal section. The dendritic shaft is characterized by paraxially oriented microtubules outlined by the dense immunoprecipitate. Along the dendrite, four unlabeled axon terminals (arrows) make synaptic contacts. Scale: 0.5 µm

Figure 4

Immunolabeled dendrite in cross-section. The microtubules appear as small dots outlined by the immunoprecipitate. The dendrite is contacted (upper left) by an unlabeled axon terminal. Both dendrite and terminal are partially ensheathed by multiple glial lamellae (arrowheads). Scale: 0.3 µm

Figure 5

Immunolabeled cross-sectioned dendritic profile in synaptic contact with an unlabeled terminal. At the point of contact, two active zones can be seen about which clear vesicles are clustered. Scale: 0.5 µm

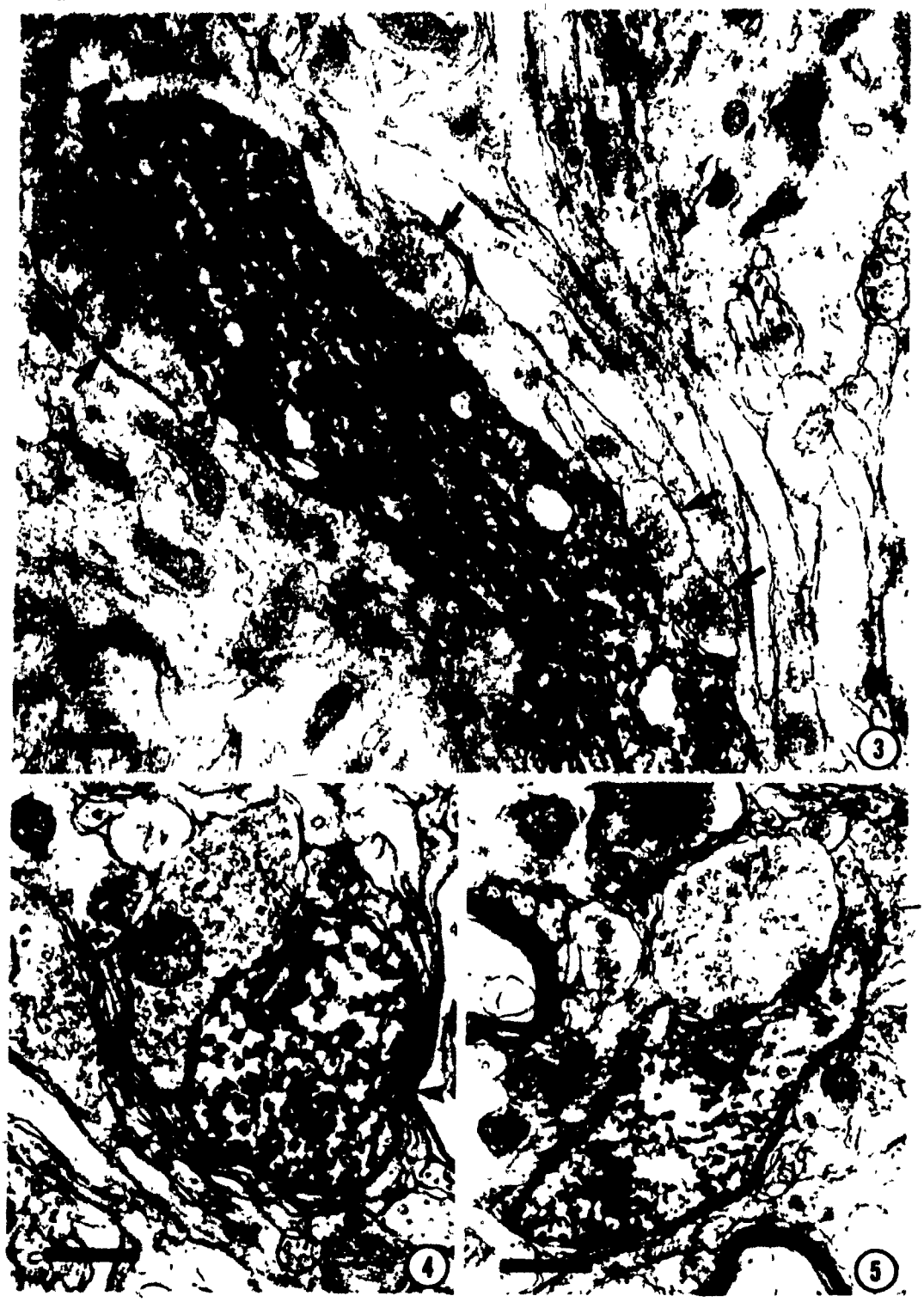
3
4
5

Figure 6

Labeled dendrites in apposition to a tanycytic process. Two labeled dendrites (d_1 and d_3) directly abut the tanycytic process (tan) coursing through the field. There are neither vesicles nor membrane specializations at the contact points. A third dendrite (d_2) appears to be in contact with a sheet emanating from the tanycytic process (arrowheads). d_1 is partially engulfed by thin tanycytic protrusions (arrows). Scale: 0.5 μm

d2
d3
d1
O

Figure 7

Labeled dendrite in apposition to unlabeled dendrite. Neither membrane specializations nor vesicles are present. The unlabeled dendrite is also contacted by two unreactive axon terminals (arrows). Scale: 1 µm

Figure 8

Two labeled dendrites in apposition. No membrane specialization or vesicles are apparent at the point of apposition. Each immunolabeled dendrite is in synaptic contact with at least one unlabeled axon terminal. The dendrites and terminals are ensheathed by glial processes. Scale: 0.5 µm

Figure 9

Labeled dendro-somatic appositions. Two labeled dendrites directly apposed to a labeled perikaryon. No membrane specialization or vesicles are apparent at the sites of apposition. Scale: 0.5 µm

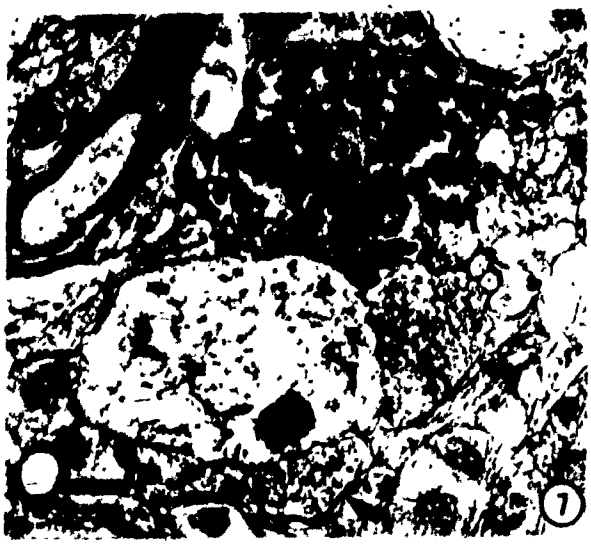

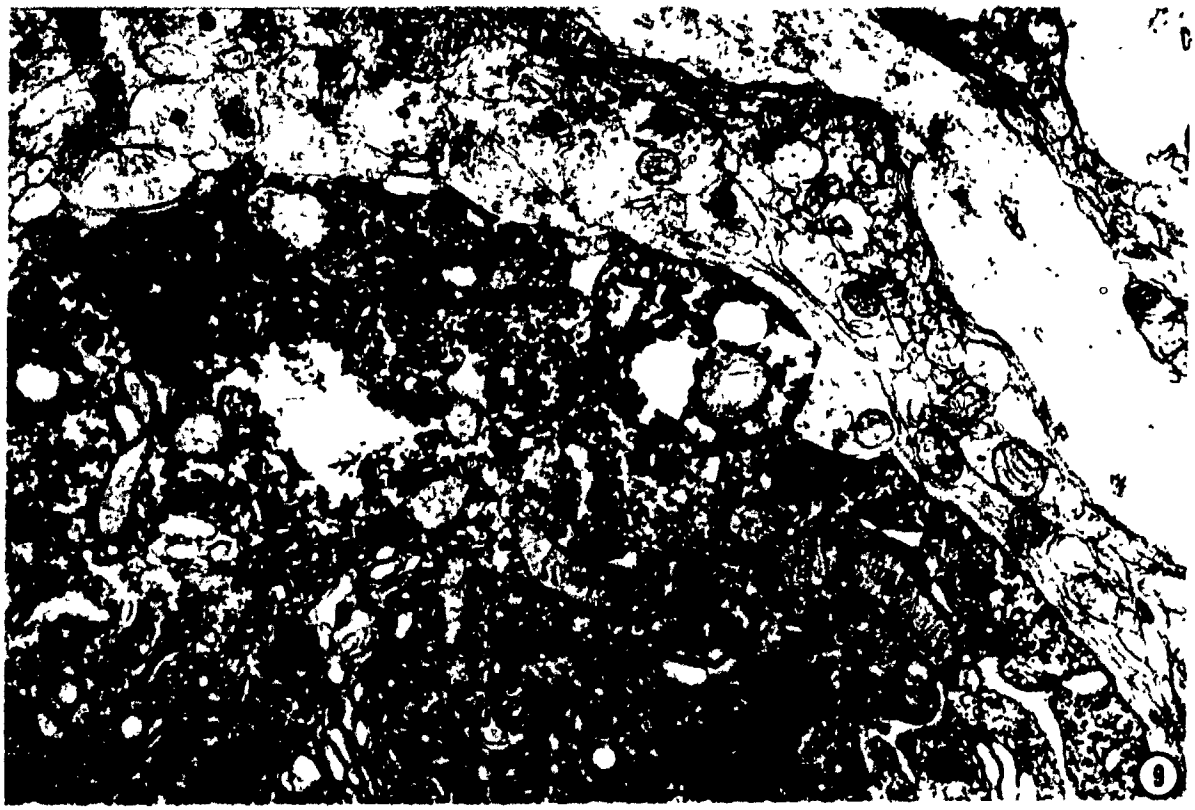

Figure 10

Labeled dendrite in apposition to unlabeled perikaryon. A labeled large dendritic shaft appears in direct apposition to an unlabeled perikaryon near the base of an emerging dendrite. Several axon terminals (arrows) are clustered in the vicinity of these two apposing elements. Scale: 0.5 μm

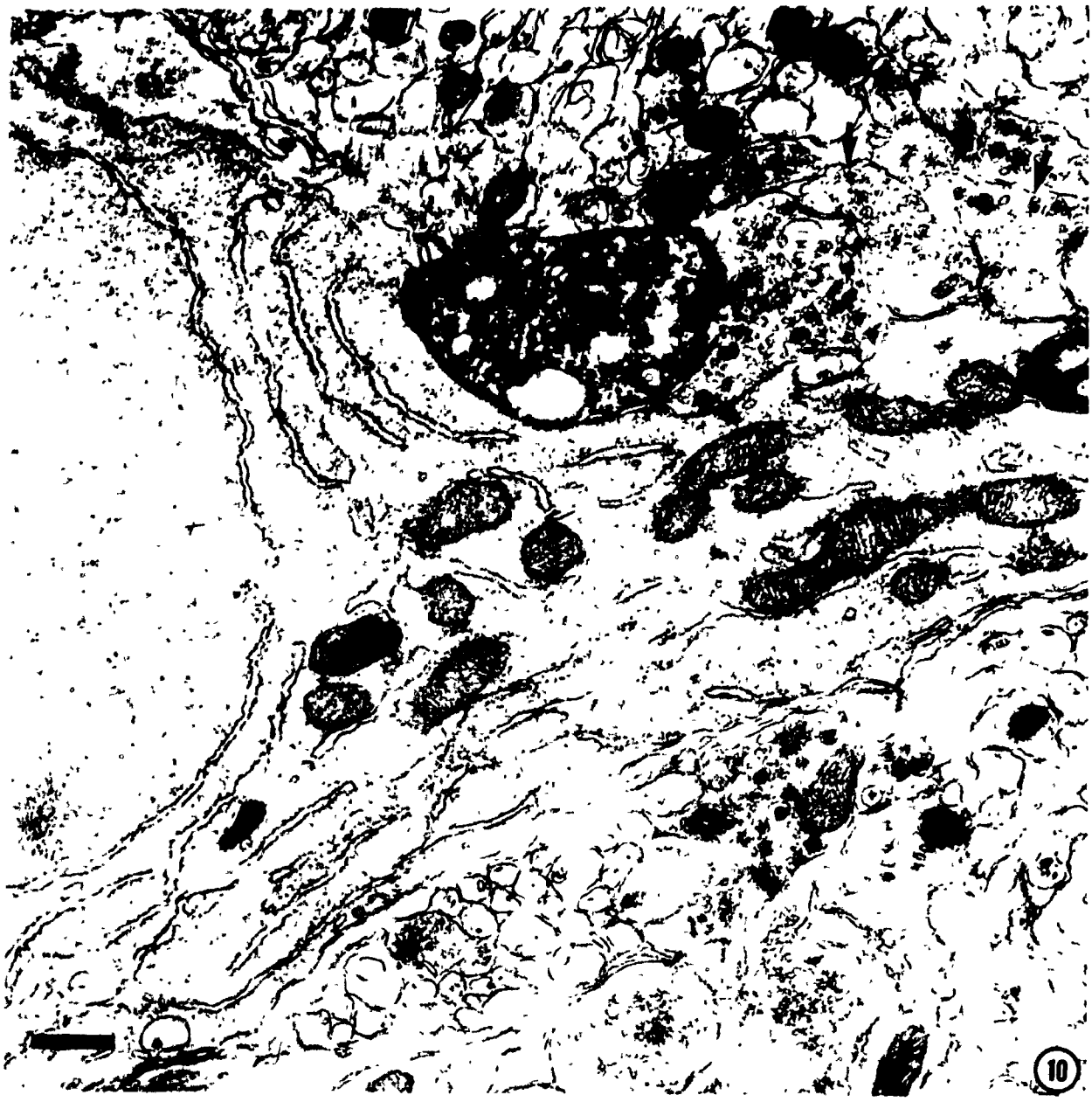
10

Figure 11

A glial sheath intercalated between a TH positive dendritic profile and an unlabeled nerve cell body. Scale: 0.5 µm

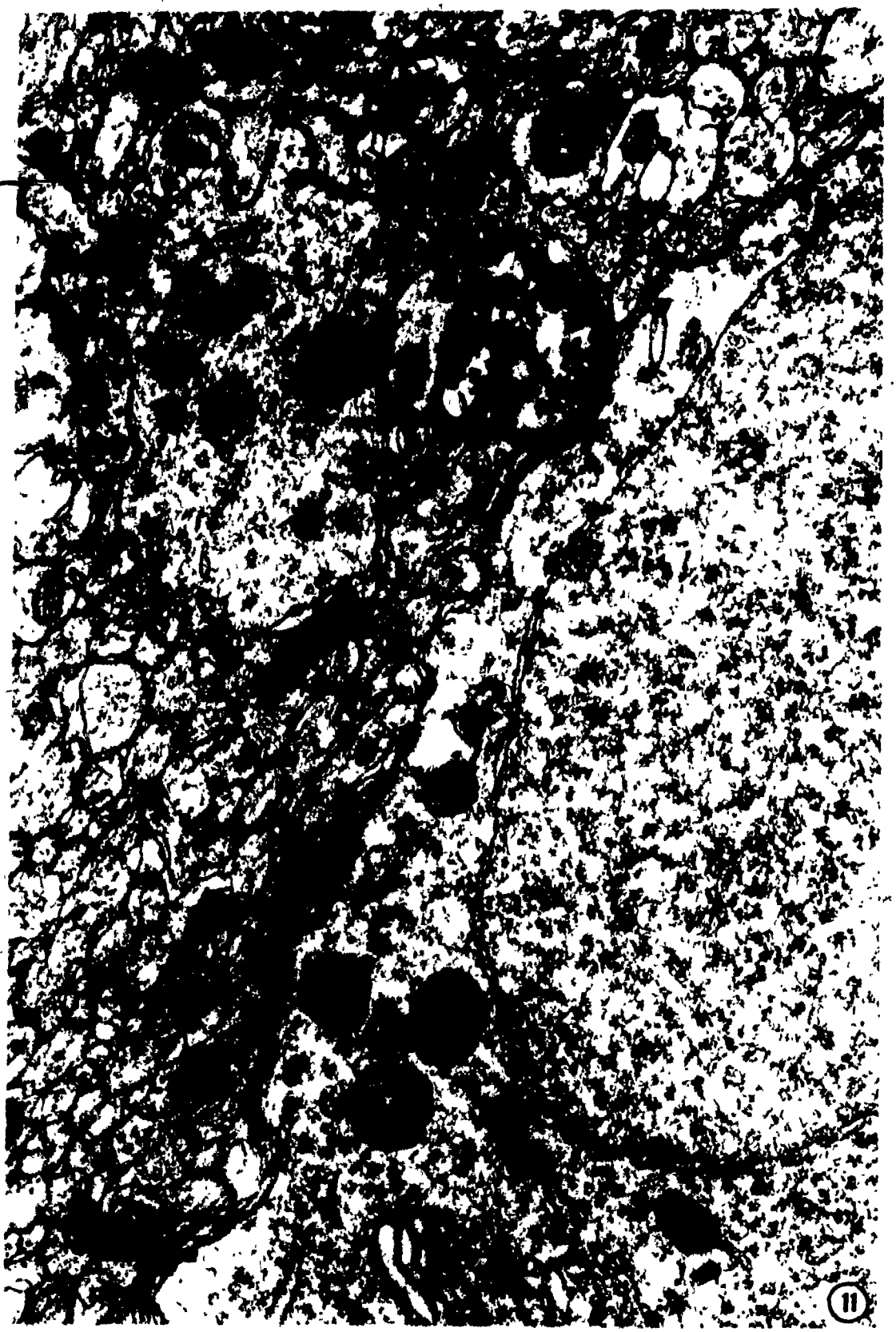
11

Figure 12

A labeled axon terminal. The profile is filled with round, densely packed, clear vesicles and a few large dense core vesicles, as well as mitochondria and profiles of smooth endoplasmic reticulum. This axon terminal is in direct apposition to two unlabeled dendrites. There is no apparent membrane specialization at the contact sites. Scale: 0.3 μm


12

Figure 13a

Axo-dendritic synapse involving a labeled axon terminal and an unlabeled dendrite. Note the presence of both membrane specialization and vesicular cluster. Scale: 0.5 μm

Figure 13b

Apposition between a labeled and an unlabeled axon terminal. Scale: 0.5 μm

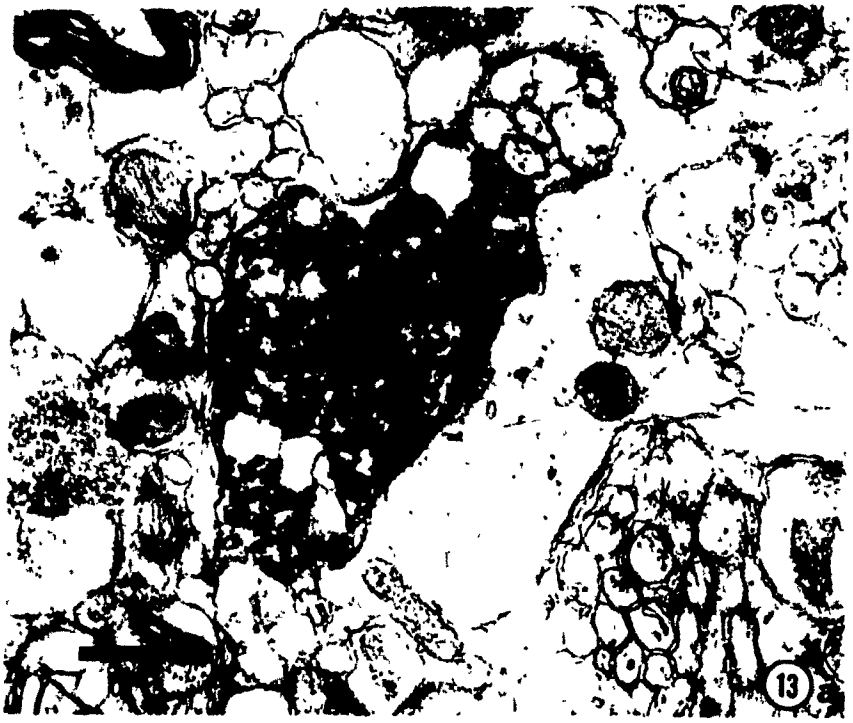
13a


13b

Figure 13c

Labeled axon terminal (arrow) in direct apposition to a tanycytic process (tan). Scale: 0.5 µm

Figure 13d

A labeled nerve terminal (arrow) in direct apposition to a TH positive nerve cell body. Scale: 0.5 µm

Figure 13e

A labeled nerve terminal in direct apposition to an unlabeled nerve cell body. Scale: 0.5 µm

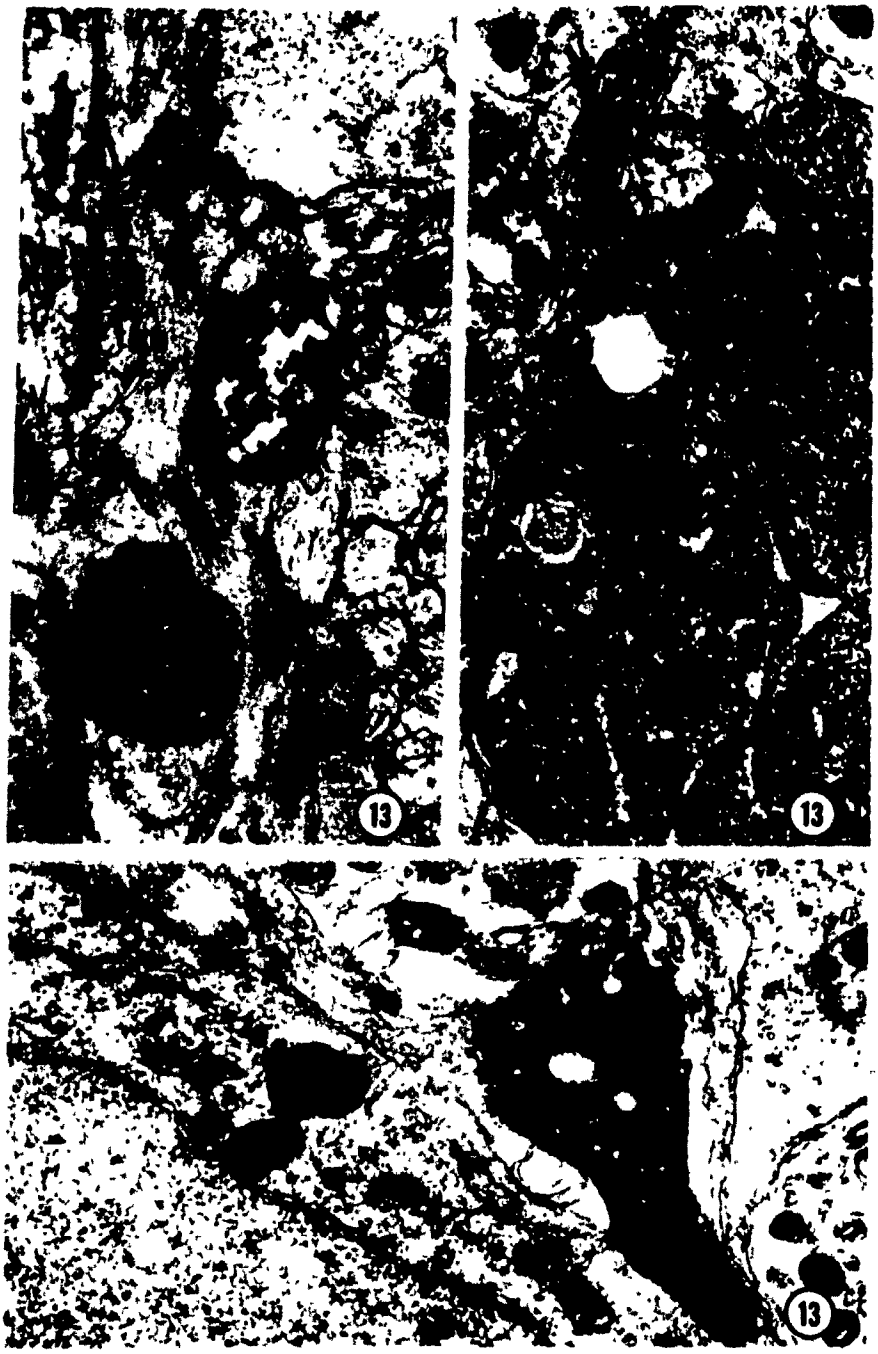
13
13
13

Figure 14

An unlabeled nerve cell body contacted by 4 unlabeled axon terminals. Two of these terminals are in direct apposition to (arrowheads), and the others form synapses (arrows) with, the perikaryon. Scale: 0.5 μm

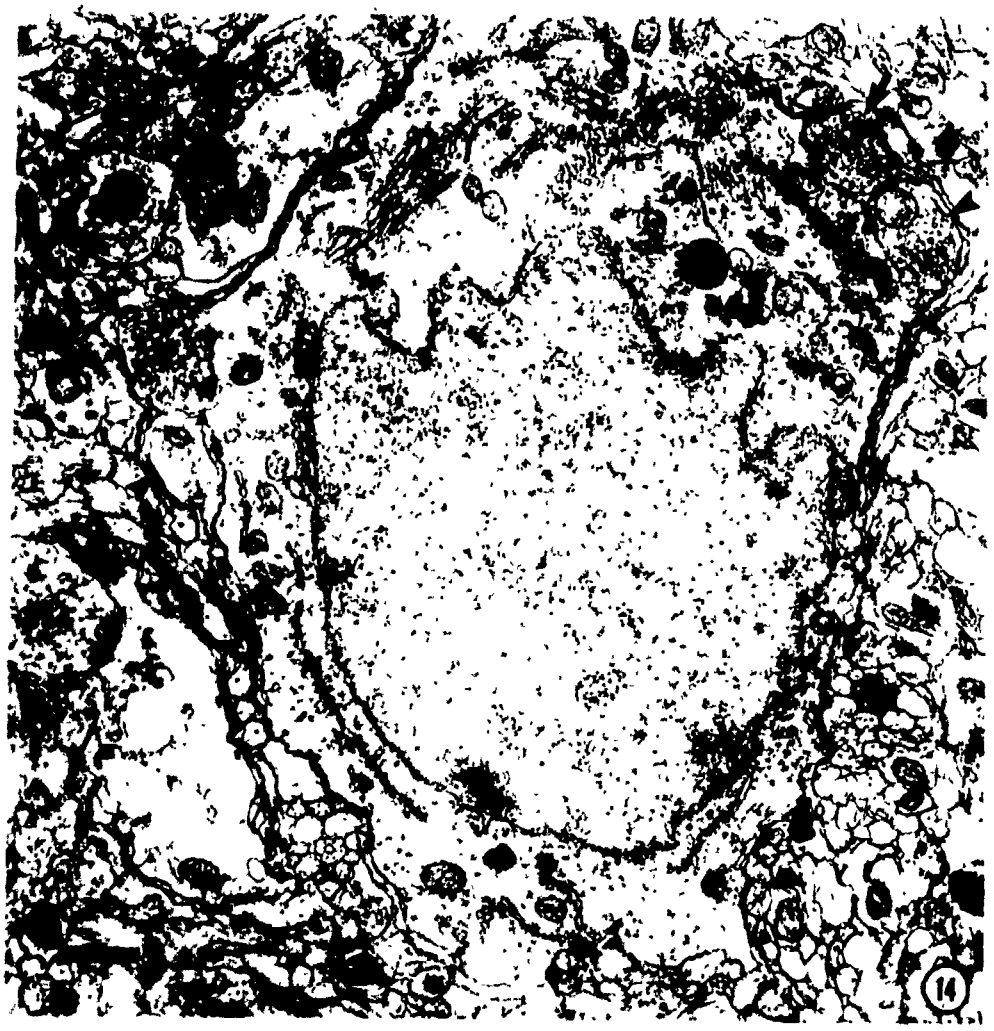
14

Figure 15

TH positive perikaryon from an intact male rat. This small neuron contains numerous mitochondria, many lysosomes, a few scattered ER cisternae and a well developed Golgi apparatus. At points where the multilamellar glial sheath surrounding the cell body is interrupted, numerous unlabeled nerve terminals contact the cell. Scale: 1 μm

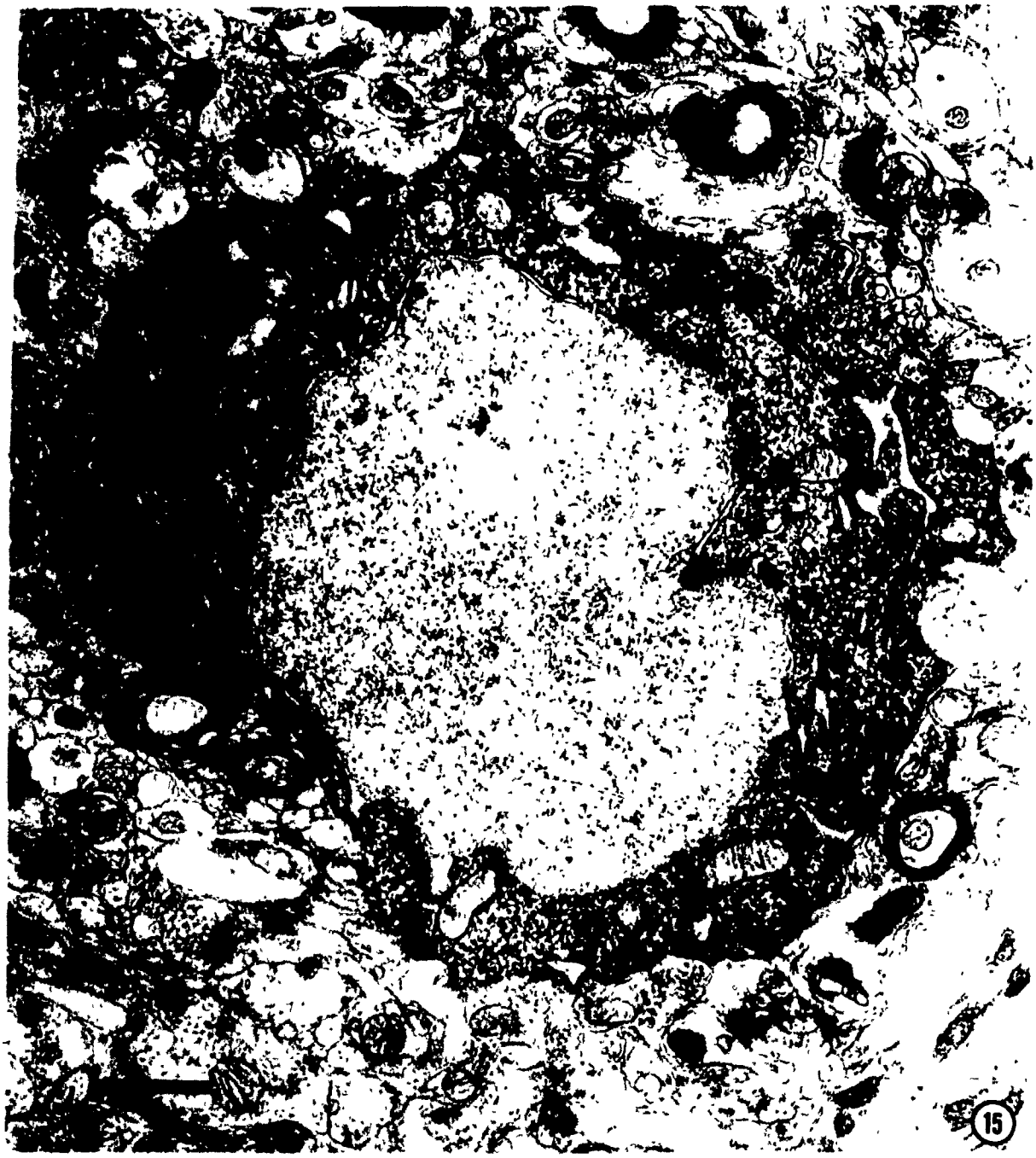
15

Figure 16

Dendro-dendritic apposition involving 2 labeled dendrites. Note the membrane specialization at the point of contact. Also, observe the membrane specialization and vesicular cluster at the site where an unlabeled axon terminal synapses on one of the immunoreactive dendrites. Scale: 0.2 µm


16

Plate 4

TH positive nerve cell bodies and processes from representative coronal sections taken from 4 different levels of a female neonatal (D1-3) arcuate nucleus. The intensely immunoreactive perikarya are filled in while the pale staining neurons are not. 2a is more rostral and 2e is more caudal. Scale: 100 µm

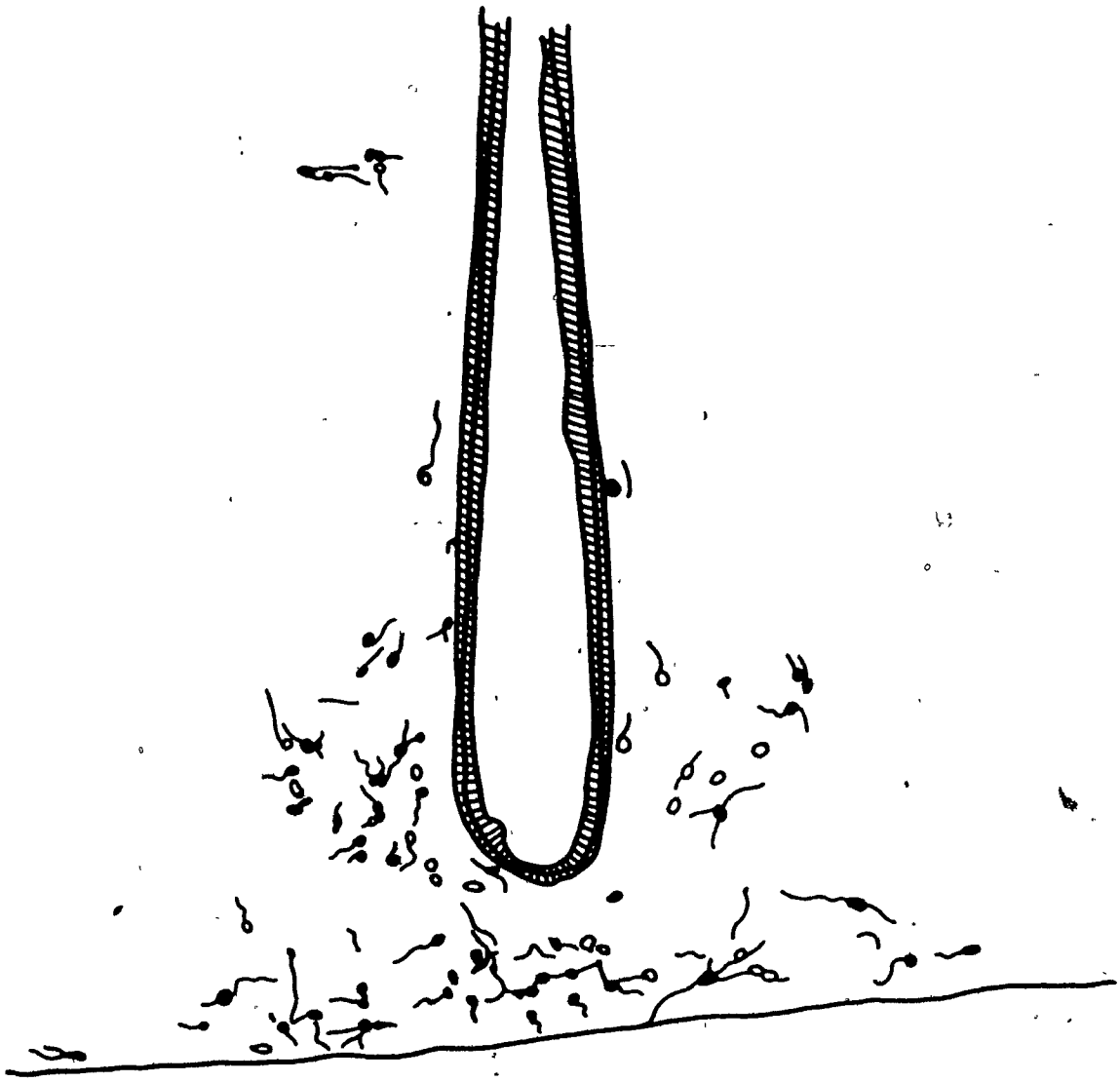

Plate 4a (level A)

Plate 4b (level B)

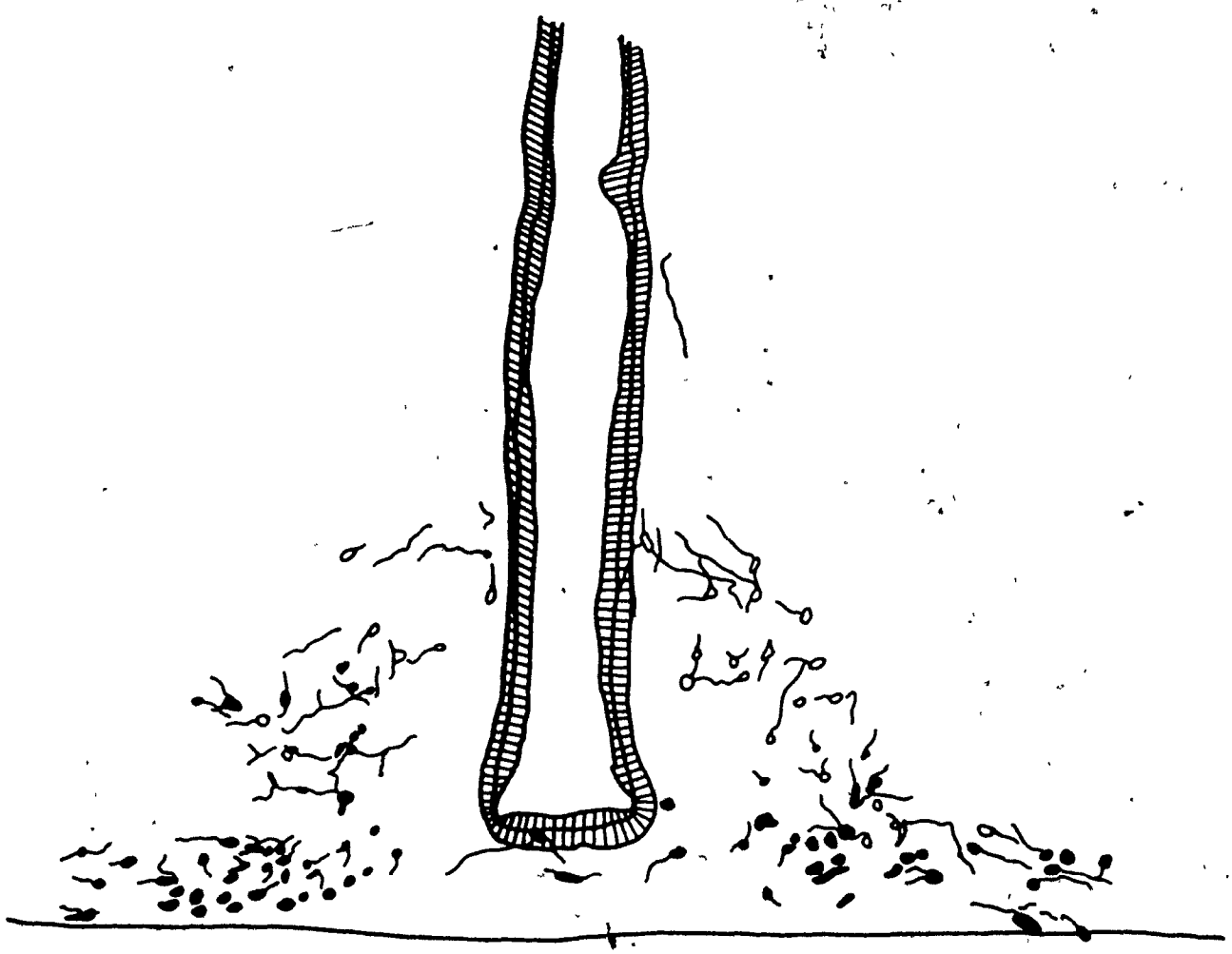

Plate 4c (level C)

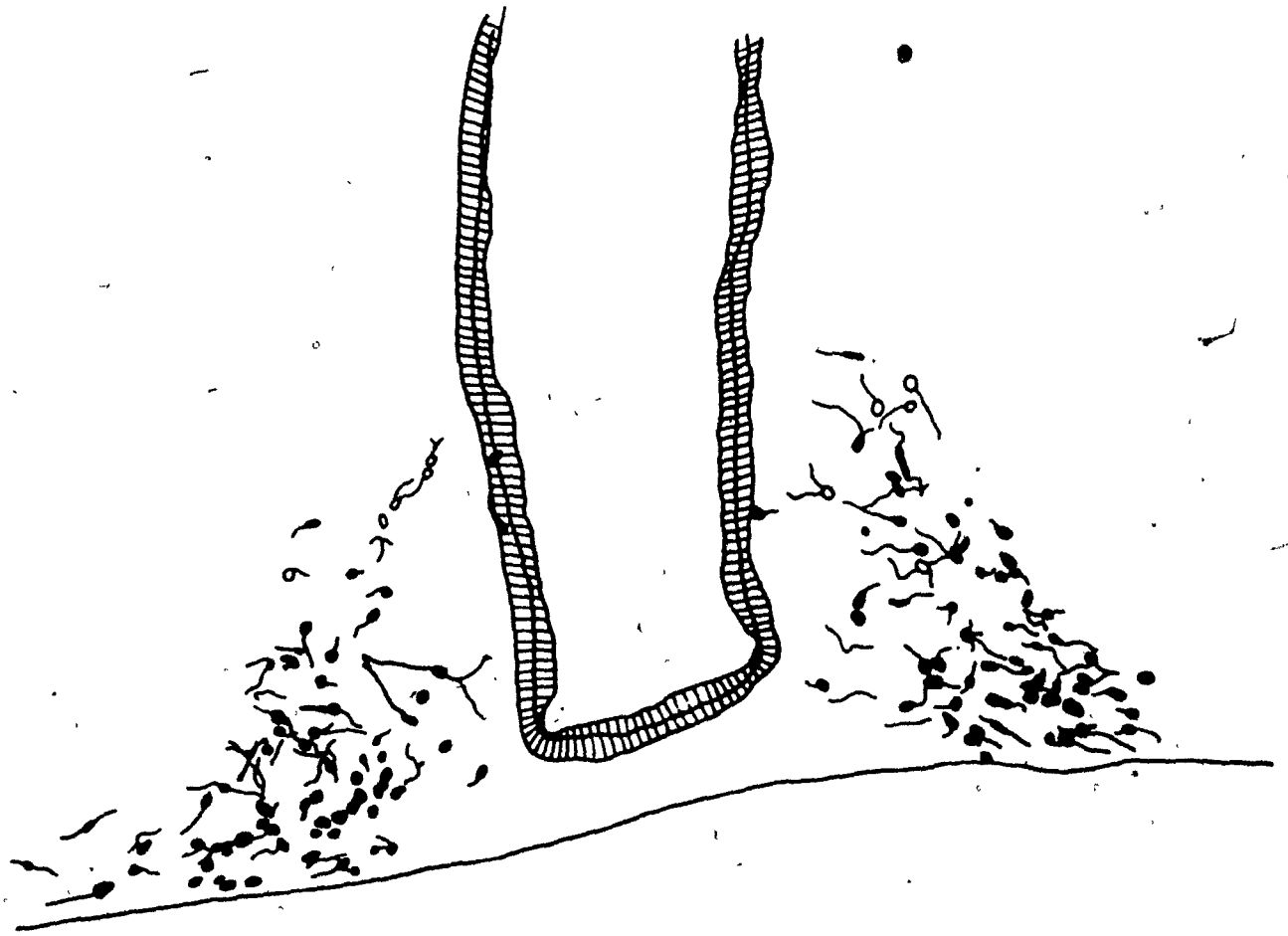

Plate 4d (level C)

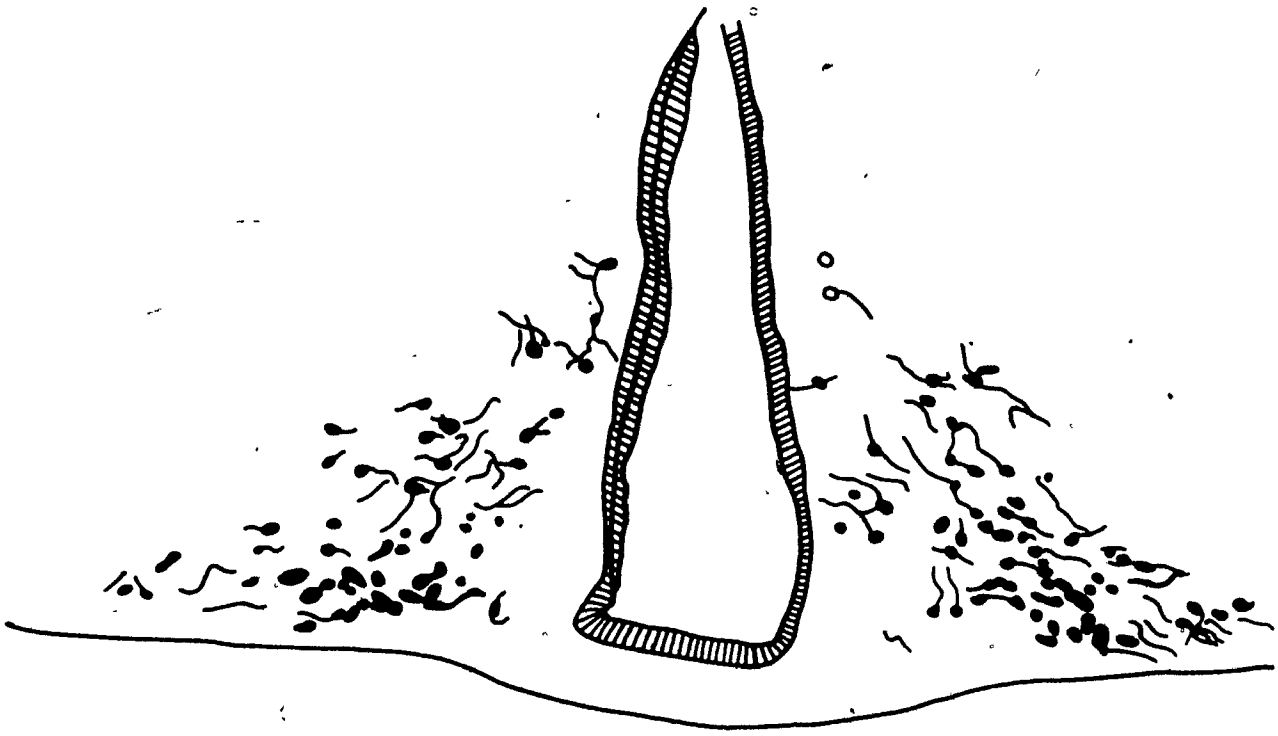

Plate 5

TH positive nerve cell bodies from representative coronal sections taken from 4 different levels of a 15 day old female (D15-2) arcuate nucleus. 5a is more rostral and 5f is more caudal. Scale: 100 µm

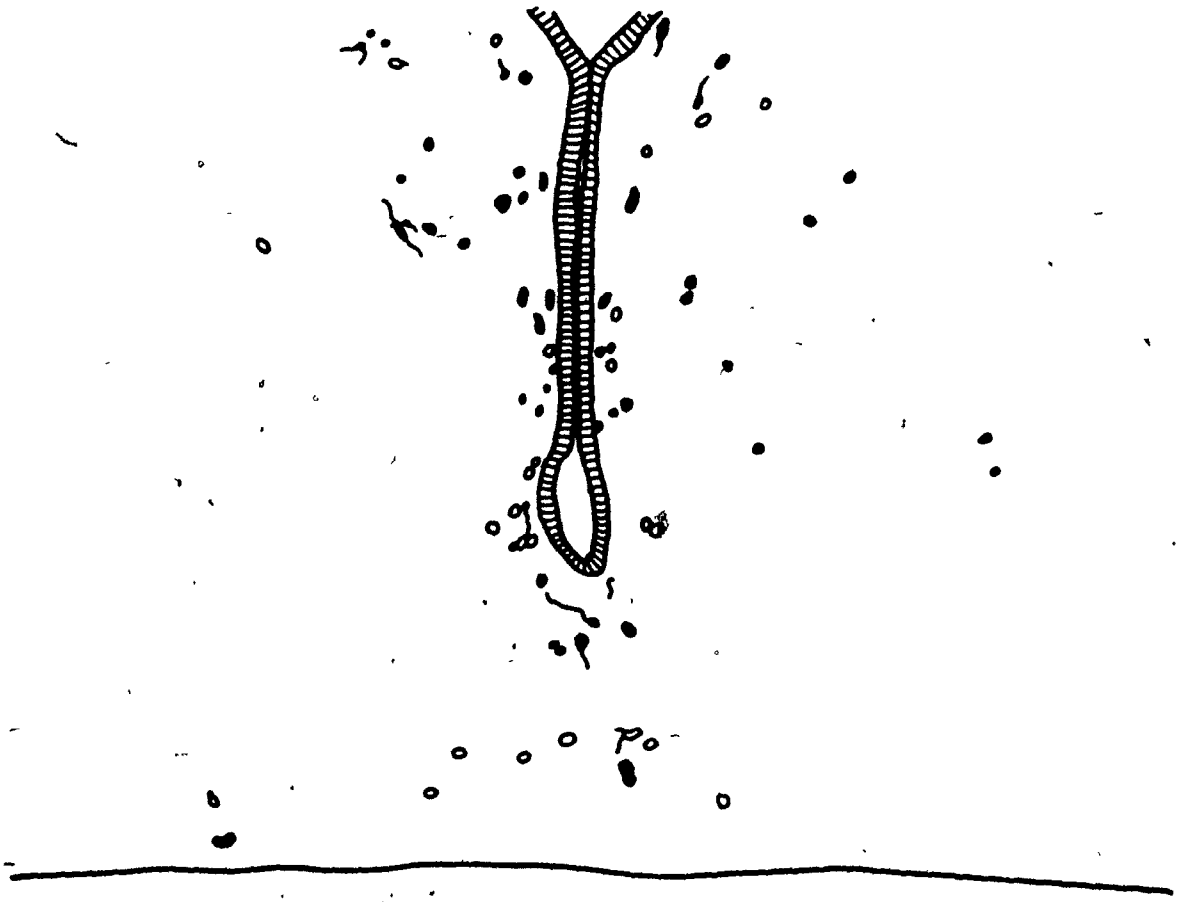

Plate 5a (level A)

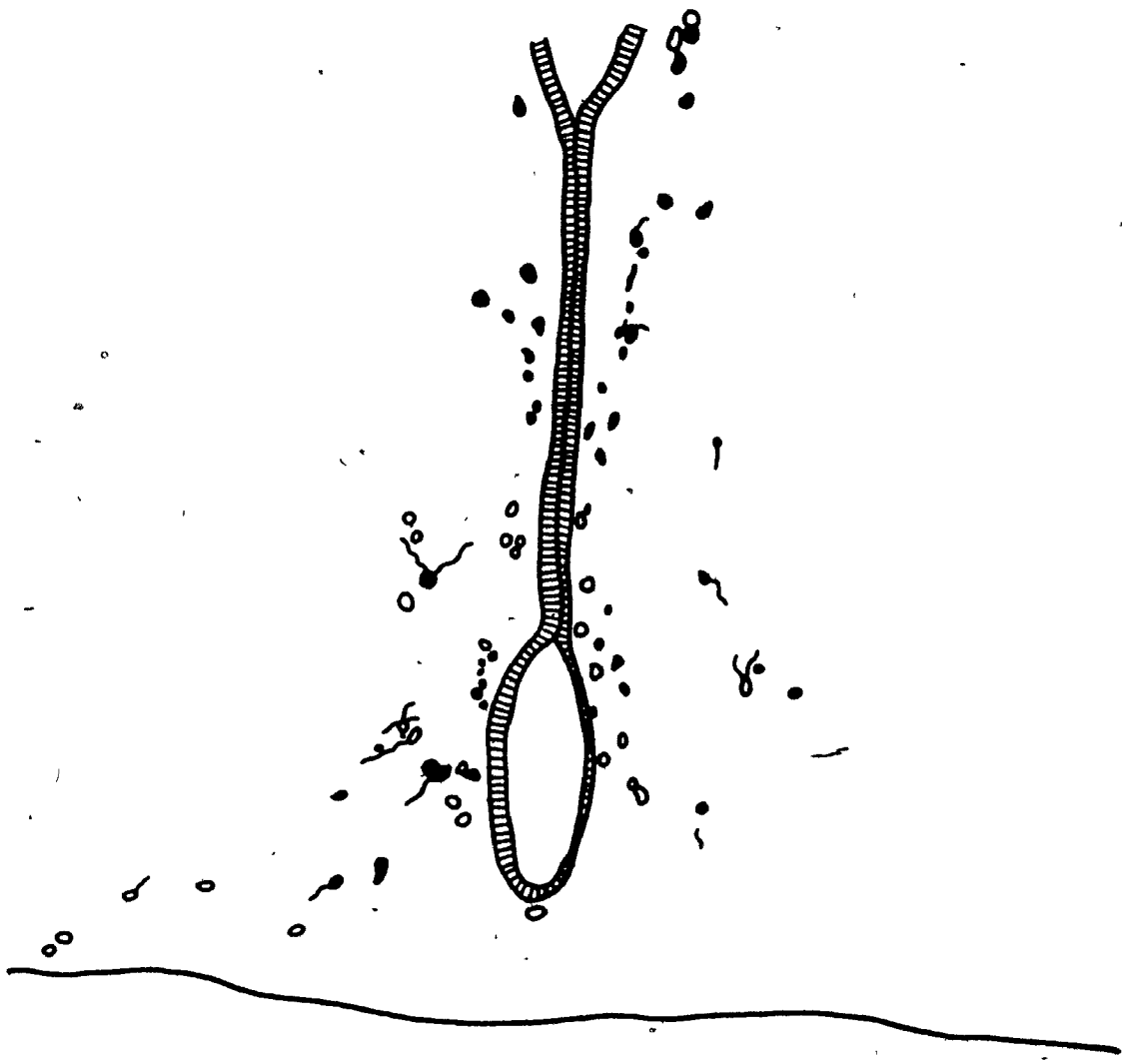

Plate 5b (level B)

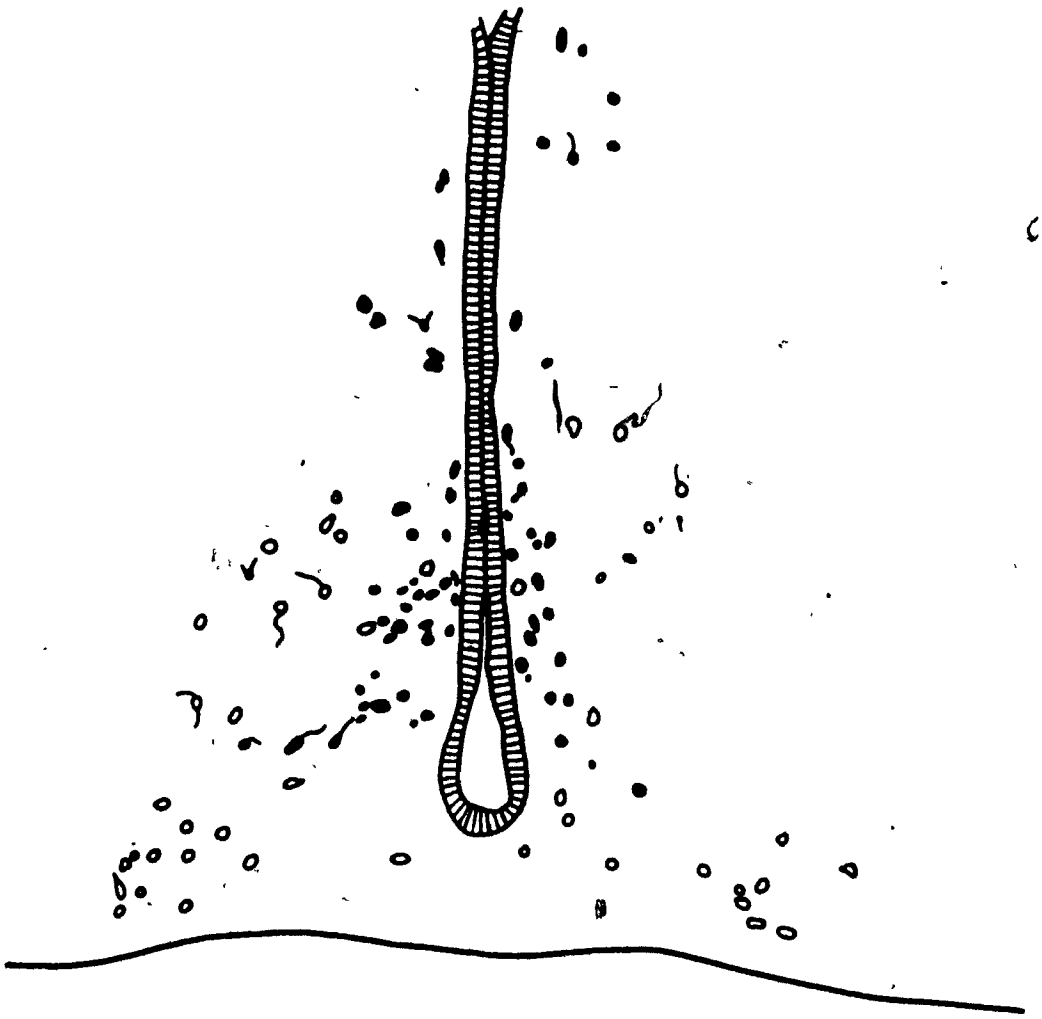

Plate 5c (level C)

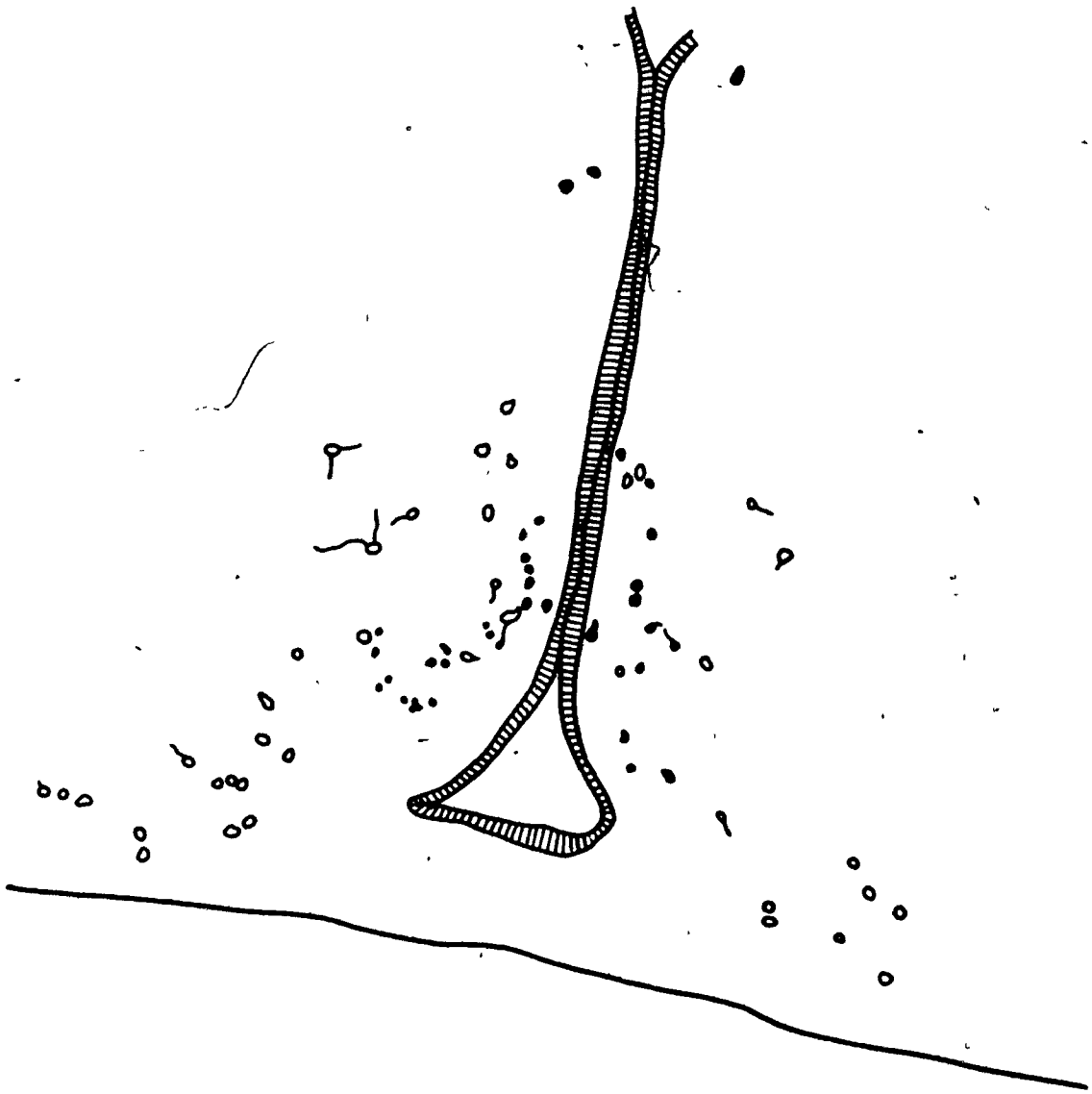

Plate 5d (level C)

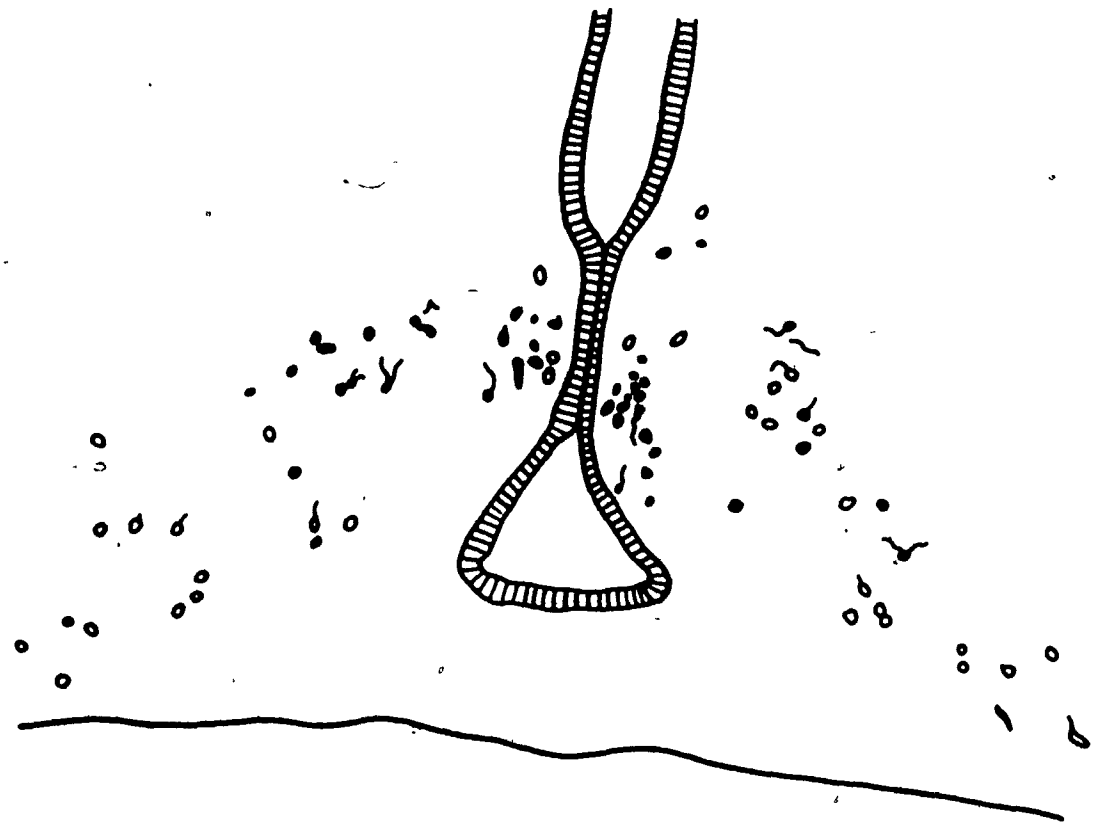

Plate 5e (level C)

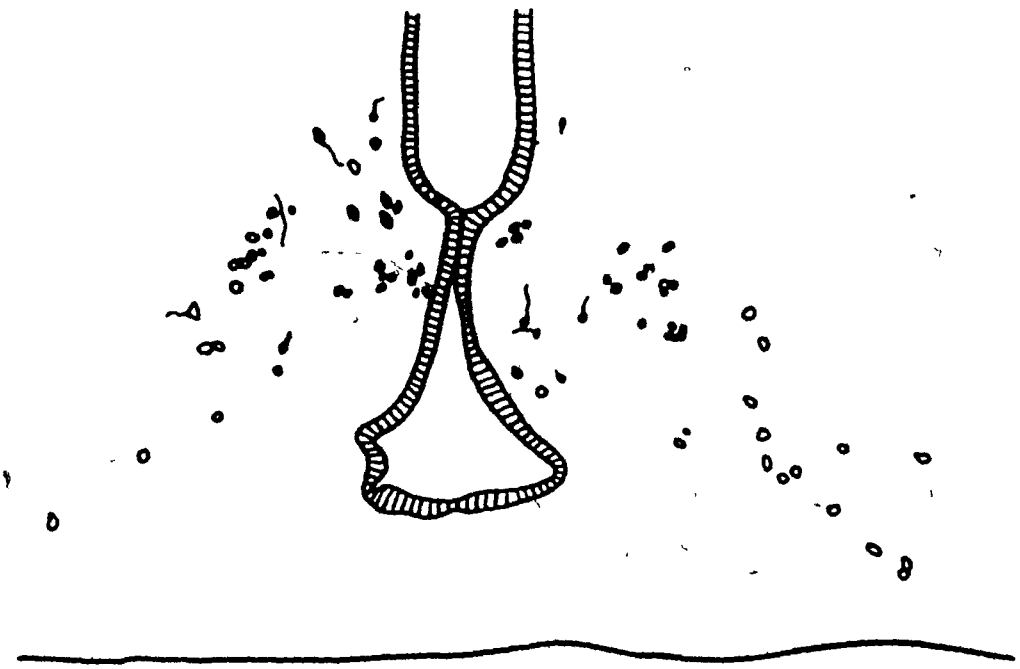

Plate 5f (level D)

Figure 17

TH positive nerve cell body from a neonatal arcuate nucleus (see text for description). Scale: 1 µm


17

Figure 18

TH positive nerve cell body from a neonatal arcuate nucleus. A tanycytic process is closely apposed to part of the external plasmalemma of the perikaryon (arrowheads). Note the presence of a multi vesicular body amongst the other cytoplasmic organelles.

Scale: 0.5 µm


18

Figure 19

Dendro-somatic apposition between an unlabeled dendrite (arrow) and a labeled perikaryon within the neonatal arcuate nucleus.

Scale: 0.5 µm


19

Figure 20a

One TH positive dendrite in direct apposition to 2 unlabeled dendrites and an unlabeled axon terminal within the arcuate nucleus of a female neonate. There is no membrane specialization nor vesicular cluster at the points of contact. Scale: 0.3 µm

Figure 20b

Dendro-dendritic apposition involving two labeled dendrites within the neonatal arcuate nucleus. There is no vesicular cluster nor membrane specialization at the point of contact, whereas a vesicular cluster is present at the synaptic junction between an unlabeled axon terminal and one of the labeled dendrites (arrow). Scale: 0.3 µm

Figure 20c

An unlabeled axon terminal synapses on a labeled dendrite. Both vesicular cluster and membrane specialization are clearly seen at the synaptic junction. The labeled dendrite is also in direct apposition to another immunoreactive dendrite and, even though no vesicular cluster is seen at the point of contact (arrow), a membrane specialization is present. Scale: 0.3 µm


20


20c

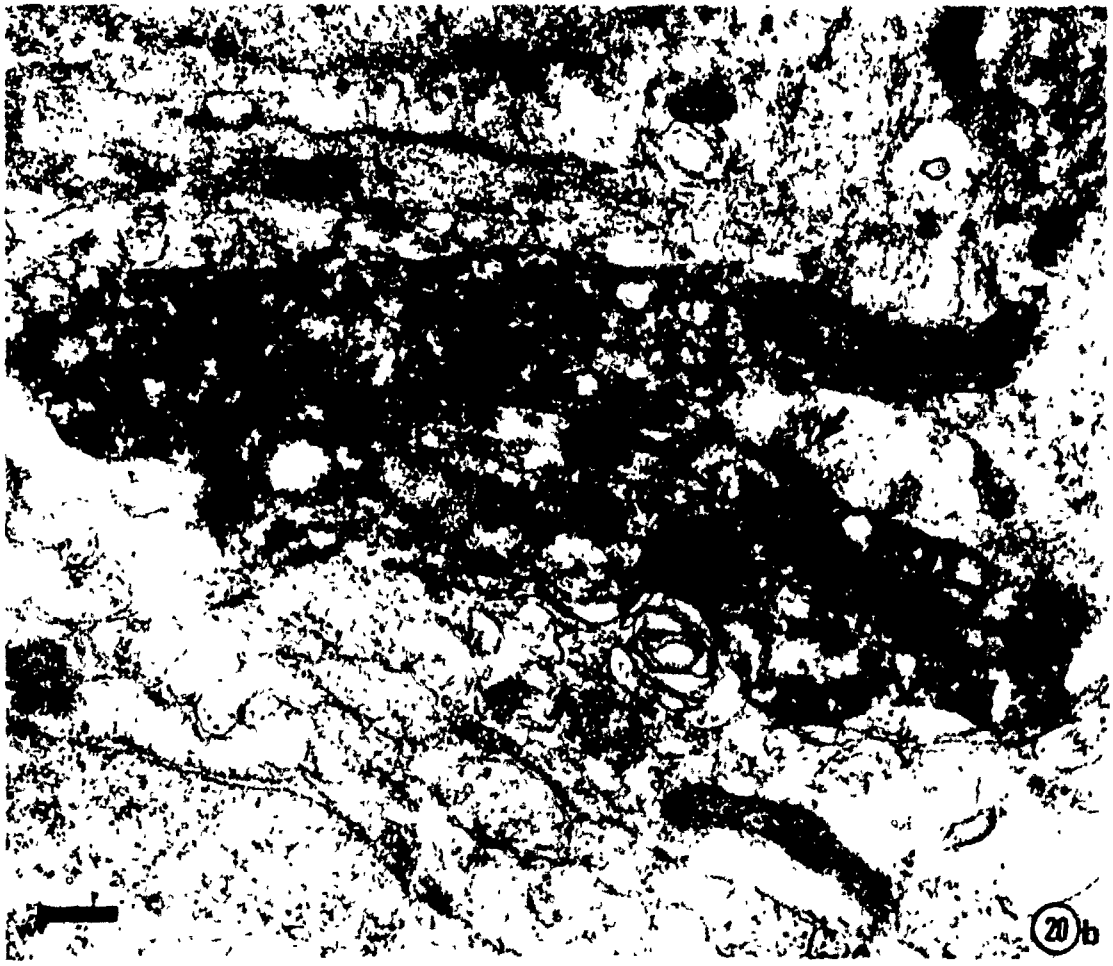
20b

Figure 21

A neonatal dendritic profile in direct apposition (arrow) to an extension of a tanycytic process (tan). Scale: 0.5 μm


21

Figure 22

A labeled dendrite in direct apposition to an unlabeled perikaryon from a female neonatal arcúate nucleus. Scale: 0.3 µm

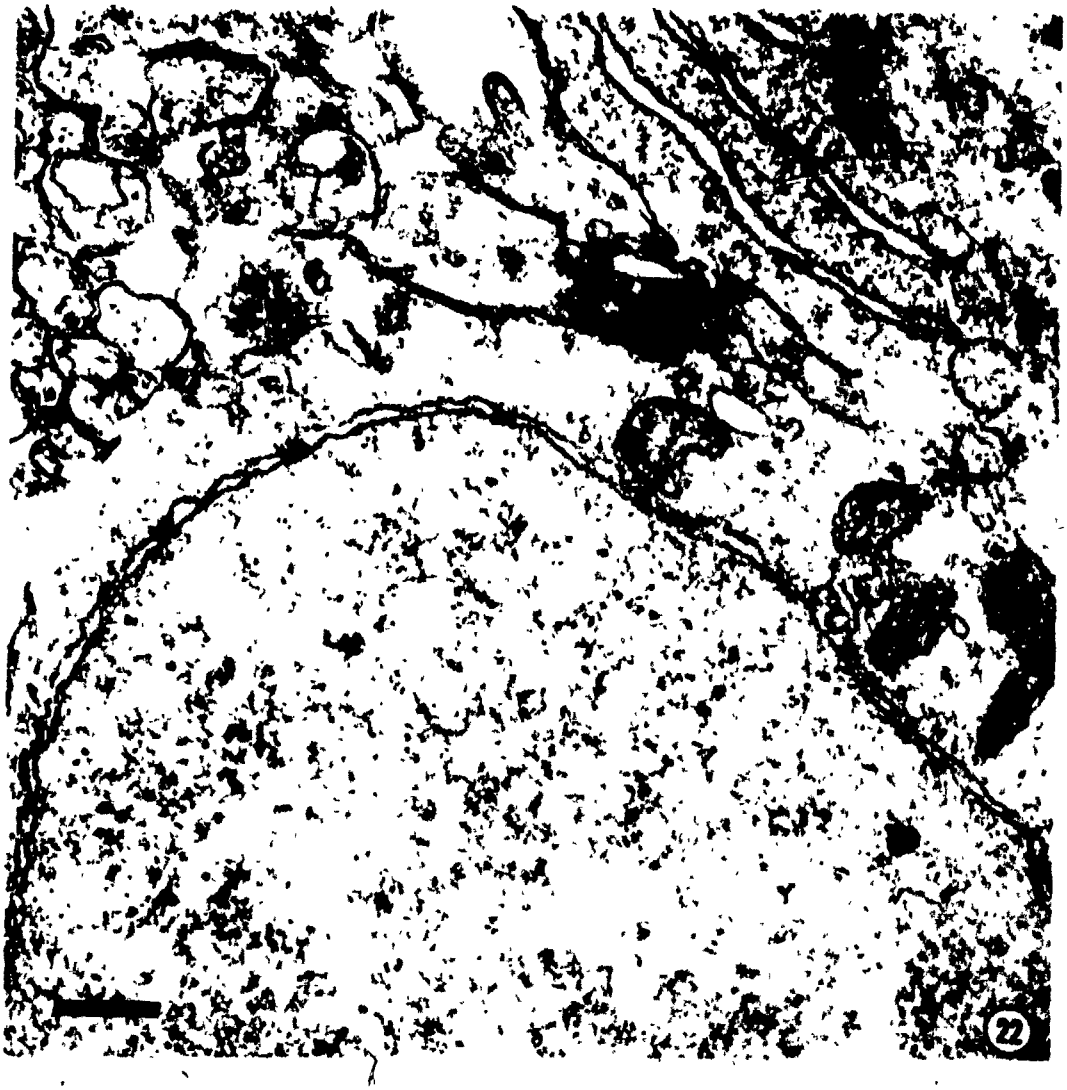
22

Figure 23

A labeled dendrite in direct apposition to a labeled and an unlabeled neonatal nerve cell body. The external plasmalemma of the two perikarya are also closely apposed for some distance.

Scale: 1 μm


23

Figure 24

Immunoreactive axon terminal within the neonatal arcuate nucleus. This terminal, filled with small, round, densely packed clear vesicles, synapses on an unlabeled dendrite. Scale: 0.2 μm


24

Figure 25

TH positive perikarya within the arcuate nucleus of a 15 day old female rat (see text for description). A TH positive dendrite is directly apposed to the soma (arrow). Scales: 1 µm